Measurements of atmospheric electricity aloft

Article

Accepted Version

Nicoll, K.A. (2012) Measurements of atmospheric electricity aloft. Surveys in Geophysics, 33 (5). pp. 991-1057. ISSN 1573-0956 doi: https://doi.org/10.1007/s10712-012-9188-9 Available at http://centaur.reading.ac.uk/32237/

Measurements of Atmospheric Electricity Aloft

K.A. Nicoll

Department of Meteorology, University of Reading.
P.O. Box 243, Earley Gate, Reading, Berks, RG6 6BB UK.
k.a.nicoll@reading.ac.uk

Abstract

Measurements of the electrical characteristics of the atmosphere above the surface have been made for over 200 years, from a variety of different platforms, including kites, balloons, rockets and aircraft. From these measurements, a great deal of information about the electrical characteristics of the atmosphere has been gained, assisting our understanding of the global atmospheric electric circuit, thunderstorm electrification and lightning generation mechanisms, discovery of transient luminous events above thunderstorms, and many other electrical phenomena. This paper surveys the history of atmospheric electrical measurements aloft, from the earliest manned balloon ascents to current day observations with free balloons and aircraft. Measurements of atmospheric electrical parameters in a range of meteorological conditions are described, including clear air conditions, polluted conditions, non-thunderstorm clouds, and thunderstorm clouds, spanning a range of atmospheric conditions, from fair weather, to the most electrically active.

1. Introduction

The study of atmospheric electricity is one of the oldest fields in natural science, dating back to the early 1700s with the suggestion that lightning was a large-scale example of effects that could be obtained with static electricity in the lab (Wall 1908). These ideas were further developed by Franklin (1751) and also Dalibart in the 1750s, who successfully drew sparks from an insulated wooden rod during thunderstorms, demonstrating that thunderclouds did indeed contain electricity (Dalibart 1752). Early investigators were also concerned with raising their measuring apparatus closer to clouds, and the kite became a popular research tool, implemented by many including de Romas (1753), and Cavallo (1776), who demonstrated that significant amounts of charge existed even in non thunderstorm clouds. At the surface, Lemonnier (1752) detected electrification in clear air, the unknown origin of which provided a major motivation for early research into atmospheric electricity.

During the 1780s, the invention of the manned hot air balloon by the Montgolfier brothers enabled investigators to make systematic and more controlled measurements of atmospheric electrical parameters above the surface. Such experiments were important in characterizing the electrical structure of the atmosphere, demonstrating that charge existed above as well as at the surface in fair weather conditions. Despite efforts by many investigators, the origin of the fair weather electric field remained an unanswered problem. Using a manned balloon platform, Victor Hess measured the vertical profile of cosmic rays (Hess 1911) and found that they increase with height from the surface to a height of ~15km, providing a source of charge generation via ionization. This, coupled with the discovery of the conducting region of the ionosphere, led CTR Wilson to propose that the observed atmospheric electrical parameters were sustained by a global atmospheric electric circuit (GEC), which was present globally, and driven primarily by thunderstorm and shower cloud activity (Wilson 1920).

Since the early 1900s, technological development of instrumentation, as well as aircraft and free balloons carrying automated radiosondes has enabled much more experimental investigation into atmospheric electricity. Investigation of the theory of the GEC as well as understanding charge and lightning generation in thunderstorms are two of the most widely studied areas in atmospheric electricity, and a great deal of the research (particularly in the case of thunderstorms) has been obtained from airborne platforms, which provide insight beyond that of surface measurements alone.

This paper presents an overview of airborne measurements of atmospheric electricity up to a height of 40km, from its inception in the 1700s to the present day. First, an introduction to the basic principles of atmospheric electricity is provided, and subsequent sections are separated into measurements in different meteorological conditions, from the least to the most electrically active. These include, clear air conditions, polluted atmospheres, non-thunderstorm clouds, and thunderstorm clouds (considering only DC measurements). Each individual section is ordered according to atmospheric electrical parameter measured. Finally, a discussion of differences between measurement platforms and common difficulties which have been encountered when measuring atmospheric electricity aloft is included.

2. The Study of Atmospheric Electricity

2.1 Small Ions and Conductivity

The weakly conductive properties of Earth's lower atmosphere result from the presence of charged cluster ions. These are created primarily by Galactic Cosmic Rays (GCRs) (up to a height of ≈60km) which enter the Earth's atmosphere from outside the solar system. GCRs are highly energetic

particles comprising mostly protons and He nuclei, with energies from ≈1MeV up to $5x10^{13}$ MeV (Bazilevskaya et al. 2008). Because of their charge, they are deflected by the terrestrial magnetic field, producing a variation in the GCR ion production rate of maximum cosmic ray ionisation at the geomagnetic poles and minimum at the equator. The 11 year solar cycle is also evident in the GCR ion production rate, varying inversely with solar activity, due to modulation by the solar magnetic field carried by the solar wind. Near the Earth's surface the ionisation rate is enhanced by natural radioactivity from Gamma rays emitted from soil and rocks, as well as the isotopes ^{222}Rn (radon) and ^{220}Rn (thoron), which can create ionisation in the lower troposphere.

Cluster ions are destroyed by ion-ion recombination, when two ions of equal but opposite charge collide, and the charge becomes neutralised, and by attachment to larger particles such as aerosol and cloud particles (Hoppel et al. 1986).

The size of an ion is determined by its mobility, μ , which is defined by the drift velocity, v, of the ion as it moves under a unit electric field, E

$$\mu = \frac{\mathrm{v}}{\mathrm{E}} \tag{1}.$$

Thus small ions, which travel faster, have higher mobility than large ions. In general the polar mobilities, μ_+ and μ_- are not equal, due to composition differences between positive and negative ions. Negative ions are smaller and have approximately 30% greater mobility than positive ions, causing the ratio of mobilities $\mu_-/\mu_+ \approx 1.3$. Ions are traditionally categorised by mobility as small, intermediate or large ions.

One of the properties of atmospheric air which is related to the mobility of ions is conductivity, σ, which describes the ability of air to conduct electric current. The total conductivity, σ_t, comprises separate contributions from positive and negative ions, and is given by the sum of the bipolar air conductivities σ_+ and σ_-.

$$\sigma_t = \sigma_+ + \sigma_- = e\left(\sum_i \mu_{i+} n_{i+} + \sum_i \mu_{i-} n_{i-}\right) \tag{2},$$

where, n_{i+} and n_{i-} are the bipolar ion number concentrations of the i different species of ions; μ_+ , μ_- are the bipolar ion mobilities; and e is the electron charge. It is mostly small ions, with mobilities greater than $5x10^{-5}$ $m^2 V^{-1} s^{-1}$ that contribute to the electrical conductivity (Elster and Geitel 1899).

2.2 The Global Electric Circuit

Early measurements of atmospheric electricity established the presence of a fair weather electric field, E, near the Earth's surface which is typically -100 Vm^{-1}, in clear air conditions (e.g. Scrase 1935)[1]. The direction of E is the direction in which a positive test charge moves under the influence of the field. In fair weather at the surface, E is negative, as it is caused by positive charge above, which drives a positive test charge downwards.

Another early fundamental discovery in atmospheric electricity was that the Earth's surface contained a net negative charge (Peltier 1842). Wilson (1906) demonstrated the presence of a vertical conduction current in fair weather, which continuously transferred positive charge to the Earth's surface at a given rate, thus seeming to neutralise the negative charge on the Earth's surface. The solution to the problem of how negative charge on Earth's surface was maintained in the presence of the conduction current was suggested by Wilson (1920), who hypothesised that continuous charge generation mechanisms were present in the form of thunderstorms and shower

[1] The term potential gradient (PG), is often used instead of electric field. Although PG and electric field have the same magnitude, PG has the opposite polarity to electric field i.e. PG = -E.

clouds, which transferred net positive charge upwards to the conducting region of the ionosphere, and negative charge to the Earth's surface by lightning, precipitation and point discharge currents. Support for Wilson's "Global Electric Circuit theory" was found from the potential gradient measurements of the sailing ship *Carnegie*, which sailed the world's oceans between 1909 and 1929, before its destruction by fire (Torreson et al. 1946). The Carnegie PG data, shown in Figure 1 by the grey curve, displays a distinct diurnal variation in fair weather PG, with a minimum at ≈0400 UTC and maximum at 1900 UTC, which was present regardless of the geographical location of the ship. The diurnal variation in PG was correlated with that of the diurnal variation in global thunderstorm activity, shown by the black curve in Figure 1, consistent with the GEC theory. Although the phase of the diurnal variation in PG matches well with the diurnal variation in thunderstorm activity, discrepancies exist between the variation in amplitudes of the two curves, which will be further discussed in section 6.3.

Wilson's theory of the GEC postulates that charge transfer in the circuit gives rise to a potential difference, V_I, between the conducting layers of the ionosphere and the Earth's surface of order 250kV (e.g. Muhleisen 1977), which drives a vertical conduction current density J_c between these regions. J_c flows globally, in all fair weather regions, and is of the order 10^{-12} Am^{-2} (e.g. Wilson 1906), requiring a sensitive electrometer to measure it. Thus the continuous flow of charge from the ionosphere to the Earth's surface provides a link between the upper atmosphere and the lower troposphere. For more detail on the GEC see e.g. Roble and Tzur (1986); Rycroft et al (2008); Aplin et al (2008).

The vertical conduction current density is related to the potential of the ionosphere by the columnar resistance, R_c, the total resistance of the column of air through which it flows from the ionosphere to the surface

$$J_c = \frac{V_I}{R_c} \tag{3}.$$

The term columnar resistance, R_c, was coined by Gish (1944) after the *Explorer II* balloon ascent which measured the conductivity in the stratosphere for the first time. R_c, is the reciprocal of the total conductance in a unit column of the atmosphere from the surface to the high conductivity region of the ionosphere, and is given by

$$R_c = \int_0^\infty \frac{dz}{\sigma_t(z)} \tag{4}.$$

R_c typically varies between 130 and 300 $P\Omega m^2$ (Roble and Tzur 1986). Most of the contribution to R_c is from the lowest 5km of the atmosphere, where the number density of atmospheric molecules is greatest and ion attachment to aerosol is abundant.

2.3 Space Charge in the Atmosphere

The non-uniformity of the electrical conductivity of the atmosphere gives rise to the accumulation of a space charge density, ρ, which is defined as the net difference between positive and negative charge per unit volume (simply referred to here as space charge). The net space charge comprises contributions from many different size charge carriers, including small ions (d≈1nm), large ions (1<d<100nm), and particles and droplets (1μm<d<10mm).

Space charge exits ubiquitously in the atmosphere, and is related to the divergence of the electric field, $\vec{E}$, by Gauss' law :

$$\nabla.\vec{E} = \frac{\rho}{\varepsilon_0} \quad (5),$$

where ε_0 is the permittivity of free space, and $\vec{E}$ is a three dimensional vector of orthogonal components E_x, E_y, and E_z. It is common to study the vertical profile of ρ, which can be derived by considering the vertical component of the electric field, E_z, (provided that variations in E_x and E_y are smaller than those in E_z, as is often the case in fair weather conditions and stratiform clouds). Thus,

$$\rho = \varepsilon_0 \frac{dE_z}{dz} \quad (6).$$

where z is the vertical coordinate, and the positive z direction is upwards. In the case of thunderstorms, E_y and E_x are not necessarily small, but their derivatives dE_y/dy and dE_x/dx are often small compared with dE_z/dz, since charge tends to accumulate in horizontally stratified regions (e.g. Stolzenberg and Marshall 1994, MacGorman and Rust 1998, P130).

In fair weather conditions, ρ is typically positive, with a maximum in the lowest few km of the atmosphere; it decreases with height. In fair weather, in unpolluted regions, the magnitude of the "ambient" space charge is small with a maximum of 1 to 10 pC m^{-3} near ground level (Scrase 1935). At the surface, space charge often shows a diurnal variation similar to that of PG (Brown 1930), sometimes exhibiting a double peak oscillation in winter and a single peak oscillation in summer (e.g. Obolensky 1925).

Space charge occurs in much larger quantities in regions where substantial particle/droplet concentrations exist, due to ion attachment to particles/droplets which creates a gradient in the conductivity and thus $\nabla.\vec{E}$. Observations inside haze layers, which form near the ground on clear and calm nights found ρ up to 160 pC m^{-3} (Lutz 1939), i.e. an order of magnitude larger than in fair weather conditions. The upper and lower boundaries of clouds and aerosol layers (e.g. dust, smoke or pollution), as well as fog and mist layers can also become substantially charged as a result of the conductivity changes near the clear air/particle laden air boundary (e.g. Tinsley 2000, Zhou and Tinsley 2007), observations of which will be discussed in section 4 (for aerosol layers), and section 5 (for non-thunderstorms clouds). For the case of stratified layers and stratiform clouds, the space charge at the cloud/ clear air boundary is proportional to the vertical gradient in conductivity $d/dz\ (1/\sigma_t)$, as well as the vertical conduction current density, J_c (e.g. Tinsley 2000):

$$\rho = \varepsilon_0 J_c \frac{d}{dz}\left(\frac{1}{\sigma_t}\right) \quad (7).$$

Similar charge layers can exist near the tops of thunderstorm clouds (known as "screening" or "shielding layers"), although the magnitude of the charge, as well as the electric fields driving the charge motion are much greater than in the non-thunderstorm case (see e.g. Brown et al 1971 or Hoppel and Philips 1971). Observations of thunderstorm screening layers will be discussed in section 6.1.3.

3. Airborne Measurements in Clear Air Conditions

Measurement of atmospheric electrical parameters aloft in fair weather, clear air conditions is essential to understand the fundamental processes that govern the electrical state of the atmosphere. Fair weather conditions are the least electrically active, where no charge separation is expected to occur, with low wind speeds and no low cloud cover or fog. This section describes

measurements of a variety of different atmospheric electrical parameters above the surface in clear air conditions, as well as the instrumentation typically used. Atmospheric electrical parameters to be discussed include the electric field, conductivity, vertical conduction current density and space charge.

3.1 Measurements of Electric Field

3.1.1 Measurement techniques

The electric field is one of the oldest and most commonly measured atmospheric electrical parameters, and has historically been measured using a passive method known as the potential probe technique, illustrated in Figure 2(a). A potential probe is a conductor, which when placed in an electric field, has a surface charge induced on it. The charged probe attracts opposite polarity ions to that of the probe, causing it to equalise with the potential of the surrounding atmosphere, and thus any subsequent changes in the potential of the probe are directly related to variations in the atmospheric potential. Probes are typically mounted at a height of 1m above the Earth's surface and the potential difference between the probe and Earth (taken to be "ground") gives E_z (this concept is illustrated in Figure 2 (a)). Often a sensitive electrometer is required to measure the potential difference between the probe and ground during fair weather conditions due to the high source impedance of signal voltages; the electrometer must draw significantly less current than the current that flows from the probe to the air. The low atmospheric conductivity at the surface, typically ≈5 fSm^{-1} (Scrase 1933) produces an equalisation rate of order 30 minutes, which is not sufficient to detect transient changes in electric field. To reduce the time constant of the measurement and increase the effective difference in impedance between the probe and the surrounding air, burning fuses, water droppers (see Figure 2(b) for an example) and radioactive sources have traditionally been used. Radioactive sources are often used to measure surface electric fields, however care must be taken in the interpretation of measurements in low wind speed conditions, due to build up of space charge around the probe surface (e.g. Muhleisen 1951). This is not a problem with most airborne platforms, due to ventilation provided by movement of the platform (with the exception of tethered balloons).

Another passive method of electric field measurement, which is commonly used to measure individual vector components of the electric field at high altitudes, is the double Langmuir probe technique (see e.g. Mozer and Serlin 1969, Holzworth 1977). This employs three orthogonal pairs of conducting probes, mounted on insulated booms, two probe pairs horizontally, and one mounted vertically. Since the conductivity is much larger at high altitudes than at the surface, equalisation of the probes with the surrounding air occurs more rapidly, without the need for additional ion sources. The electric field in the direction of each boom is found by dividing the voltage difference (measured using a high impedance voltmeter) between each pair of probes by the distance between them. When used on a balloon platform, the probes must be mounted far enough from the central gondola to minimise the local electric field distortion due to the central payload.

Corona/point discharge probes can also be used to measure electric field, both at the surface and aloft. These probes consist of a sharp conducting point, connected to an electrometer circuit, through which a corona current flows whenever the electric field exceeds a certain corona-onset threshold (found to vary generally between 1 to 6kVm^{-1} (MacGorman and Rust 1998, p77)). This technique has been widely used for electric field measurement in thunderstorms from a free balloon platform (e.g. Byrne et al 1983, 1987, 1989), however, careful interpretation of measurements is required due to corona current dependency on pressure, temperature, wind speed and water vapour.

An additional instrument for electric field measurement, which is generally robust to all meteorological conditions is an electric field mill. An electric field mill typically consists of an electrode, connected to an electrometer circuit, which is alternately exposed and shielded from the atmospheric electric field (see Figure 2 (c) for an example). As the electrode is exposed to the electric field, a charge is induced on the electrode, the magnitude of which is proportional to the field (see Chubb (2010) or Ch6 of MacGorman and Rust (1998) for a more detailed description). Modern field mills (e.g. Bateman et al 2007), are often capable of measuring the full range of electric fields encountered in the atmosphere (spanning six orders of magnitude from $1Vm^{-1}$ to $100kVm^{-1}$), with a fast time response which enables measurement of both ac and dc fields (e.g. Chubb, 2010).

3.1.2 Electric field measurements aloft

One of the first methods of investigating the electrical characteristics of the free atmosphere was by manned balloon, in the late 1800s. On these ascents, E_z was typically found by measuring the potential difference between two water-dropper collectors, separated by distance of a few meters underneath the gondola e.g. Tuma (1899), Gerdien (1904), (1905a), (1905b). The manned balloon electric field apparatus of Tuma (1899) is shown in Figure 2 (b), which illustrates the position of the four water dropper potential sensors in relation to the balloon basket. Linke (1905) modified the water dropper technique by using alcohol instead of water, due to its lower freezing temperature (Israel 1971). During these early ascents, which were typically made to a height of ≈5km, E_z was generally found to decrease with altitude. This was also found by the measurements of Gerdien (1905a), who observed a surface E_z of $70Vm^{-1}$, which decreased to $21Vm^{-1}$ at 1.5km and $3Vm^{-1}$ at 5km. Further details of some of these early manned balloon ascents are given in Harrison and Bennett (2007).

Manned balloons were typically limited to ascents within the troposphere, due to the lack of oxygen at greater heights for the observers, as such, the first information about electric fields in the stratosphere was provided by the recording flights of Idrac (1928). These free balloon ascents reached up to 20km, and were instrumented with two glow collectors ("wicks") which acted as potential probes. The voltage difference between the probes was recorded by photographing the needle setting of a milliammeter. The 1950s saw much development into radiosonde based electric field sensors, typically using radioactive probes (Koenigsfeld and Piraux 1950; Venkiteshwaran et al. 1953; Stergis et al 1957a), and allowed the data to be sent back in real time by radio, avoiding the need for recovery of the instrumentation. Koenigsfeld (1955) made numerous radiosonde flights measuring E_z in fair weather conditions and deduced that generally, above several km, E_z decreases approximately exponentially with height as found by the early manned balloon flights, reaching values between 0 and $1Vm^{-1}$ in the lower stratosphere. He also observed that in the first few km of the atmosphere there was often an increase in E_z with height, and changes in E_z occasionally occurred at the boundary layer between the troposphere and stratosphere.

Further radiosonde measurements were made by Hatakeyama et al (1958), who carried out two balloon borne measurement campaigns to measure E_z, the first using radioactive probes, and the second using a mechanical electric field mill. A similar type balloon borne electric field mill to that of Hatakeyama (1958) was developed by Jones et al (1959), who expressed concern that using radioactive probes or point discharge currents to measure electric fields pollutes the atmosphere with ions, therefore possibly contaminating any additional atmospheric electrical measurements being made nearby or in the wake of the ion plume.

In addition to balloon platforms, aircraft have also been used to measure E_z aloft. Early aircraft measurements were made by Lecolazet (1948) who measured E_z using a radioactive collector mounted on a glider. The glider was thought preferable to normal aircraft for making atmospheric electrical measurements as there were no exhaust emissions to interfere with measurements, such

as through ion attachment, or charged particle generation. The excess charge on the glider was neutralized using a jet of water, acting as a water dropper. When the glider passed into the boundary layer from above, large increases in E_z were observed. Aircraft measurements of E_z were also made by Gunn et al (1946), Gunn (1948) and Gish and Wait (1950) using two electric field machines above and below the wing to remove the effect of aircraft charge on the electric field measurements. The effect of excess aircraft charge on electric field measurements will be further discussed in section 7.2.

Using a similar electric field mill technique to measure E_z, Clark (1957) and (1958) made a number of aircraft flights in fair weather conditions in polar regions and over the oceans. From the results of these flights he devised a rough parameterisation for the rate of change of E_z with height in the troposphere as

$$E_z = E_0 \exp^{-az} \quad (8),$$

where E_0 is the surface electric field, the scale height a =0.25km^{-1}, and height, z, is in km. Additional insight into the behaviour of E_z aloft in fair weather has also been made by scientists from the Soviet Union. Over 425 profiles of fair weather E_z measurements were made over Russia, which were categorised into 4 different groups, depending on the shape of the vertical profile of E_z (Imyanitov and Chubarina 1967), some of which are shown in Figure 3. In category 1 flights (which comprised ≈ 40% of profiles) E_z decreased exponentially with height, similar to the measurements made by Clark (1957), but with a scale height of a=1km^{-1}, demonstrating that differences exist in the vertical distribution of space charge between land and ocean. Figure 3 also shows that in the other 40% of flights, E_z increased with height in the lowest few km of the atmosphere before decreasing rapidly (category 3). Similar results were reported by Clark (1957), who frequently observed that in the lower atmosphere, the vertical profiles of E_z differed substantially from flight to flight, with E_z often not decreasing with height in the expected manner until above several km altitude. This is consistent with the existence of a boundary layer in the lowest few km of the atmosphere, where turbulent mixing determines the vertical distribution of ions and aerosol particles, and therefore atmospheric electrical parameters (further discussed in section 4).

3.1.3 Ionospheric Potential Measurements

The potential of the ionosphere, V_I, is a fundamental atmospheric electrical parameter which is of great importance to the GEC theory. V_I is found by integrating the vertical profile of E_z from the surface to a height of at least 5km (where 80% of the change in E_z has taken place), but as ≈ 99% of the change in E_z occurs from 0 to 20km, measurements to greater heights are desirable. V_I can also be determined from simultaneous measurements of J_c and R_c, and application of Ohm's Law, as given by equation (3). The 1935 flight of the manned balloon *Explorer II* provided the first indirect determination of V_I from onboard measurements of R_c (Gish and Sherman 1936), and direct measurements of V_I followed from the aircraft flights of Clark (1958). Extensive work was done by Mühleisen, who made over 300 balloon ascents of V_I during a 15 year period, mainly over Germany (data tabulated in Budyko 1971). Measurements of V_I ranged from 145 to 608kV, with a mean of 278 kV (Mühleisen 1977). The anomalously large values of V_I > 500kV during the 1960s have been attributed to increases in ionisation in the upper atmosphere as a result of the nuclear weapons tests during this period (Markson 2007). Mühleisen's measurements also demonstrated the similarity between the diurnal variation in V_I to the Carnegie curve, providing direct support for Wilson's GEC hypothesis. This finding is supported by the extensive aircraft measurements of V_I by Markson (1976), (1977) and (2007), in which comparisons between the diurnal variation in V_I on single days and the Carnegie curve are reported, with the two measurements showing close agreement.

Additional evidence in favour of the GEC hypothesis is that V_I measured from different locations varies together, e.g. Mühleisen (1971), Markson (1985), and Markson et al (1999). Mühleisen (1971) reported on measurements of V_I made by simultaneous balloon soundings over Weissenau, Germany and the Meteor research ship in the equatorial Atlantic (separated by a distance of 6000km). Figure 4 shows a comparison of the V_I measurements made from Weissenau and the north Atlantic, where it is obvious that there is close agreement between the two sites.

Measurements of V_I have also been made from tethered balloon platforms by Vonnegut et al (1973) (also implemented by Willet and Rust (1981)), Holzworth et al (1981), and Holzworth (1984). The maximum potential measured by Willett and Rust (1981) was 195kV, at a height of 5.3km above mean sea level, and 170kV at a height of 0.55km by Holzworth et al (1981). Concerns about the validity of the measurements by Holzworth et al (1981) were expressed by Markson (1984), who pointed out that the potential measurements were unusually large compared to previous aircraft measurements at the same height. Although the tethered balloon technique of measuring V_I generally permits higher time resolution measurements than aircraft or free balloon platform, several problems are commonly encountered, including engineering difficulties associated with a 1km long tethered cable, the error incurred by extrapolation to ≈ 65km of the potential measurement from low altitudes, and the influence of local meteorological conditions on the atmospheric electrical parameters, in particular convection currents and aerosol concentration.

3.2 Measurements of Conductivity

3.2.1 Measurement techniques

Another atmospheric electrical parameter of importance to the GEC is the electrical conductivity of the air, σ. Most conductivity instruments are based on the principle of Gerdien's cylindrical condenser which was initially designed to make measurements above the surface on a manned balloon (Gerdien 1905c). The instrument consists of two concentric cylinders, a central and outer electrode, through which air is drawn, illustrated in Figure 5(a) and (b). A bias voltage applied to the outer electrode deflects ions of the same polarity as the bias voltage towards the inner electrode where they induce a current and associated voltage change, either of which can be measured by a sensitive electrometer.

An additional method of measuring conductivity above the surface is the relaxation probe (or Langmuir Probe) method, typically deployed on balloon and rocket flights. The operating principle of relaxation probes is similar to that described in section 3.1 for measurement of electric field by potential probes, but for measurement of σ, the probe must be biased at some potential different to the surrounding air. The relaxation probe method works best at high altitudes, where the conductivity of the air is substantial, and creates considerable ion conduction currents in the sensor, hence this technique is mostly deployed in the stratosphere and mesosphere. Vertical profiles of conductivity have been measured by this method by many investigators including Kellogg and Weed (1968); Hale et al (1968); Mozer and Serlin (1969); Mitchell and Hale (1973); Byrne et al (1988); Hu and Holzworth (1996); Holzworth and Bering (1998); Bering et al (2005) and John et al (2009) using free balloons, constant altitude balloons and rockets. The relaxation method is also popular on space missions, as the same probe instrument can be used to determine both conductivity and electric field, thus saving space and power, which is in small supply e.g. (Berthelier et al. 2000). The technique was implemented successfully on the Huygens space probe, which measured the conductivity of the atmosphere of Titan, in which a strongly ionised layer was measured at ≈ 60km above Titan's surface (Fulchignoni et al. 2005).

To investigate possible differences between Gerdien condenser and relaxation probe methods of measuring conductivity, simultaneous measurements of conductivity obtained by a relaxation probe

and three different Gerdien condensers from balloon flights were compared during an international workshop on atmospheric electrical measurements in 1978 (Rosen et al. 1982). The vertical profiles measured by the Gerdien condensers were very similar, however the conductivity profile from the relaxation probe was a factor of two lower than the others. The reason for this discrepancy is still not understood, but to the author's knowledge, no further comparisons have been made.

3.2.2 Measurements of conductivity aloft

The first measurements of conductivity above the surface were made by Gerdien, who made several manned balloon ascents with his σ apparatus between 1903 and 1905, and his ascent from Berlin, Germany on August 30th 1905 shows a clear increase in σ with height from the surface up to 5km (Gerdien 1905b). A rendering of the balloon apparatus is shown in Figure 5 (c), which illustrates the sampling tube inlet on the left of the image, the electrometer beneath the sampling tube, and the fan on the right. The increase in σ with height found by Gerdien was corroborated by the 1913 flights of Wigand (Everling and Wigand 1921), where the maximum altitude reached was 9km. At higher altitudes, stratospheric conductivity was first measured by the *Explorer II* manned balloon (Gish and Sherman 1936), which showed an increase in σ with height from the surface to 18km, but a decrease with height from 18 to 22km, the maximum altitude of the flight. The decrease in σ above 18km was unexpected, but was attributed to the presence of condensation nuclei in the stratosphere.

The Gerdien condenser was originally a large bulky instrument, designed for use on manned balloons where weight constraints were not a problem, however by the 1950s σ instrumentation could be made small enough to fly on free balloons. An example of more modern σ apparatus designed for use on a free balloon platform is shown in Figure 5(d). The apparatus, described in Nicoll and Harrison (2008) measures bipolar conductivity simultaneously, and weighs 300g, considerably lighter than the 4.5kg apparatus of Woessner et al (1958) and Paltridge (1965). Some of the earliest free balloon measurements of clear air σ were made by Stergis et al (1955), Koenigsfeld (1953), Woessner et al (1958), Jones et al (1959), Hatekayama et al (1958), Paltridge (1965), and Morita et al (1971). They generally found an increase in σ with height in accordance with the results of Gish and Sherman (1936) to 18km. Stergis et al (1955) observed large fluctuations in the σ data measured during the ascent stage of the flight, but were not present in the descent data. They deduced that the fluctuations were due to instrumental error, most likely insufficient ventilation of the Gerdien condenser on the ascent, and not representative of actual fluctuations in σ. Thus it is essential to ensure that Gerdien conductivity apparatus is adequately ventilated in order to make accurate measurements. Ventilation of relaxation probes is not so vital, thereby allowing the technique to be implemented on high altitude constant level balloons, where horizontal or vertical speeds may be low.

A substantial number of radiosonde measurements of σ were made by the group of Muhleisen during the 1970s and 80s, using a variant of the Gerdien condenser. From these, Gringel (1978) compared profiles of positive conductivity during periods of maximum solar activity and minimum solar activity, and parameterized them according to an expression of the form

$$\sigma_{+}(z) = 1x10^{-14} \exp(a + bz + cz^{2} + dz^{3}) \quad (9),$$

where the coefficients *a, b, c*, and *d* vary depending on the solar cycle, e.g. for solar minimum *a*=0.636, *b*=0.36008, *c*=-0.008605, *d*=0.00010331, and for solar maximum *a*=0.66837, *b*=0.35653, *c*=-0.0095435 and *d*=0.00012313, with height, *z* in km. Gringel's measurements are plotted in Figure 6 (a), where the black dashed line denotes solar maximum and blue dot dashed line solar minimum conditions. It is clear there is a decrease in conductivity during periods of solar maximum compared

to solar minimum, which results from deflection of incoming galactic cosmic rays (GCRs) by the solar magnetic field. Figure 6 (a) shows a number of conductivity profiles obtained by different researchers (Woessner et al 1958; Rosen et al 1985; Gish and Sherman 1936; Callahan et al 1951) during periods close to solar maximum (with the exception of Gish and Sherman (1936)). Although these profiles were obtained during periods of similar solar activity there is considerable variability between profiles, likely to be attributable to instrumentation and location differences, as well as variation in aerosol concentration profiles, however the approximately exponential increase in conductivity with height is common to all.

Considerable research has been undertaken into the vertical distribution of conductivity, however it is also important to determine its variation horizontally, particularly with respect to latitude, as the GCR flux which provides the main source of atmospheric ionisation is known to vary substantially with latitude (e.g. Bazilevskaya et al 2008). At low latitudes, low energy GCRs are deflected by the geomagnetic field, thus only high energy GCRs can penetrate the atmosphere. Nearer the geomagnetic poles, the energy barrier to incoming particles reduces, therefore at the poles, the full energy spectrum of GCRs can penetrate the atmosphere. The latitudinal variation of conductivity has been investigated by several researchers using high altitude balloons (Byrne et al 1988; Hu and Holzworth 1996) and aircraft (Markson 1985; Driscoll et al 1996). Driscoll et al (1996) measured the latitudinal distribution of conductivity in the stratosphere using the high altitude ER-2 aircraft. Flights were made over a range of geomagnetic latitudes from 56°N to 28°S between 1991 and 1993. Conductivity measurements were normalized according to pressure and temperature, and the following parameterization was derived for the latitudinal variation in positive conductivity at 20km during 1993,

$$\sigma_+ = a_0 + a_1 \mid \Lambda \mid + a_2 \mid \Lambda \mid^2 + a_3 \mid \Lambda \mid^3 \qquad (10),$$

where $a_0 = 0.972$, $a_1 = 2.00\text{x}10^{-4}$, $a_2 = 3.80\text{x}10^{-4}$ and $a_3 = 1.25\text{x}10^{-6}$ Sm^{-1} (at pressure 54.748 mbar and temperature 216.65°K, valid for a geomagnetic latitude range $28°S \leq \Lambda \leq 49°N$). A plot of Driscoll et al's parameterized conductivity as a function of geomagnetic latitude is shown in Figure 6 (b) as the solid black line. Also shown in Figure 6(b), by the dashed black line, is the positive conductivity parametrization of Hu and Holzworth (1996), obtained from high altitude balloon measurements at an altitude of 26km, spanning a geomagnetic latitude range of 15 to 80°S. From this data it is clear that the stratospheric conductivity exhibits an obvious dependence on geomagnetic latitude, with the largest values of σ_+ near the geomagnetic poles, where the incoming cosmic ray flux is greatest. Also evident from Figure 6(b) is the effect on σ_+ of the cosmic ray "knee", where the cosmic ray flux, and thus conductivity ceases to increase with increasing Λ at polar latitudes.

As well as characterisation of the vertical and horizontal profiles of conductivity, it is important to investigate the typical ratio of bipolar conductivities, σ_-/σ_+. Simultaneous measurement of both positive and negative conductivity can provide information about the dominant polarity of charge in a region through σ_-/σ_+. From equation (2), it can be seen that

$$\frac{\sigma_-}{\sigma_+} = \frac{n_- \mu_-}{n_+ \mu_+} \qquad (11),$$

where $n_{-/+}$ and $\mu_{-/+}$ are the polar ion number densities and mobilities respectively. Positive and negative ions are created in equal numbers, therefore $n_+ = n_-$, and thus σ_-/σ_+ should be equal to the ratio of negative small ion mobility to positive ion mobility, i.e. ≈1.3. In practice, this is rarely observed, particularly at lower altitudes, where meteorological conditions can have substantial influences on ion number concentration, for example at cloud edges. Measurements of σ_-/σ_+ in the

fair weather atmosphere above the surface by different investigators are given in Table 1. It is seen that there is a large variability in σ_-/σ_+ between different flights, and at different altitudes, and in general σ_-/σ_+ does not agree with the theoretically predicted value of 1.3.

3.3 Measurements of Vertical Conduction Current Density

Another parameter of importance to the GEC theory is the vertical conduction current density, J_c, which can be determined at and above the surface by *indirect* or *direct* methods. The indirect method requires the simultaneous measurement of electric field and conductivity, and the assumption of Ohm's law. If E_z and σ are measured in the same volume element (e.g. $1m^3$), the product of these two parameters gives J_c, however, small scale variations and measurement difficulties often mean that simultaneous co-located measurements of E_z, σ and J_c do not give the result expected from Ohm's law (Israel 1973). Using the indirect method, Kraakevik (1961) found that from aircraft measurements over the ocean, J_c varied by only 10% from 15m to 6km, providing evidence that J_c is approximately constant with height, as predicted by conservation of charge and current continuity. Similar results were found by the Gringel et al (1986) balloon measurements of E_z and conductivity. The derived values of J_c were found to be approximately constant with height between 3 and 12km, and the mean value of J_c over the entire flight was 2.35 ± 0.15 pAm^{-2}. Holzworth et al (2005) used the indirect method of determining J_c to investigate links between temporal variations in the GEC over Antarctica and global lightning flash rate. Using E_z and σ data measured from a double Langmuir probe on board constant level stratospheric balloons at an altitude of ≈30km, they calculated J_c (found to vary between 2 and 4 pAm^{-2}) and compared it with observations of global lightning using the World Wide Lightning Location Network (WWLLN). A strong correlation between the temporal variation in the two datasets was found, providing further support for the GEC theory.

Direct measurements of J_c are typically made using either a well-insulated horizontal plate which measures the total charge flowing to the plate in a given period of time (Wilson 1906), a horizontal long-wire antenna (Kasemir 1955; Ruhnke 1969), or a double hemispherical conductor (Burke and Few 1978). The long-wire antenna (Kasemir 1960), has been successfully flown on a balloon platform and J_c calculated from the current measured between the lower and upper halves of a vertically oriented wire antenna, and dividing it by the effective area of the antenna. Such apparatus has been flown by several investigators (Olson 1971; Uchikawa 1977; Cobb 1977; Rosen et al 1982), however, accurate derivation of the effective area of the vertical wire (Tammet et al 1996) and careful interpretation of the current measurement is essential when deriving J_c from this apparatus (Few and Weinheimer 1986).

3.4 Measurements of Space Charge

Like the vertical conduction current density, space charge, ρ, can be determined indirectly, or measured directly. The indirect method of determining space charge derives the total space charge from all sizes of charge carriers. The total space charge is directly proportional to the gradient of the change in E_z with height, as given by equation (6). Space charge in clear air conditions has been derived using the indirect method by Vonnegut and Blume (1957) who used radioactive probes mounted on an aircraft to measure the rate of change of E_z, and Koenigsfeld (1955) using a radiosonde platform, who found marked changes in space charge at cloud levels. Kraakevik and Clark (1958) also derived space charge using the indirect method. Their measurements in clear air showed several space charge layers located above each other.

Direct methods of measuring space charge are based on charge detection. These include filtration methods, where air is passed through an adequately thick filter of cotton wool or metal wool, which retains the charge carriers from the air. The method was pioneered by Obolensky (1925) and the

apparatus is known as an Obolensky filter. The electrification of the filter is directly related to the excess positive or negative charge carried by the absorbed charges. This method is used to measure the total space charge due to all charge carriers trapped by the filter. Other investigators who have used similar types of filters include Smiddy and Chalmers (1960) and Moore et al (1961). Moore et al (1961) used a filter composed of glass microfibers, after expressing concerns that the traditionally used steel wool filters did not trap all of the space charge carriers. They flew their space charge apparatus successfully on 35 aircraft flights over Illinois, mostly in clear air conditions, alongside additional apparatus to measure E_z. They found that the space charge measured directly by their apparatus was in close agreement with that derived from the measurements of E_z via the indirect method, giving confidence in their space charge apparatus.

3.5 Electrical parameters aloft during solar energetic particle events

Although the main source of atmospheric ionisation above the Earth's surface is from GCRs, ionisation at high altitudes can also result from Solar Energetic Particles (SEPs) (mostly MeV protons). A transient flux of SEPs into the Earth's atmosphere typically occurs following a solar flare, which accelerates electrons, protons and heavy ions to high speeds. SEPs access to the atmosphere is restricted by magnetic rigidity cutoff, in a similar way to GCRs, whereby SEPs are generally restricted to polar regions. Direct observations of atmospheric electrical parameters during SEP events have been made from high altitude, long duration balloon flights, typically instrumented with double Langmuir probes to measure the vector electric field and conductivity (via the relaxation method). Holzworth and Mozer (1979) report a decrease in E_z from 250 mVm^{-1} to 0 mVm^{-1} during an SEP event, at an altitude of 30km at 55.8°N, 97.9°W (geographical coordinates). The decrease in E_z was interpreted as a result of increased conductivity (which was measured during the same flight, but with insufficient time resolution (every 30 minutes) to examine the period around the SEP event in any detail).

Subsequent measurements by Holzworth and Norville (1987) during an SEP event in February 1984, detected a decrease in the magnitude of E_z and increase in $\sigma_{tot,}$ where both polarities of conductivity were enhanced by a factor of two (see Figure 7). The ionisation rate was also measured during the same balloon flight (altitude 26km, 44.6°S, 142.7°E geographical coordinates), which showed an increase from ≈30 to 100 counts per minute, coincident with the SEP event, accounting for the observed increase in $\sigma_{tot,.}$ A second balloon at similar altitude but different geomagnetic latitude (38.7°S, 65.7°E geographical coordinates) showed no detectable change in E_z and $\sigma_{tot,}$, allowing the spatial extent of the SEP event on the electrical environment to be determined. Thus the rigidity cutoff at the poleward balloon enabled SEPs to perturb the electrical environment, but not at lower latitudes. The simultaneous measurement of σ_{tot} and E_z from these balloon flights also allowed the determination of J_c via the indirect method, which showed an increase by a factor of two (from 2 pAm^{-2} to 4.5 pAm^{-2}) at the poleward balloon during the SEP event, but no change at the equator-ward balloon. Providing the indirect method yields an accurate determination of J_c, this suggests that if the upward charging current to the ionosphere from thunderstorms remains constant, J_c should decrease at lower latitudes to maintain current continuity. This was not evident from the equator-ward balloon measurements, possibly because the duration of the J_c change (of order 30 minutes) was not long compared with the total relaxation time of the GEC, which is thought to be between 5 and 40 minutes (Chalmers 1967).

More recent measurements by Kokorowski et al (2006) during an SEP event in 2005 found a similar decrease in E_z from 100 mVm^{-1} to near zero, and an increase in σ_{tot}, from a balloon at 30km altitude at 70.9°S, 10.9°W (geographical coordinates). J_c was found to vary between ±5pAm^{-2} for a period of 12 hours, in contrast to the 30 minute perturbations in J_c detected by Holzworth and Norville (1987). Thus the electrical changes observed by Kokorowski et al (2006) took place over much longer timescales than the relaxation time of the GEC, however no simultaneous measurements at other

latitudes were available to asses the spatial extent of the atmospheric electrical changes. Although it is generally found that SEP events increase the conductivity and decrease E_z locally at high altitudes, the effect of such events (and indeed other space weather events) on the global behaviour of the GEC has yet to be fully investigated, requiring simultaneous measurements at a variety of geomagnetic latitudes.

3.6 Summary of Clear Air Atmospheric Electricity Aloft

Systematic measurements of atmospheric electricity aloft in fair weather conditions began in the late 1800s with the pioneering manned balloon measurements of Tuma, Gerdien and Wigand, who established the general behaviour of atmospheric electrical parameters above the surface. Their findings, that E_z decreases approximately exponentially with height, and σ increases exponentially with height, have mostly been corroborated by numerous subsequent measurements, many of which have been described in this section. Table 2 provides a list of the investigators who have made atmospheric electrical measurements above the surface in fair weather conditions, including details of the measurement platform and instrumentation used.

Despite the consistency of electrical measurements above the lowest few km of the atmosphere, considerable variability between flights is found near the surface, even in clear air conditions. This variability can be explained by the presence of particulate matter in the atmosphere, which is generally emitted from the surface, and can have substantial effects on atmospheric electrical parameters, as will be discussed in the following section.

4. Airborne Measurements in the Polluted Atmosphere

It is well known that atmospheric electrical parameters are influenced by meteorological conditions, both at the surface and above, however this was not always the case. Early measurements of atmospheric electrical profiles showed considerable variability between flights, and sharp discontinuities were often observed in seemingly fair weather conditions. The explanation for these effects lies with the existence of aerosol and haze particles, which can become charged by diffusion of ions to their surfaces, or by collision with each other, thus perturbing E_z and σ locally. Furthermore, the existence of the boundary layer, which resides in the lowest few km of the atmosphere, acts to trap these particles, further perturbing the atmospheric electrical parameters from their clean air values. This section will describe measurements of atmospheric electrical parameters aloft in conditions when haze or aerosol layers (including dust and volcanic ash) are present. As in the preceding section, sub sections are separated according to atmospheric electrical parameter measured.

4.1 Measurements of Electric Field

4.1.1 Boundary Layer

The boundary layer (or atmospheric Exchange layer or Austach region as it is sometimes known) is the lowest few km of the atmosphere that is directly influenced by the surface. In this layer, aerosol particles, which are typically emitted at the surface, are transported upwards by convection and turbulence, and trapped at the top of the layer by a temperature inversion (where the temperature increases with height). This inversion acts as a lid to upward motion, the height of which is determined by the amount of incoming solar radiation, and thus the time of day, location and season of the year. Some of the first detailed measurements of the electric field in the boundary layer were made by Clark (1957), who found substantial variations in the E_z profile from its average value within the lowest few km of the atmosphere. Measurements often showed a large decrease in

E_z with height up to a certain altitude, then a more gradual decrease. The height at which the gradient in E_z changed was often accompanied by a temperature inversion, and differed according to location.

The measurements of Imyanitov and Chubarina (1967) also supported evidence of an atmospheric boundary layer which affects atmospheric electrical parameters. Measurements of E_z from an aircraft instrumented with an electric field mill over Russia showed that during days when smoke or dust was trapped under a temperature inversion, E_z increased with height up to the inversion layer, and subsequently decreased above it. Approximately 43% of their measured E_z profiles were of this type (category 3 profiles shown in Figure 3), and agree with the results of Koenigsfeld (1955), and Hatekayama et al (1958), who also found sustained large values of E_z in the lowest few km of the atmosphere, with sharp decreases at temperature inversions. The measurements of Srivastava (1972), from balloon ascents over India also found variations in electric field between different seasons. They note that high values of E_z often occurred during summer in the boundary layer due to increased dust concentration and also dense haze near the ground.

4.1.2 Aerosol Layers

Another common reason for large values of electric field in the seemingly fair weather atmosphere is the presence of aerosol layers above the surface. Some of the first documented measurements of E_z in haze layers above the surface were made from a glider platform by Rossman (1950), described in Israel (1973). Rossman made several flights through haze layers, which occurred during anticyclonic conditions, which created well defined haze boundaries. During a flight on 16th March 1943, E_z remained close to its surface value (≈60Vm^{-1}) up to an altitude of 2500m, where it decreased rapidly to ≈15Vm^{-1}, signifying the top of the haze layer. Markson (2007) has also detected sharp changes in E_z thought to be associated with aerosol above the surface during a balloon flight over Hawaii. The vertical profile of E_z shows an increase in electric field from 25 to 60Vm^{-1} at ≈3km, then decrease back to 20Vm^{-1} which occurs over a vertical distance of a few hundred meters.

4.2 Measurements of Conductivity

A substantial number of fair weather vertical profiles of conductivity by many different investigators show that conductivity increases approximately exponentially with height, in agreement with theory. However, in the presence of particulate matter, conductivity is expected to decrease, due to ion-particle attachment, which decreases the mobility of the ions. In addition to the decrease in conductivity, the particles themselves become charged, leading to the generation of space charge. Such decreases in conductivity are observed in a number of atmospheric phenomenon which occur at and above the surface such as aerosol layers, haze and dust. Observations inside each of these phenomena will be discussed in the following section.

4.2.1 Boundary layer

Substantial insight into the processes governing atmospheric electrical parameters in the lowest few km of the atmosphere have been gained by the measurements of Sagalyn and co-workers in the US. In Sagalyn and Faucher (1954; 1956) simultaneous measurements of conductivity, large ion concentration, temperature, pressure and humidity were made from an instrumented B-17 aircraft over New Hampshire, Texas and California in the US. From the 40 or so flights that were made in fair weather conditions, the existence of a boundary layer was apparent, in which the vertical distributions of ions and thus the conductivity are controlled primarily by turbulence. An example of the typical vertical profile of conductivity in the boundary layer is given in Figure 8(a) which shows that within the boundary layer, the conductivity is typically low, and increases dramatically within a small vertical distance at the upper boundary of the layer. A comparison between the conductivity expected from GCR ionisation data and observed values from 9 different flights of Sagalyn and co-

workers showed the conductivity to be less than half of its expected value within the boundary layer. Above the layer the observed conductivity agreed with that predicted by theory.

4.2.2 Aerosol layers

Substantial reductions in conductivity within haze layers have been observed by the aircraft measurements of Callahan et al (1951), who found that the average value of negative conductivity on hazy days was up to 40% less than on clear days. Conductivity decreases have also been observed in haze layers by Scott and Evans (1969) who measured conductivity with a dropsonde based instrument. On a descent on a fair weather day, a sharp decrease in positive conductivity was measured at around 12km, thought to be attributable to a thin layer of haze. On the same flight, a second layer of haze was encountered at 9.5km, where the positive and negative conductivities again decreased, but did so asynchronously, suggesting that the layer was unipolar charged. Similar asynchronous behaviour of the polar conductivities was found at the top of the boundary layer, where the positive conductivity increased at 3km, but the negative conductivity did not increase until 3.5km. A clear example of the conductivity decrease between clear and particle laden air is also shown by the balloon flights of Gringel and Muhleisen (1978), during a flight through a Saharan dust layer approximately 2km deep. The vertical profile from this flight shows a distinct decrease in the positive conductivity at the base of the dust layer (≈ a factor of two smaller than its clear air value), and an increase at the top of the layer back to its clear air value.

The existence of aerosol particles in the stratosphere was demonstrated by Junge et al (1961), who measured vertical profiles of small Aitken nuclei, with typical diameters between 0.1 and 1 μm at high altitudes, well above the tropopause. Changes in conductivity due to aerosol layers in the stratosphere have been observed by Kondo et al (1982a; 1982b); Rosen et al (1985); and Byrne et al (1988) mainly from balloon platforms. Gringel and Muhleisen (1978) measured the number concentration of small particles and conductivity simultaneously from a balloon platform, in which conductivity was found to decrease by ≈11% in a layer in which the particle number concentration was 2000cm^{-3} above the background value. This allowed derivation of a parameterization for aerosol particle concentration using only measurements of conductivity, which has been used by several investigators including Kondo et al (1982a), who also measured conductivity from a balloon platform, from Garmisch-Partenkirchen, Germany, during the early 1980s. Flights were made before and after the eruption of Mt St Helens on 18th May 1980 (Kondo et al 1982b). Approximately a month after the eruption, a decrease in conductivity was found over a broad altitude range around the tropopause and above (from ≈12 to 17km). Similar effects were observed during subsequent flights, but the authors note that it was difficult to attribute the decreases in conductivity to solely volcanic effects, due to the common existence of aerosol layers around the tropopause, even during periods of low volcanic activity. They did note, however, that ground based lidar retrievals showed increased backscatter ratios above 10km, which were generally not observed for aerosol layers during non-volcanic periods, suggesting that at least some of the conductivity decreases in the lower stratosphere were a result of the Mt St Helens eruption.

Further decreases in conductivity as a result of high altitude aerosol layers have also been detected by Rosen et al (1985) who measured bipolar conductivity and small ion concentration simultaneously with the same instrument. The number concentration of Aitken nuclei was also measured during some of these flights. During one flight a layer of Aitken nuclei with concentration of ≈400cm^{-3} was detected near 30km, which caused a 10% decrease in the conductivity. Other observations of aerosol layers at different altitudes did not generate noticeable decreases in conductivity, despite containing similar number concentrations of particles. This suggests that the effect of aerosol particles on the conductivity depends on the size of the particles, as well as the altitude and temperature, as this plays an important role in the mobility of the ions.

4.3 Measurements of Space Charge

The vertical profile of space charge in the fair weather, clear air atmosphere has typically been obtained by calculating the vertical gradient in electric field (i.e. indirectly), and is found to decrease with height, from a few pCm^{-3} at the surface to $\approx 10^{-3}$ pCm^{-3} at a height of 10km. In the presence of particles, large variations in space charge are often found, observations of which are described in the following section.

4.3.1 Boundary Layer

Measurements of the vertical profile of space charge within the boundary layer have been derived from the aircraft electric field measurements of Sagalyn and Faucher (1954). During a flight in August 1953, shown in Figure 8(b) a very well defined layer of positive space charge, with $\rho > 6$ fC m^{-3} was observed at the top of the boundary layer. This was coincident with an increase in conductivity above the boundary layer, due to the decrease in particle concentration.

4.3.2. Aerosol Layers

The existence of space charge due to haze layers in the lower atmosphere was observed indirectly from the dropsonde electric field measurements of Mecklenburg and Lautner (1940). Electric field was measured using two radioactive collectors, mounted a vertical distance one above the other, and their potential difference was photographically recorded with a Lutz string electrometer. Their instrumented dropsonde traversed several haze layers, in which positive space charge up to 1.9 pC m^{-3} existed at the top of each layer. Aircraft measurements of electric field by Vonnegut and Blume (1957) have also found large changes in electric field at haze boundaries. During a flight in May 1955 from Massachusetts, US, two temperature inversions located between 0 and 1km were accompanied by substantial changes in electric field. Using the indirect method of determining space charge, negatively charged regions of -3 fC m^{-3} and -23 fC m^{-3} were found in the lower and upper haze layers respectively. Negative space charge has also been found at the base of haze layers by Moore et al (1961), who measured charge directly using a filter type apparatus mounted on an aircraft. At the base of the haze layer, the charge apparatus detected a layer of negative charge, and the electric field (also measured on the aircraft using a separate instrument) increased rapidly. Positive charge was observed towards the top of the layer, where the electric field decreased to its ambient value.

Direct measurements have also been obtained of charge inside volcanic ash layers well above the surface by Harrison et al (2010). Unlike the measurements of Kondo et al (1982b), who measured conductivity aloft a month after the eruption of Mt St Helens, the measurements of Harrison et al were made 32 hours after the volcanic plume was emitted from the Eyjafjallajokull volcano in Iceland during April 2010, shortly after a period of intense volcanic lightning. Measurements were made from a balloon instrumented with a space charge sensor, aerosol particle counter, and meteorological radiosonde with GPS position information. The space charge sensor consisted of a spherical electrode, which measured the total space charge per unit volume directly, from induction and impaction from charged particles (see Nicoll and Harrison (2009) for a detailed description). During an ascent from Stranraer, Scotland, UK, on 19th April 2010 (a horizontal distance of 1200km from the volcano), a distinct layer of aerosol particles, with mean diameter 1.4 µm was detected at approx 4km altitude, shown in Figure 9(a). Coincident with this layer, a region of charge, the same depth as the aerosol layer (≈700m) of $\rho \approx 0.5$ pC m^{-3} was detected (shown in Figure 9 (b)), demonstrating that volcanic ash layers can retain their charge up to several days after being emitted from the vent.

Measurements of charge inside layers of Saharan dust, several km above the surface have also been made by the group of Harrison and colleagues, using the same instrumentation used to investigate volcanic plumes. Nicoll et al (2011) report direct observations of space charge measured from

balloon flights from the Cape Verde Isles, approximately 600km from the west coast of Africa, which are frequently affected by Saharan dust outbreaks carried across the sea by upper level winds. During four ascents within a two week period, several elevated layers of dust were found, many of which were charged. Observations during one flight on 26th August 2009, detected a layer of dust at 4km altitude with up to 60 particles cm^{-3} (particle diameters <2.6μm), containing charge up to 25 pC m^{-3}. Although dust particles are expected to charge during the lofting stage, the horizontal distance between their source region and the measurement location suggests that, in the absence of continuous particle charging mechanisms, the charge on the particles should have decayed long before reaching the measurement location due to interactions with atmospheric ions. Nicoll et al (2011) suggest several reasons for the charge observed in the layer, including charging at the layer edges by the vertical conduction current density (see section 5), but this effect is too small to account for the charges observed. Neglecting potential instrumental errors, this suggests the existence of a continuous charge generation mechanism.

Investigation of charge generation mechanisms in dusty environments, particularly with respect to the triboelectrification of dust from contact electrification is an ongoing area of research. Electrification is known to exist in dust devils, which can be significantly charged, often possessing electric fields of tens of kVm^{-1}, (e.g. Frier 1960, Renno et al 2004, Farrell et al 2004). They are abundant on Earth as well as Mars, where they are thought to create large enough fields to enable electric discharges (e.g Kok and Renno, 2008).

4.4 Summary of Measurements in the Polluted Atmosphere

Atmospheric electrical observations in polluted conditions show that there is a close relationship between the vertical distribution of aerosol particles and atmospheric electrical parameters. Measurements described in this section shown that the altitude distribution of aerosol particles and atmospheric electrical parameters is significantly affected by the state of the atmosphere, in particular by the presence of temperature inversions and other capping inversions. Strong gradients in electric field and conductivity, as well as significant regions of space charge are frequently observed near these temperature inversions, particularly in the lowest few km of the atmosphere, where aerosol particles are abundant.

5. Airborne Measurements in Non-Thunderstorm Cloud

Although convective clouds that give rise to thunderstorms are often the only cloud type usually regarded to be charged, all cloud types have the propensity to be electrified, due to ion collection by cloud droplets. Specifically, charge can accumulate at the upper and lower cloud edges as a result of vertical flow of the conduction current density, J_c, through the cloud layer, theoretically creating a layer of positive charge at the cloud top and negative charge at cloud base (given by equation (7)). In this paper, non-thunderstorm clouds are defined as those which are not highly electrified convective clouds leading to thunderstorms, which also do not produce precipitation e.g Stratus (St), Stratocumulus (Sc), Altostratus (As), fair-weather Cumulus (Cu), Altocumulus (Ac), Cirrus (Ci), Cirrostratus (Cs). Non-thunderstorm clouds have been relatively under explored in comparison with thunderstorm clouds, hence the vertical structure and magnitude of charge in non-thunderstorm clouds is generally not well characterised. This section presents an overview of atmospheric electrical measurements made in non-precipitating, non-thunderstorm clouds from airborne platforms. As previously, sections will be divided according to atmospheric electrical parameter measured.

5.1 Measurements of Electric Field

Some of the first documented airborne measurements of atmospheric electrical parameters in non-thunderstorm clouds were made by Koenigsfeld (1955) who found marked changes in electric field at cloud level (cited by Chalmers 1957). In the UK, a balloon-borne electric field mill was developed by Jones et al (1959) and flown alongside the UK Met Office's Kew MK II radiosonde. A flight through a layer of Sc cloud showed a gradual increase in electric field within the cloud to a maximum of 300Vm^{-1}, and a sharp decrease above the cloud top from 300 to 50Vm^{-1}, indicating charge near the cloud top (see Figure 10). The balloon measurements of Venkiteshwaran (1958) also found large fluctuations in electric field where cloud was present, and they generally increased and decreased sharply when the balloon entered and exited clouds, suggesting the presence of charge layers on the cloud boundaries. Balloon borne measurements of electric field have also been made inside cirrus cloud over India by Srivastava et al (1972). They noted sharp increases in electric field from 10 to 42 Vm^{-1} and 1 to 30Vm^{-1} as the sonde passed through two separate cloud layers.

More recently, measurements of E_z in high altitude cloud layers have been made by Berthelier et al (2008) (also described by Cairo et al. 2010) using a double Langmuir probe technique over Niamey, Africa. Observations showed the existence of thin layers (tens of meters vertically) of ice crystals above the tropopause, presumably due to layers of cirrus clouds, where E_z was found to fluctuate compared with its background level.

The most extensive measurements of electric field within non-thunderstorm clouds have been made by Imyanitov and Chubarina (1967) who produced a review of the charge structure in St, Sc, As, and Cs clouds, by measuring E_z inside the clouds with an electric field meter mounted on an aircraft. Each cloud was divided into ten individual layers, regardless of the cloud thickness, and the same layer from each of the clouds was compared to determine the typical electric structure of each cloud type. A summary of their measurements is given in Table 3, where it is seen that the mean value of electric fields in non-thunderstorm clouds is several hundred Vm^{-1}, but field strengths up to 6.5kVm^{-1} can occur, even in non-precipitating clouds.

5.2 Measurements of Conductivity

Measurements of conductivity within clouds are rare in the literature and, self evidently, very difficult to make, as the abundance of cloud droplets contaminates the conductivity measurement, which is usually dominated by small ions. Despite the difficulties, some sensible measurements of conductivity within non-thunderstorm clouds do exist. One example is the balloon borne conductivity measurements of Jones et al (1959), shown in Figure 10, which found a decrease in conductivity on entering the base of a layer of Sc cloud (where σ_+ decreases from ≈ $1x10^{14}$ mho (10 fSm^{-1}) beneath the cloud layer, to ≈$0.2x10^{14}$ mho (2 fSm^{-1}) inside the layer), and an increase above the cloud top. A decrease in conductivity within cloud is expected as the high concentration of cloud droplets should reduce the conductivity from its clear air value, due to ion-droplet attachment. Additional in-cloud conductivity measurements have also been made by Rust and Moore (1974), who created an extensive array of equipment on a mountain ridge in New Mexico, 3225m above sea level. They measured conductivity and electric field with instruments suspended 40m below a tethered balloon, and measured bipolar conductivity by alternating the polarity of the bias voltage on their Gerdien condenser. The Gerdien condenser was fitted with a specially designed circular inlet on the entrance to the electrode to minimise point discharge and to reduce the number of rain drops entering the sensor (see Figure 15 for further details). Conductivity measurements were made inside fair weather clouds (presumably cumulus clouds), and developing thunderclouds. A flight into the base of a weakly electrified cloud showed a distinct decrease in both polarities of conductivity when the cloud base was entered. A reduction of ≈ 70% from the clear air value

beneath the cloud was observed, and a region of negative space charge in the cloud base was indicated by the greater value of negative conductivity than positive.

More recently, Gondot et al (1988) developed a conductivity sensor with a segmented electrode which measured multiple ion mobilities simultaneously. It was flown on a CESSNA aircraft, and was designed to detect screening layers in thunderstorms. On a test flight, 200m below altocumulus cloud, they detected a decrease in bipolar conductivity and bipolar ion number concentration. The decrease in σ_+ was larger than the decrease in σ_- (70% and 40% decrease respectively), corresponding to a negative space charge of -110 pCm^{-3} measured at the cloud base. During a flight through the middle of the cloud σ_+ and σ_- were found to be 95% and 92% less than their clear air values respectively. The value of the negative space charge decreased over a distance of ≈200m into the cloud, providing one of the few measurements of the depth of charge layers on the edges of cloud.

Further aircraft measurements of conductivity in clouds have been reported by Raj et al (1993), who flew an instrumented Douglas DC-3 aircraft through Sc and Cu clouds over India. Conductivity was measured from a specially designed Gerdien condenser, mounted on the underside of the aircraft, with a measurement range from 10^{-11} to 10^{-12} Sm^{-1}. Flights at a constant level of ≈300m above cloud base often found increases in conductivity inside cloud from its clear air value. Inside cloud, the conductivity was ≈10^{-12} Sm^{-1}, which is several orders of magnitude larger than that found in clear air at similar altitudes by other investigators. However, it is not clear whether the large values of conductivity within the cloud are real measurements, or instrumental effects. There is no mention of the effect of aircraft charge, which may have had substantial influence on the conductivity measurements by attracting ions of opposite polarity to the charge on the aircraft, and no evidence is provided to suggest that the effect of impacts with cloud droplets on the central electrode did not occur, contributing to the measurement current.

Attempts to measure conductivity inside ice cloud have also been made, however this is even more difficult than measuring conductivity inside liquid water cloud, as shown by Kraakevik (1958), whose aircraft based conductivity instrument was taken off-scale in the negative direction inside a cirrus cloud. He interpreted this as negative charge flowing to the central electrode, most likely due to tribo-electric charging of the central electrode by ice crystals. Venkiteshwaran et al (1962) also found anomalous behaviour of their balloon borne conductivity apparatus inside cirrus clouds. They found that generally, on entering the cloud region, there was an average increase in the electric field of ≈ +180Vm^{-1}, and an increase in voltage on the central electrode of the conductivity apparatus. Values of positive conductivity inside cirrus clouds showed an increase of up to 70% of its value beneath such clouds. The most likely explanation for the conductivity increase is the presence of highly positively charged ice crystals inside the cirrus cloud that were drawn into the conductivity sensor, suggesting it was not a true measurement of conductivity.

5.3 Measurements of Space Charge

The electric field measurements of Imyanitov and Chubarina (1967) almost certainly provide the most extensive dataset of space charge in non-thunderstorm clouds, via the indirect method, which calculates ρ from the rate of change of E_z (from equation (6)). In their investigation of stratus clouds they found that even though there was a large amount of variation between the electrical structure of individual stratus clouds, they could generally be separated into four different categories. From a total of 70 soundings, 28 stratus clouds (41%) contained positive charge in their upper parts and negative charge in the lower parts (referred to as positively polarised clouds). The mean space charge density was calculated to be 7.3 pC m^{-3} in the upper part, and -5.3 pC m^{-3} in the lower part. In 7 flights (≈10%) they found a reversal of charge polarity, with negative charge in the upper regions, and positive charge in the lower regions. Clouds that were positively charged at all levels

were discovered in 16 flights (27%), and clouds that were entirely negatively charged were measured on 6 flights. These results show that the dominant polarity structure in stratus clouds, with positive charge towards the top of the cloud and negative charge near the bottom, agrees with that predicted by the theory of conduction current flow through clouds (e.g. MacGorman and Rust 1998 p43; Tinsley 2000). A summary of space charge measurements in different types of non-thunderstorm clouds measured by Imyanitov and Chubarina (1967) is given in Table 3, where it is seen that the maximum magnitude of space charge of ρ = 1236 pCm^{-3} was found to occur in As clouds.

Direct measurements of space charge in non-thunderstorm clouds were made by Barklie et al (1958), who installed an Obolensky type space charge apparatus in the nose of an instrumented research aircraft. During penetrations into a Sc cloud over Greenland, the apparatus frequently sampled negative charge up to 1 nC m^{-3} whenever the cloud top was entered. Flights through fair weather cumulus cloud over the English channel found that the net space charge within the cloud was <16 pC m^{-3}. On subsequent flights, a different apparatus for the measurement of space charge was installed on the underside of the aircraft. This cylindrical impactor probe was flown through 25 fair weather cumulus clouds, which were typically quite shallow, with bases ≈ 0.75km and cloud tops ≈1km. Positive charge was found during each cloud penetration, with the average space charge ρ=5nC m^{-3}. The authors note that there was also some evidence that the currents measured by the sensor were often greater in the cloud top than near cloud base.

More recently, Harrison (2001) developed a balloon borne electrometer which flew alongside a Vaisala RS80 meteorological radiosonde. The sensor consisted of two electrodes, separated by a vertical distance of 7.5cm with the voltage on both electrodes measured by a sensitive electrometer circuit. On a preliminary test flight the sensor detected a distinct layer of charge at the top of the boundary layer. Further development of this sensor was detailed in Nicoll and Harrison (2009), in which the double electrode configuration was replaced by a single spherical electrode, named the *Cloud Edge Charge Detector (CECD)*. Voltage changes in the electrode arose from displacement currents generated by changes in electric field and impaction events with regions of charged droplets. The apparatus was also designed to operate with the updated Vaisala RS92 radisosonde, via a specially designed data acquisition system which allowed the extra sensor data to be sent over the radio link synchronous with the meteorological data. ρ was measured at 1Hz, providing a vertical resolution of 4m (for a typical 4ms^{-1} ascent rate of the balloon). The CECD was flown through a small number of stratocumulus clouds in which charge was frequently measured near the upper and lower cloud boundaries. Nicoll and Harrison (2010) described one particular flight of this sensor in which a distinct layer of charge, of maximum ρ = 35 pC m^{-3}, approximately 90m deep was measured at cloud base (depicted in Figure 11 (c)). The charge was only present in the region where the cloud droplet number concentration (shown in Figure 11 (a)) was changing (the same region in which the conductivity was changing – see equation (7)), and the magnitude of the measured charge agreed well with that predicted by theory.

5.4 Measurements of Droplet Charge

Knowledge of the typical charge carried by cloud droplets in non thunderstorm clouds is important to assess the effect of charge on cloud microphysical processes. Recent theoretical work has shown that even small charges (< 20e) present on cloud droplets can influence the collection behaviour of droplets (Khain et al. 2004), their interactions with ice forming nuclei (Tinsley et al. 2000), and droplet formation (Harrison and Ambaum 2008). However, very few measurements of charges on individual cloud droplets have been made above the surface. Measurement of cloud droplet charge is difficult due to the small signals involved, thus a highly sensitive electrometer and good insulation are required. Due to the ability to make long term measurements, most investigations of cloud droplet charge have been made from mountain observatories. There is concern, however, whether

observations in such locations are representative of the electrical environment of the cloud well above the surface, particularly in the case of the lower cloud boundary which can be perturbed by e.g. electrode layers at the surface and convection currents, among other effects (e.g. Beard et al 2004).

Some of the first apparatus for measuring charge on cloud droplets above the Earth's surface was developed by Gunn (1952), who designed a centrifuge type instrument which separated the space charge associated with cloud droplets from that due to small ions. Droplets entered the centrifuge through an inlet, and due to the centrifugal action, the largest droplets ($d>10\mu m$) were thrown to the walls of the centrifuge, and the resulting current measured. The smaller particles and droplets ($d<0.01\mu m$) were passed through an ion filter, consisting of a series of alternately charged parallel plate capacitors. Depending on the polarity of the ions, they would be attracted to one or the other of the charged plates, and the charge was inferred from the voltage discharge of the system with time. The instrumentation was developed for use in the nose of a B-25 bomber, and subsequently installed at the mountain-top observatories of Mt Weather (530m) and Mt Mitchell (2000m) in the US. Preliminary measurements in a B-25 bomber aircraft (Gunn 1952) through the middle of several fair weather cumulus clouds showed that the mean charge carried by droplets greater in diameter than $10\mu m$ was approximately 32e per droplet. Gunn (1952) also noted that when the aircraft flew below the apparent lower limit of clouds, appreciable currents were still measured by the apparatus, indicating the presence of charge below the cloud, possibly from evaporating cloud droplets.

Measurements of the charge on small droplets in convective clouds have also been made over Russia by Petrov (1961). Droplet charge measurements were made from an aircraft platform with an apparatus that measured the angle of deviation of droplets in a perpendicular electric field. Droplet sizes could also be determined by photographing the droplets (reported in Shishkin 1965). Petrov found that in 25 out of 30 cases, the lower part of "powerful cumuli clouds" were negatively charged. In the cloud interior, bipolar charge droplets were found, but occasionally regions of unipolar charge occurred, which had diameters similar to the size of the convection currents. Petrov found the mean charge on $2\mu m$ radius droplets in clouds was $\approx$25e, and on $10\mu m$ droplets $\approx$220e.

Selvam et al (1978) also measured cloud droplet charge from an instrumented aircraft, using a double induction ring apparatus. Only measurements from the lower ring were taken, to avoid the effects of droplet splashing on the upper ring. Flights were made through Cu clouds, with an average base of 0.6km, and top 1.6km, over maritime and urban locations around India. Cloud penetrations were made at constant level $\approx$300m above cloud base, with positive droplet charges being found in the bases of maritime clouds (average max droplet charge 38e from 8 flights), and negative charges in the bases of clouds over urban locations (average min droplet charge -8e from 3 flights).

The most recent measurements of droplet charge in non-thunderstorm clouds are by Beard et al (2004) who made aircraft measurements in layer clouds over Lake Michigan. During an ascent through a 600m deep layer of Sc cloud, maximum droplet charges of -54e to -83e were measured towards the middle of cloud, in regions of strong updrafts. It was suggested that the presence of the negatively charged droplets originated from the base of the cloud, which were transported upwards in the updrafts. In contrast, a descent through a layer of 250m thick layer of altostratus found positive currents near the top of the cloud, with droplet charges of between 83e and 95e in regions of downdrafts. Upon further penetration into the cloud, the positive currents weakened, giving rise to negative currents and droplet charges of -40e for $12\mu m$ diameter droplets near the base of the cloud.

5.5 Summary of Measurements in Non-Thunderstorm Clouds

Although non-thunderstorm clouds are generally hundreds of times less active than thunderstorms, they cover a horizontal area several hundred times more than thunderstorms, covering up to half of the Earth's surface at any one time (Klein and Hartmann 1993). Despite the importance of non-thunderstorm clouds to the radiative budget of the atmosphere, very few electrical measurements have been made inside these clouds above the surface. From existing measurements, it is clear that the electric field increases from its clear air value inside clouds, the strength of the field being determined by the cloud type, height, temperature and vertical depth, as well as precipitation characteristics (e.g. Imyanitov and Chubarina 1967). Inside non-thunderstorm clouds the conductivity typically decreases inside the cloud from its clear air value, causing an accumulation of space charge at the lower and upper cloud edges. Measurements have shown that the depth of the space charge region in stratus clouds is similar to the vertical distance over which the conductivity changes, in agreement with theory (Nicoll and Harrison 2010).

6. Airborne Measurements in Thunderstorm Clouds

Atmospheric electrical measurements inside thunderstorms are essential to understand the processes that give rise to thunderstorm electrification, however the turbulent conditions inside these clouds, as well as precipitation and extremely high electric fields make it very difficult to obtain accurate measurements. Despite the difficulties, many measurements of atmospheric electrical parameters have been made inside thunderstorms, which will be reviewed in this section, due to the relevance of the techniques to the non-thunderstorm cases. Although the measurements will be described, it is not within the scope of this review to give a detailed explanation of the electrical characteristics and charge generation mechanisms in thunderstorms. For an overview of thunderstorm properties, see e.g. Krehbiel (1986); MacGorman and Rust (1998); and Stolzenberg and Marshall (2008), and for charge generation mechanisms see e.g Saunders (1993), Williams (1985) or Yair (2008). As previously, sections are divided according to atmospheric electrical parameter measured.

6.1 Measurements of Electric Field

As in other atmospheric situations, the electric field is the most commonly measured electrical parameter inside thunderstorms, and has been measured most frequently from balloons, but also from instrumented aircraft and rockets. Many measurements of electric field during different stages of thunderstorm electrification have been made, a detailed list of which is given in Table 4. Unlike stratiform clouds, which are generally regarded as having quasi-static behaviour, thunderstorms evolve and change almost constantly, thus electric field measurements made during different stages of the life cycle of a thunderstorm vary widely. As such this section will be divided according to measurements made during different stages in the life cycle of a thunderstorm. This approach illustrates how the electrical characteristics of a thunderstorm change with time from initial electrification to the decay stage. A distinction will also be made between isolated thunderstorms and Mesoscale Convective Systems (MCS), as the thermodynamic characteristics, kinematic structure and microphysical properties of these convective clouds can be very different. Most observations of space charge density in thunderstorms have been made using the indirect method, by deriving the vertical rate of change of electric field. Since it is only the electric field that is measured, some of the derived space charge values will be reported here, to avoid repetition of material in a later section.

6.1.1 Initial Electrification

Cumulonimbus clouds develop when continuous uplift of cumulus clouds occurs in an unstable atmosphere. In this initial stage, the cloud circulation pattern is dominated by updrafts, and, as the

cloud grows upwards, the temperature decreases, leading to the formation of ice and graupel particles. During the early days of thunderstorm research, investigators set out to answer the question of how a cumulonimbus cloud becomes electrified – their results have proved essential to our present day understanding of cloud electrification mechanisms.

Some of the first electric field measurements made during the developing stage of thunderstorm clouds were those made as part of the Air Force Cambridge Research Laboratory's long running measurement program between the 1950s and 1970s. Using a B-17 aircraft instrumented with an induction type electric field meter, Fitzgerald and Byers (1958) found in clouds where no ice was present, that the magnitude of electric fields ranged from 100-1000 Vm^{-1}, and that regions of maximum updrafts and liquid water content contained the most charge. Fitzgerald and Byers (1958) also reported that in clouds containing solid precipitation particles (i.e. ice, groupel, hail), the magnitude of the horizontal component of the electric field was 10 to 100 times larger than the typical fields measured in liquid water clouds, suggesting a charge generation mechanism linked to the presence of ice. This finding is supported by the measurements of Moore et al (1958) and Vonnegut et al (1959) at Mt Withington, who measured electric fields within several thunderstorms from a tethered balloon system. Their results indicate that thunderstorm electrification is linked to the vertical development, and thus temperature of the cloud, which is generally supported by the results of most investigations of thunderstorm electrification.

A novel method of investigating initial thunderstorm electrification was implemented by Dye et al (1986), who used an instrumented glider known as the "Explorer". The glider was frequently used to measure the electric field in thunderstorm updrafts using several electric field mills mounted on the aircraft. Measurements of the initial electrification inside a small thunderstorm in Montana demonstrate the short timescales during which thunderstorm electrification can occur. Initially the electric field within the cloud was <100 Vm^{-1}, which increased to 800 Vm^{-1} within 4 minutes and only once the graupel particle size was above 5mm (Dye et al. 1986). 5 minutes after this, the electric field had increased by an order of magnitude to 8000 Vm^{-1}. A summary of electric fields measured within 20 developing thunderstorms is given in Dye et al (1989), who found that the height of cloud tops at initial electrification ranged from 8-12km, and at the time of the first lightning flash they were >9.5km. After the electric field had reached >1000Vm^{-1}, the time interval to the first lightning flash was as brief as 1 minute. Measurements also showed that precipitation had to be present for tens of minutes before the electric field exceeded 200Vm^{-1} (Dye et al 1989), again suggesting an electrification mechanism linked to precipitation.

Merceret et al (2008) describe aircraft measurements of electric field in developing thunderstorms over Kennedy Space Centre, Florida, as part of a NASA campaign to investigate lightning risk to space launch vehicles (also reported in Christian et al (1993) and Merceret and Christian (2000)). More than 80 developing cumuli clouds were sampled using an instrumented Learjet 28/29 aircraft. They observed that the vast majority of clouds with tops between 0 and -10 °C had fields <1 kVm^{-1}, and the electric field depended strongly on cloud top height. Electric fields greater than 3-5k Vm^{-1} did not develop in the clouds until the cloud top had grown higher than the -10 °C level (≈ 6.4km above sea level) and lightning did not occur until the tops were higher than the -20 °C level.

6.1.2 Mature Stage

The mature stage of thunderstorm is the most intense phase, and is generally characterised by the appearance of a downdraft. Strong updrafts and downdrafts are usually present in the middle of the cloud, creating severe turbulence, and precipitation is commonly present. Most measurements of electric field within thunderstorms have been made during the mature stage of thunderstorm electrification, as it is the most electrically active phase. Early measurements were made by Simpson and Scrase (1937) and Simpson and Robinson (1941) who launched instrumented balloons from Kew

Observatory near London. Balloons were equipped with an alti-electrograph to record corona caused by the vertical component of the electric field. Data was recorded on a clock driven disk of aluminium, which contained a chemically treated paper and was used to infer the polarity of the electric field. They found that more point discharge resulted in a wider trace on the paper, which could be used to give a crude estimate of the magnitude of the electric field, but only up to 10kVm^{-1} (see section 6 in McGorman and Rust (1998) for a detailed description). Their measurements indicated that the main charges in a thunderstorm typically formed a tripole, with a region of positive charge at cloud base, negative charge above this, and positive charge in the top of storm. This basic tripolar model of a thunderstorm was generally accepted by the atmospheric electrical community for many years, however, more recent measurements suggest that this is an over simplified model and that many more charge layers typically exist in thunderstorms e.g (Rust and Marshall 1996).

Since the early electric field measurements of Simpson and Scrase (1937) a large number of electric field measurements have been made in thunderstorms, from various platforms. For instance, Gunn (1947) describes several flights made through thunderstorms from a B25 bomber. The aircraft was instrumented with two electric field mills, one on the underside of the aircraft, the other on top of the fuselage. During one flight the aircraft was struck by lightning – which left a considerable burn mark where it entered the aircraft on the right wing tip and exited through the nose. The electric field just before the lightning flash was 340 kVm^{-1}, and the average electric field over a horizontal distance of 13 km was 70 kVm^{-1}. Gunn remarked that on one flight, the maximum electric fields encountered were near the freezing level, and decreased towards the ground. In addition to aircraft measurements, dropsonde techniques have also been used to probe the internal structure of thunderstorms, such as by Evans (1969), who parachuted 32 rotating electric field mills into thunderstorms from a manned aircraft. Evans (1969) obtained 16 vertical profiles of electric field through convective clouds and thunderstorms around Tuscon, Arizona. The maximum value of electric field measured was 39 kVm^{-1} at an altitude of ≈8.5 km.

Rockets have also been used to measure electric fields within thunderstorms. The instrument described by Winn et al (1974), launched from Langmuir Laboratory, New Mexico, mostly measured the horizontal component of the electric field, which is likely to be smaller than the vertical component. The distribution of the maximum measured values of electric field from several flights was found to approximate a log normal distribution, with median value 43 kVm^{-1}. It was also found that maximum electric field values above 100 kVm^{-1} were only measured on 6 occasions out of 61, suggesting that very high values of electric field exist in thunderstorms, but only occasionally.

During the mid 1970s, the Langmuir research group migrated from a rocket platform to balloon based electric field measurements. The electric field sensor, commonly referred to as the *Electric Field Meter (EFM)*, initially consisted of two horizontally rotating aluminium spherical electrodes of 15cm diameter (Winn and Byerley 1975; Winn et al 1978), a schematic of which is shown in Figure 12(a). The voltage on each electrode was measured by a circuit located inside one of the spheres, which also acted as the radio antenna. The spherical design of the instrument minimised the risk of corona discharge in regions of high electric field. Although the initial instrument measured only the horizontal component of the electric field, subsequent variations could also measure the vertical component. A detailed description of the electric field meter and its operation is given by Stolzenberg (1998b) and MacGorman and Rust (1998) (Ch 6). The EFM has been flown extensively by a number of investigators, detailed in Table 4.

One of the first flights of the EFM is described by Winn et al (1978), who give a detailed account of the balloon trajectory through a thunderstorm over Langmuir Laboratory, New Mexico. The storm consisted of two cloud layers, with clear air in between. An abrupt decrease in electric field was

detected when the balloon exited the lower cloud layer and entered the clear air, indicating evidence of a screening layer. Screening layers are formed due to ion-droplet attachment, and occur when ions which have the same polarity as the charge within the cloud are repelled, whilst those having the opposite polarity are attracted to the cloud edges. The presence of screening layers is thought to reduce the ambient electric field outside the cloud (measurements of which are described in section 6.1.3).

A balloon borne electric field sensor was also developed by Christian (1976), which is further described in Christian and Few (1977) and Weber et al (1982). The sensor, known as the *Balloon Electric Field Sensor (BEFS)*, consisted of a spherical super-pressure balloon with a conductive coating on the outside – shown in Figure 12(b). The metal surface of the balloon was divided into sections, electrically separated from each other, which acted as the sensing electrodes, allowing determination of both horizontal and vertical components of the electric field. A change in orientation of the balloon with respect to the external electric field caused a redistribution of induced surface charge on the balloon, which was measured with circuitry housed in the interior of the balloon.

A different technique to electric field meters was implemented by Byrne et al (1983) using a corona probe (see section 3.1.1). This instrument measures the corona-point discharge current induced through a conducting wire by the electric field, and is described by Weber and Few (1978), and Weber et al (1983). Flights through 4 thunderstorms showed a bipolar charge structure with a lower negative charge region, and upper positive charge region. The negative charge region was consistently located between 0 and -10°C, with a vertical depth of ≈1km, and average charge densities from -0.7 to -1.8 nCm^{-3}. The positive charge region was ≈1.5 km deep with charge densities ranging from 0.5 to 1.7 nCm^{-3}.

In contrast to the bipolar charge structure measured by Byrne et al (1983), Marshall and Rust (1991) found that from 12 profiles through thunderstorms there were typically between 4 and 10 distinct charge layers, of vertical depth 130m to 2100m, with charges ranging from 0.2 to 13 nCm^{-3}. The largest value of electric field measured was 146kVm^{-1}. Measurements of electric field were made from a balloon platform, using the EFM. A further 11 vertical profiles of electric field by Marshall et al (1995a) also found up to 9 individual charge layers within thunderstorms. The electrical charge structure was different between updraft and downdraft regions, causing them to classify soundings according to the ascent rate of the balloon. This approach was also adopted by Stolzenberg et al (1998a), (1998b) (1998c) where soundings made in convective regions where the vertical wind speed > 1 ms^{-1} were “updraft” soundings, whilst those made in weaker or downward vertical wind speeds were “non-updraft” soundings. Stolzenberg et al (1998c) collated results from nearly 50 balloon flights through isolated thunderstorms and MCSs. The two types of convective cloud were found to have a common basic electrical structure, but differences were found between the heights and temperatures at which the charge layers occurred. From these measurements, Stolzenberg et al (1998c) developed a conceptual model, in which four distinct charge regions were present in updrafts (consisting of a weak lower positive charge region, main negative and upper positive charge regions (often referred to as the main dipole), and a negatively charged screening layer near the cloud top). This is similar to the early tripolar model, but with an additional negatively charged screening layer at the cloud top. Outside updrafts, there were typically at least six charge regions (again alternating in polarity, with positive charge at the base and negative charge at cloud top). A representative sounding of the typical electric field profile found inside updraft regions is shown in Figure 13(a), and outside updrafts in Figure 13(b), from Stolzenberg et al (2002). It is seen that the profile inside the updraft region is simpler and has fewer charged regions than outside the updraft, thus it is important to determine the location of the measurements in respect to the thermodynamical structure of the thunderstorm.

Recent evidence has suggested that "inverted" charge structures can also exist within thunderstorms. Inverted storms contain opposite polarity charged regions to the normal tripole i.e. the main charge region in the interior of the cloud is positively charged, and is surrounded by upper and lower negative charge regions. Such inverted storms were detected several times during the Severe Thunderstorm Electrification and Precipitation Study field program in 2000, and are described fully in Rust et al 2005; MacGorman et al 2005; Wiens et al 2005 and Tessendorf et al 2007. Large numbers of positive cloud to ground lightning strikes have been observed in these inverted polarity storms, and it was found that positive cloud to ground flashes did not occur without the presence of the lower negative charge region (Weins et al 2005). This gives credence to the hypothesis that the lower negative charge region could be important in producing positive cloud to ground lightning flashes (e.g. Williams 2001).

6.1.3 Anvils

The anvil of a cumulonimbus (Cb) cloud is the flat topped, uppermost section of the cloud, which is formed by advection of ice crystals from the outflow from the top of a mature Cb cloud. Anvils can extend over a much greater horizontal distance than the main convective center of the storm, covering up to hundreds of km, and can last several hours. Measurements of electric field inside the anvils of thunderstorms have been made by Marshal et al (1989); Byrne et al (1989); Stolzenberg et al (2004); Dye and Willet (2007); Dye et al (2007) and Merceret et al (2008) using balloon and aircraft platforms. Balloon measurements by Marshall et al (1989) in New Mexico and Oklahoma using an electric field meter (EFM) found a rapid change in electric field at the lower boundary of the anvil cloud, suggesting a layer of charge present at the cloud edge. The change in electric field was -81kVm^{-1} over a vertical distance of 1.1km, and the derived space charge ρ = -0.7nCm^{-3}. These measurements support the idea of screening layers at the edges of anvil clouds predicted by Grenet (1947) and Vonnegut (1953) which form as a result of droplet capture of ions drifting in the ambient electric field. Marshal et al (1989) observed a simple charge structure within the anvil, with positive charge in the anvil interior and negative charge at the upper and lower edges, with peak electric fields of -72kVm^{-1} and -94kVm^{-1} in two different thunderstorm anvils. This simple vertical charge structure is often observed in thunderstorm anvils, demonstrating that ion attachment can be a significant charging mechanism in such layer clouds.

Information about the horizontal distribution of charge inside a thunderstorm anvil was provided by the corona sonde measurements of Byrne et al (1989), who launched two instrumented balloons into the same supercell thunderstorm in Oklahoma in 1983. Electric field profiles from the two balloon flights were similar, despite a horizontal separation distance of 30-35km, suggesting that charge regions within the anvil extended several tens of km. More recently Stolzenberg et al (2004) launched three electric field meter instrumented balloons through the anvil of a New Mexico thunderstorm during a period of 75 minutes (reported in Stolzenberg and Marshall (2008)). Soundings were made at 25 minute intervals after the last lightning flash was observed. By the time of the third sounding, 75 minutes after the last lightning flash, no enhanced electric field was observed within the anvil, giving an estimate of the time duration required for the charge within an anvil to dissipate to fair weather values.

Highly electrified anvil clouds present a hazard to aircraft and spacecraft, due to their large horizontal extent, and the threat of triggered lightning. NASA conducted two airborne campaigns over Kennedy Space Centre, Florida – named ABFM-I in the early 1990s and ABFM-II from 2000 to 2001 to measure electric fields in and around thunderstorms to asses the risk to space launches. A series of papers by Merceret et al (2008), Dye and Willet (2007), and Dye et al (2007) describe the results of these findings in respect to anvils clouds. During the ABFM-II campaign, a Citation Jet II aircraft was instrumented with 6 specially designed electric field mills, with a measurement range

from 1Vm^{-1} to 150 kVm^{-1} (described in Bateman et al (2007)), as well as five separate instruments for measuring cloud microphysical properties. They concluded that even though electric fields several km inside anvils clouds were tens of kVm^{-1}, electric fields outside anvil clouds were small, generally <1kVm^{-1}.

6.1.4 Above Storm Tops

The commonly observed presence of screening layers at the upper boundaries of thunderstorms suggests that electric fields above storms should be smaller than those within the storms. Observations of electric field above thunderstorms began in the late 1940s with the aircraft observations of Gish and Wait (1950) who flew a B29 bomber, instrumented with two electric field mills (one mounted on the upper surface of the aircraft, and the other on the lower surface) over 21 thunderstorms in the central United States. The largest electric fields measured were ≈ 5-10 kVm^{-1}, i.e. significantly lower than those generally observed within thunderstorm clouds, but no mention of the height of the cloud tops, or the distance of the aircraft above cloud tops is given. Similar measurements were made by Stergis et al (1957b) who observed electric fields ranging from 0.15 to > 0.5 kVm^{-1} (which was instrument saturation), and Vonnegut (1966), who found that the electric field was generally close to zero, except in the region over penetrating convective tops, with peak electric fields of 0.4kVm^{-1}. The increase in electric field above the convective tops was explained by penetration of the convective tops through the screening layer, exposing the cloud's internal charge.

Substantial fluctuations in electric field above thunderstorm tops have been observed on the instrumented U-2 aircraft flights of Blakeslee et al (1989), and balloon flight of Marshall et al (1995a). These fluctuations have been attributed to lightning flashes in the storm below, which cause abrupt increases in the electric field of up to 10kVm^{-1}, followed by an exponential decay to the background level. An example of this is shown in Figure 14 from Marshall et al (1995a). Above the storm top (≈13km), the magnitude of the electric field decreases from > 10kVm^{-1} to <1kVm^{-1}, but at 13.6km, transiently increases to 4kVm^{-1} due to a lightning flash. The exponential decay to background levels after this increase was observed to occur during a timescale of ≈50 seconds, consistent with the relaxation time in ambient air at those altitudes. Transients in electric field above thunderstorms due to lightning discharges have also been observed on a large number of flights by Mach et al (2009). Their study contains the most extensive set of measurements of electrical properties above thunderstorms, taken from 850 flights over electrified clouds during a ten year period. During this study, two aircraft – one manned (NASA high-altitude ER-2), the other unmanned (Altus-II), were instrumented with up to 8 electric field mills (Bateman et al. 2007). The maximum electric fields observed above thunderstorms ranged from -1.0kVm^{-1} to 16 kVm^{-1}, with a mean value of 0.9kVm^{-1}.

A relatively recent area of atmospheric electrical research is measurement of transient luminous events (TLEs), which include sprites, jets, elves, halos and trolls. Sprites are perhaps the most intensively studied of these phenomenon, and are observed to occur in the mesosphere and ionosphere, at about 40-95km, above active thunderstorms (Sentman and Wescott, 1993). Observations show that sprites are often produced in association with positive cloud to ground lightning strokes, typically within the stratiform region of Mesoscale Convective Systems (e.g. Hu et al 2002, Lyons et al 2003). Much uncertainty exists about the generation mechanism of sprites, with several theories in contention, however most theories require the existence of large electric field transients in the mesosphere and ionosphere for sprite formation, hence measurement of electric fields at these high altitudes is a motivation for current research. Several large campaigns have attempted to measure electric fields above TLE producing thunderstorms including campaigns in 1999 (Bering et al. 2004a; 2004b), 2002 (Thomas et al. 2009; Holzworth et al 2005) and 2006 (Sao Sabbas et al. 2010). Electric field instrumentation typically comprises three orthogonal double Langmuir probes to measure ac and dc vector electric fields (basic description is given in section

3.1.1), flown on a balloon platform (see e.g. Bering et al 2002 and Thomas et al 2004 for a description of the instrumentation). Holzworth et al (2005) report the measurement of an electric field change of 140Vm^{-1} at an altitude of 34km, which originated from a two stroke lightning flash, 34km from the balloon. The electric field change recorded was an order of magnitude larger than previously measured values at such altitudes, suggesting that the sufficiently large electric field changes required for sprite formation may occur in the atmosphere, however a major challenge remains in the detection of such field changes over sprite-producing thunderstorms at sprite altitude.

6.1.5 Decay Stage

The dissipating/decay stage of a thunderstorm is generally defined as when the updrafts weaken, cutting off the energy source of the storm. Despite several surface measurements made during the decaying stage of thunderstorms (from which a phenomenon known as the End Of Storm Oscillation (EOSO) period has been observed to occur), very few measurements have been made of the electrical properties aloft. Of these, the balloon ascents of electric field by Marshall and Linn (1992) using the EFM, showed the existence of substantial electric fields even twenty minutes after the last lightning flash. Ascents through two decaying thunderstorms over Langmuir Laboratory, New Mexico, measured maximum electric fields of 35 and 71kVm^{-1}. In both storms the charge structure was simpler than is generally observed within thunderstorms during the mature stage – with a main negative charge centre in the middle of the cloud, surrounded by two positively charge screening layers at the upper and lower cloud boundaries. The upper screening layer was the most weakly charged region in both storms, with $\rho \approx 0.1 nC\ m^{-3}$. More recent flights were made by Marshall et al (2009) who launched multiple balloons through a dying storm, and observed substantial changes in the charge structure of the storm during a 50 minute period. Substantial regions of charge were also observed below the cloud base (a phenomena also reported by Marshall and Linn (1992), and supported by surface observations of electric field beneath decaying storms), which were linked to precipitation falling from the cloud.

6.1.6 Mesoscale Convective Systems

A Mesoscale Convective System (MCS) is an extensive storm system, consisting of a group of long lived thunderstorms which interact with each other, and is characterised by a convective region with vigorous updrafts and a precipitating stratiform region in which only weak vertical motions occur (Houze 2004). The electrical structure and charge generation mechanisms within these two regions can be quite different, as such measurements within them will be described separately in the following sections.

The Stratiform Precipitation Region (SPR) of an MCS generally occurs near the rear of the storm, and has typical dimensions of 10 000 km^2 (Houze et al. 1990). The electrical structure of SPRs have been investigated by Chauzy et al (1985); Schuur et al (1991); Hunter et al (1992); Marshal and Rust (1993); Stolzenberg et al (1994); Shepherd et al (1996) and Mo et al (2003), all using the balloon borne Electric Field Meter developed by Winn et al (1978) and described in section 6.1.2. From the analysis of many of these balloon soundings, Marshall and Rust (1993) found that vertical electric field structures fell into two distinct categories - Type A and Type B, and that comparison of electric field soundings from several different storms in the same type showed remarkable similarities between charge regions, whose spacing and depth was almost identical between different storms. It was also found that there is often a distinct layer of charge around the 0°C isotherm in the SPR region. This charge layer is present in both Type A and B soundings, and is often the region of highest electric field magnitude, discussed further by Shepherd et al (1996).

The most extensive research into the electrical structure in the convective region of an MCS has been accomplished by Stolzenberg et al (1998a), who took all 7 existing electric field profiles in

convective regions of MCS, notably those of Byrne et al (1987); Marshall and Rust (1991); Marshall et al (1995a), and compared them with 9 new profiles, to determine whether a typical electric field structure exists in these regions. Stolzenberg et al (1998a) found that there was a typical electrical structure in convective regions of MCSs, which just as for isolated thunderstorms, differed between updraft and non-updraft regions. The electrical structure was similar, with the same number of charge layers to those found in isolated storms, but the height at which the charge layers occurred was generally higher than in isolated storms, linking the charge structure to cloud top height.

6.2 Measurements of Conductivity

6.2.1 Conductivity inside thunderstorms

The conductivity inside a thunderstorm is one of the least well understood electrical properties of thunderstorms. Not only is conductivity inside a storm difficult to measure, theoretical calculations vary widely due to the variety of assumptions about cloud microphysics that have been made. An extensive range of possible values for conductivity inside thunderstorms has been calculated in the scientific literature, ranging from Phillips (1967) value of <0.05 to 0.1 of its clear air value, (also supported by the calculations of Griffiths et al (1974)), to Freier's value of 20 times greater than the conductivity of the surrounding air (Freier 1962). An additional complexity was stated by Vonnegut (1963) who noted that conductivity may even be an invalid concept within a thunderstorm. This was further touched upon by Kamra (1979) who pointed out that although the small ion conductivity inside a thunderstorm may be low, the presence of charged cloud droplets and precipitation particles may mean that the total conductivity due to all charge carriers is high.

The simplest way to resolve the controversy surrounding the conductivity inside a thunderstorm is to measure it. However, despite more than 50 years of thunderstorm research, only a handful of measurements of conductivity inside storms exist, and apparently none within the most electrically active regions of storms. Scott and Evans (1969) used a dropsonde technique to measure the conductivity inside three electrically active clouds using a modified Gerdien condenser. Several precautions were taken to reduce the effect of the hostile environment on the conductivity measurement, including shielding the central electrode with wire mesh to guard against possible displacement current effects from large changes in electric field. A secondary precaution was to remove the bias voltage between the electrodes at defined intervals during the flight and measure the central electrode current. This yielded a point measurement of charged particles impacting the central electrode, which is a common problem when measuring conductivity inside clouds, and voids the small ion conductivity measurement. During a descent through an electrically active cloud (maximum electric field ≈-40kVm^{-1}), the positive conductivity at ≈ 6km was measured to be 3.5x10^{-14} Sm^{-1}, which the authors interpret to be a reliable measurement as it occurred immediately after a calibration period. From these limited measurements they concluded that the conductivity inside the thunderstorm measured was unlikely to be much less than the conductivity in clear air at the same altitude.

Further investigation of conductivity inside thunderstorms was made in subsequent dropsonde flights by Evans (1969), using a different instrument, which measured electric field, and also enabled the conductivity to be derived from the same measurement, but only when the electric field was not changing appreciably. The range of the conductivity measurements was thought to be 10^{-13} to 10^{-11} Sm^{-1}, with errors of 25 to 40%. A number of descents through thunderstorms were made, and conductivities of 10-100 times the clear air value at the same altitude were measured. Evans comments that generally only small sections of the conductivity profiles from each flight were valid, due to the behaviour of the electric field and its effect on the derivation of conductivity. Additional concern about the ability of the instrument to accurately measure conductivity in regions of high electric field was expressed in a comment by Vonnegut (1969), who noted that charge on the outer

surface of the instrument, as well as point discharge may be occurring , which adversely affected the measurement of conductivity.

Measurements of the conductivity in the bases of electrically active clouds were made from a tethered balloon platform by Rust and Moore (1974), described in section 5.2. A schematic representation of the specially designed conductivity apparatus is shown in Figure 15. Measurements were made within weakly electrified clouds and developing thunderstorms over Langmuir Laboratory, New Mexico. Rust and Moore (1974) reported that within all of the clouds studied, the conductivity was invariably less than that in fine-weather, clear air at the same altitude. Typically the conductivity of cloudy air was ≈ $1/6^{th}$ to $1/10^{th}$ that of the adjacent clear air. Their results showed that the mean bipolar conductivity in the lower regions of 12 clouds was $\sigma_+ = 2.1$ fSm^{-1} and $\sigma_- = 2.3$ fSm^{-1}, where electric fields were< $2kVm^{-1}$. Hence on average $\sigma_- > \sigma_+$ and the ratio of $\sigma_-/\sigma_+ > 1$ denoting the presence of negative space charge in the lower levels of the clouds. As noted by MacGorman and Rust (1998), although these results are valuable to our understanding of weakly electrically active clouds, they do not contribute much to our understanding of conductivity in highly electrified clouds.

6.2.2 Conductivity above Thunderstorms

Although very few measurements of conductivity inside thunderstorms have been made, a number of investigators have measured the conductivity above thunderstorm tops. Some of the first to do so were Gish and Wait (1950), who measured bipolar conductivity above 6 thunderstorms using two Gerdien condensers mounted under the wing of a B-29 aircraft. They found that in general, the conductivity of the air above thunderstorms was not appreciably different from its value at the same altitude at distances far from the cloud. These results are supported by the Gerdien condenser measurements of Stergis et al (1957b) and Blakeslee et al (1989) both from balloon platforms, and Bailey et al (1999) and Mach et al (2009), both from aircraft platforms. Measurements of conductivity above storms using the relaxation technique from a constant level balloon platform, however, have found contradictory results (e.g. Bering et al 1980; Holzworth et al 1986; Pinto et al 1988; Hu et al 1989; Saba et al 1999). For example Holzworth et al (1986) flew a double Langmuir-probe, measuring bipolar conductivities from super pressure balloons at altitudes of 26km over thunderstorms. They found that in seven of nine cases the total conductivity increased at some point over the storms. The reason for the discrepancies in the measurements from the relaxation probe method and Gerdien condensers is currently unknown, and measurements by Barcus et al (1986) using the relaxation probe method found no variation in conductivity above a thunderstorm, suggesting that different measurement techniques alone do not explain the discrepancies between measurements.

6.3 Current flow above thunderstorms

Wilson's GEC hypothesis is based around the assumption that thunderstorms are the main drivers of the GEC, transferring positive charge upwards into the ionosphere. Early measurements of currents above thunderstorms estimated the average total upwards current from an individual storm to be +0.5A (Gish and Wait 1950) and +1.3A (Stergis et al 1957b), using simultaneous measurements of electric field and conductivity to derive the conduction current. Similar results of positive polarity upward flowing currents were found by Blakeslee et al (1989) (+1.7A), and Thomas et al (2009) (+2.5A). Recent aircraft measurements reported by Mach et al (2010) have generated a substantial database of measurements of currents flowing above thunderstorms. The measurements provide support for the GEC hypothesis in that on 93% of 850 flights over electrified cloud systems, upward flowing currents were of positive polarity. However, interestingly, negative polarity currents were found on occasion, (7% of flights), presumably from inverted polarity thunderstorms such as those observed by Rust and MacGorman (2002) and Tessendorf et al (2007). More research into these inverted polarity storms is required to fully understand their contribution to the GEC. A summary of

the current measurements by Mach et al (2010) is given in Table 5, which also illustrates that in a small number of storms, no measurable upward current exists.

The aircraft measurements of Mach et al (2011) have also provided insight into an issue that has long perplexed atmospheric electricians - the difference in amplitude between the Carnegie curve and lightning activity. Although the phase of the diurnal variation in fair weather PG (known as the Carnegie curve - see section 2.2) matches well with the diurnal variation in lightning activity, discrepancies exist between the variation in amplitudes of the two curves (Carnegie curve varies by ≈15% whilst lightning flash rate varies by ≈35% about its mean) (e.g. Whipple and Scrase 1936). The reason for this is thought to be the contribution of electrified shower clouds (which do not produce lightning) to the GEC. Recent measurements by Mach et al (2011) have for the first time characterised the upward current flow from electrified shower clouds, which are found to produce 1/4 to $1/8^{th}$ of the current per cloud as storms with lightning. This led to an estimate that thunderstorms contribute 90%, and electrified clouds contribute 10% to current flow in the GEC. Mach et al (2011) also observed large differences between land and ocean storms, with land storms generating greater lightning rates, but smaller mean conduction currents than ocean storms. Thus most of the observed amplitude variation of the Carnegie curve can be accounted for by correctly including the differences that exist in the mean currents and flash rates between land and ocean thunderstorms.

6.4 Measurements of Space Charge

Most estimates of space charge in thunderstorm regions originate from the indirect method - by calculating the vertical gradient in electric field, as given by equation (6). Strictly it is the electric field which is measured, therefore space charge measurements using this method are described in section 6.1 which discusses measurements of electric field in thunderstorms.

To the author's knowledge, the only direct measurement of space charge within a thunderstorm are those of Scott and Evans (1969), using a Gerdien condenser with no bias voltage applied between the central and outer electrodes. On a dropsonde flight through a thunderstorm, a tripolar charge structure was measured, with a 200m deep layer of negative space charge near the cloud top, a region of positive space charge, with charge large enough to saturate the instrument, detected below this, and negative charge in the cloud base. No estimates of the magnitude of the charge, or the vertical profile of relative humidity within the cloud are given.

6.5 Measurements of Droplet Charge

The investigation of charge carried by individual precipitation particles and cloud droplets is useful to understand cloud electrification processes. It is particularly important to determine the typical magnitude and polarity of charge on individual particle and droplets, as well as how they acquire their charge, and whether they are the main contribution to the large electric fields commonly observed in thunderstorms. During the last 60 years many investigators have attempted to measure individual precipitation charge from both aircraft and balloon platforms, with some success, but the measurement of charge on individual cloud droplets, which can be several order of magnitudes smaller than precipitation particles, is still an elusive area.

Some of the first charged precipitation measurements from an airborne platform were made by Gunn (1947), using an induction sensor mounted on a B52 aircraft. This technique has also been implemented by Latham and Stow (1969), who made several flights through developing cumulus clouds over Arizona, from a Piper Aztec aircraft which was also instrumented with an electric field mill mounted on the nose of the aircraft. By combining data from a number of flights, the general distribution of particle charge with temperature was found to be negative in the upper regions of clouds, but became increasingly positive as the temperature increased towards 0°C. Unipolar charge

regions were occasionally observed, but in most regions a mixture of both positively and negatively charged particles existed, with individual particle charges occasionally being large enough to saturate the charge sensor (>300pC).

As well as measuring the charge on individual precipitation particles, it is also important to measure their size and composition (i.e. liquid water, graupel or ice) to understand particle charging mechanisms. Gaskell et al (1978) and Christian et al (1980) describe simultaneous measurements of charge and particle size made from an instrumented Schweitzer plane, mostly over Langmuir Laboratory, New Mexico. The aircraft was instrumented with 5 electric field mills, an induction type particle charge sensor, and a particle size detector which operated using a shadowgraph technique. For this, a light beam was directed perpendicular to the axis of the induction cylinder, and was detected by an array of 64 photodiodes. Interruption of the beam by a particle produced a voltage change in the photodiode output which was measured. The range of detectable particle sizes was 0.5 to 4.4mm, and particle charges of up to ±130pC could be measured, with an accuracy of ±5pC (extended to ±300 pC by Christian et al (1980)). Gaskell et al (1978) report on an aircraft flight through the base of a thunderstorm in which the sensors detected bipolar charges, but with a much larger proportion of negatively charged particles than positive. Substantial charges of -50 to -100pC were present on the particles, which were generally smaller than 1mm diameter, and extended over distances of several km or more. They also observed that many particles were smaller than the lower limit of the size sensor, emphasizing the need for more sensitive instrumentation. Similar measurements of individual particle charge and size in thunderstorms from aircraft have also been made by Vali et al (1984), Cupal et al (1989) , Weinheimer et al (1991) and Mo et al (2007).

Measurements of charge on individual precipitation particles have also been made from balloon platforms. Early investigations of the charge in the bases of thunderstorms was made by Rust and Moore (1974) using a tethered balloon over Langmuir Laboratory, New Mexico. Balloons were instrumented with electric field and conductivity sensors, as well as two different sensors to measure charge on precipitation particles. A Faraday funnel was used to measure the total charge flux from precipitation particles (whereby charged particles transfer their charge to a conducting funnel on impact), and a second instrument consisted of two induction rings with a Faraday cup beneath the rings, to detect the charge on individual precipitation particles. Measurements in the bases of developing thunderstorms demonstrated that the polarity of charge on individual precipitation particles was almost always that of the local electric field, but no clear correlation was found between the magnitude of the precipitation charge and the size of the electric field.

Free balloons have also been used to investigate charge on individual precipitation particles, most of which used an induction type device similar to the one described by Marshall and Winn (1982), and shown in Figure 16 (a). The original particle charge instrument consisted of three vertically separated induction cylinders of 3.8cm depth and 8.3cm in diameter, housed inside a spherical container (see Figure 16(b) for a vertical cross section of the instrument). The range of detectable particle charges was from -350pC to +450pC, with a minimum detectable particle charge of 10 pC. A secondary sphere was used to house the electronics and the radio transmitter to transfer the data back to ground. An updated version (Bateman et al. 1994) replaced the lowest induction cylinder with a particle size detector using a light source positioned opposite a light detector. Droplet size was determined from the amount of light blocked as a droplet passed through the beam. The particle charge device was mounted on a boom to minimise contact with particles rebounding from the surface of the balloon, and flown alongside a meteorological radiosonde and Electric Field Meter (Winn et al. 1978).

During a balloon sounding through a small thunderstorm over Langmuir Laboratory, new Mexico, on August 1st 1984, Marshall and Marsh (1993) detected individual particle charges >400 pC. The storm

consisted of four distinct charge regions, with a lower positive charged region, main negative charged region, main positive charged region and uppermost screening layer. Profiles from this flight are given in Figure 17 which shows electric field and the number of charged particles detected per minute, as well as the polarity of their charge. Within the lower positive charge region, many positively charged precipitation particles were detected, and comparison between the charge density calculated from the electric field measurements and that from the charged precipitation particles showed that the two were similar, suggesting that the charge carried by precipitation made a significant contribution to the electric field. A similar finding was made for particles in the main negatively charged region (denoted by the vertical bars in Figure 17) where Figure 17 shows that the polarity of the electric field and the observed charged particles are both negative. Above a height of 9.5km, no charged precipitation particles were found, prompting Marshall and Marsh (1993) to suggest that the $\rho \approx +0.4 nCm^{-3}$ in the main positive charge region was carried mainly by small cloud droplets below the detection threshold of the instrument. The finding that charge carried by precipitation makes a substantial contribution to the electric field, particularly in the lower regions of thunderstorms, is also supported by the observations of Marshall and Winn (1982); Marsh and Marshall (1993); Stolzenberg and Marshall (1998); and Mo et al (2007). However, it is clear that measurements of cloud droplet charge, in addition to precipitation charges are required in order to fully assess charging mechanisms in the upper regions of thunderstorms.

Although the balloon measurements of Marshall and colleagues measured individual particle charge and size, they were not able to determine the composition/state of the particles. During a period of more than 40 years Takahashi has made a substantial number of measurements of charge on individual precipitation particles from balloons, as well as their size and composition (e.g. Takahashi 1965; 1978; 1983). Takahashi (1978) describes a radiosonde package to measure the charge and phase of precipitation particles which consisted of an induction ring, with a roll of filter paper mounted beneath the ring. An optical scanner, comprising a light source and photocell was swept back and forth perpendicular to the direction of the moving filter paper, detecting a change in the light intensity when a liquid droplet impacted the filter paper. The instrument was also equipped with a microphone to detect impacts from graupel particles and large raindrops onto the filter paper. Large raindrops were detected by both the filter paper and microphone, whilst graupel particles were only detected by the microphone. The sensor was flown through several thunderstorms occurring over Ponape, Micronesia, and on one particular flight encountered a tripolar charge structure, with positive charge near the freezing level, an extensive region negative charge between the -5°C and -35°C isotherm levels, and positive charge at heights above -60°C. A more detailed representation of particle type was achieved by development of a “videosonde” (Takahashi 1990; Takahashi et a.l 1995; 1999), which was designed to measure the shape, phase, size and charge on individual precipitation particles. Precipitation particles passed through an induction cylinder, which measured their charge, and were then imaged by a video camera. A flash lamp was positioned above the camera lens, which was triggered by interruption of an infrared beam by a precipitation particle greater than 0.5mm diameter. A variety of precipitation types could be identified from the resulting images, including liquid water droplets, supercooled water droplets, graupel, hailstones, and ice crystals. The instrument detected particle charges in the range of 0.1-200 pC, and was suspended 50m below three large balloons. A variant on the videosonde has also been developed by Boussaton et al (2004), who, like Takahashi, used an inexpensive CCD video camera to directly image precipitation particles, and an induction ring to measure their charge. The size range of particles detectable with this instrument was 0.5mm to 2cm diameter, and particle charges of ±1 to ±400 pC.

6.5 Summary of Measurements in Thunderstorms

In-situ measurements of atmospheric electrical parameters inside thunderstorms have provided a wealth of data to assist our understanding of the electrification processes of thunderstorms, that is

not possible from surface measurements alone. Free balloons, have been particularly instrumental in characterizing the typical magnitudes, vertical extent and vertical structure of charge layers and electric fields. It is now known that a typical E_z structure exists within thunderstorm convection regions, but that it differs between updraft and non-updraft regions. In-situ measurements aloft have shown that magnitudes of electric fields within thunderstorms can reach up to $150Vm^{-1}$, but fields of this magnitude generally occur in a relatively small fraction of the thunderstorm cloud, and exist in regions from a few hundred meters to a few km deep vertically. Investigation of the role of precipitation charge in creation of the large electric fields within thunderstorms has also been made possible by airborne platforms, particularly balloons, and it is generally found that charges carried by precipitation particles dominate the electrical structure of the lower regions of storms (i.e. <7km), whereas cloud droplet charge is likely to dominate the upper regions.

Recent measurements by Mach et al (2010; 2011) have investigated the role of thunderstorms as generators in the GEC, finding differences in the current output between land and ocean storms, as well as contributions to upward current flow from electrified shower clouds which do not produce lightning. Mach et al. (2011) concluded that the mean total conduction current is 2.0 kA, where contributions to the GEC from land and ocean thunderstorms are 1.1 kA and 0.7 kA, respectively, and electrified shower clouds contribute 0.04 kA and 0.22 kA for land and ocean storms, respectively. Measurements such as these are essential to our understanding of the GEC and will aid in the development of future GEC models.

Despite these advances, many questions regarding the electrical nature of thunderstorms still remain. For example lightning triggering mechanisms are not well understood. Conventional electrical breakdown processes require electric fields much greater than the maximum electric fields observed in thunderstorms, therefore an alternative breakdown process is required (e.g. Roussel-Dupre et al. 2008). Runaway breakdown, which requires smaller electric fields than conventional breakdown and is stimulated by secondary electrons from cosmic rays, may provide a possible answer, but the details are not yet understood (e.g. Gurevich and Zybin, 2005). Charge transfer in lightning strokes, why some storms produce only intra-cloud lightning, generation of TLEs, and generation of inverted polarity storms are all areas which warrant further research.

7. Discussion

7.1 Differences between Measurement Platforms

Multiple measurement platforms have been used to make measurements of atmospheric electricity aloft including kites, tethered balloons, manned balloons, radiosonde-balloons, high altitude balloons, rockets, and aircraft. However, it is important to realise that the characteristics of the measurements made differ widely, as well as the problems encountered when using each platform. This section will describe some of the differences between aircraft and radiosonde-balloon platforms (which have been widely used to measure atmospheric electricity aloft), as well as their benefits and limitations.

One of the main differences between balloons and aircraft is their rate of motion. The large horizontal speeds of aircraft make them more suited to horizontal, rather than vertical, measurement profiles, and such fast speeds mean that in order to achieve high resolution measurements, the on-board instruments must be sampled at rapid rates. For example an instrument which samples at 1Hz on board an aircraft moving with horizontal speed 100 ms^{-1}, will give a horizontal resolution of 100m. Measurement of atmospheric electrical parameters with an aircraft has several additional complications above measurement of other meteorological parameters, e.g. (i) the aircraft is a conducting body which will perturb the ambient electric field,

and (ii) the aircraft body will itself become charged due to collisions with exhaust particles or cloud droplets. The problems associated with aircraft charging and the methods used to solve this issue are described further in section 7.2. Care must also be taken not to fly through the exhaust plume from the engine when making multiple passes of an area with an aircraft, as the exhaust gases may be highly charged and long lived. An additional limitation of aircraft is that measurement campaigns are expensive to fund, but they can, however, carry heavier instrumentation than balloons or rockets, and can also carry human observers. They also provide a more stable measurement platform for instrumentation than radiosonde-balloons. The development of Unmanned Aerial Vehicles (UAVS) is likely to provide an additional measurement platform for future measurements of atmospheric electricity, as they present a less expensive alternative to manned aircraft, with slower flight speeds, and the ability to probe areas where it is dangerous for manned aircraft to fly, such as thunderstorms and around volcanoes (e.g. Mach et al 2009).

Radiosonde-balloons are more suited to vertical profiling rather than aircraft as their horizontal speeds are much smaller. They can also provide better resolution measurements for the same sampling rate i.e. a sampling rate of 1Hz and vertical ascent rate of $5ms^{-1}$ gives a vertical resolution of 5m. One of the main advantages of radiosonde-balloons as a measurement platform is that they are inexpensive and thus allow many flights to be performed for the same cost as only a few aircraft flights. This can be useful as there is great variability in the atmosphere, requiring many measurements to accurately measure the typical range of electrical properties. An additional advantage is the ability of radiosonde-balloons to enter regions where it is dangerous for humans to fly, such as thunderstorms and near volcanoes. Indeed most of the research into electrification of thunderstorms in their mature stage has been made using radiosonde-balloons. There are no engines to produce separation of charges on a balloon, however the surface of the balloon is at least partially conducting and so the ambient electric field is distorted by the presence of the balloon. It is therefore desirable to have the instrumentation as far below the balloon as possible. The basic limitation of radiosonde-balloons is that they cannot be guided, and as their flight path is determined by the wind, they can land several hundreds of km from their start position in strong horizontal winds. Tethered balloons are more controllable, but are only suitable for altitudes less than ≈1km, and the tether is problematic in high electric fields and strong winds. Radiosonde balloon flights are short lived, and generally only provide one vertical profile through a region (as descent profiles rarely occur over the same horizontal region sampled during the ascent. An alternative to the relatively short lifespan of radiosonde-balloons, are high altitude balloons (e.g. Hu and Holzworth 1996; Saba et al. 1999; Bering et al. 2005; Holzworth et al. 2005). These can float at altitudes of ~30km for periods up to several months, and are particularly useful for quantifying latitudinal and longitudinal profiles, or flying over thunderstorms.

7.2 Difficulties Associated with Airborne Measurements of Atmospheric Electricity

Obtaining accurate measurements of atmospheric electricity aloft can be a challenge, due to instrumental problems as well as demanding measurement environments. Often the atmospheric electrical environment is affected by the presence of the measurement platform itself, and each different platform has its own problems and solutions. Table 6 describes some of the most common problems encountered when measuring atmospheric electrical parameters from airborne platforms, and provides suggestions on how to minimise these unwanted effects. For example, distortion of the ambient electric field around sharp points is a common occurrence, which can lead to corona discharge in large electric fields. This effect can be minimized by designing instrumentation to be spherical (such as the EFM of Winn et al (1978) and droplet charge apparatus of Marshall and Winn (1982)) as well as mounting the measurement apparatus far from any sharp points e.g. radiosonde antennae.

One of the most common problems encountered when measuring atmospheric electrical parameters from an aircraft is that of excess charge on the body of the aircraft, which perturbs the local electric field. By measuring the electric field in multiple directions, from several points on the aircraft body (often 5 or 6) it is possible to separate the component of the measured field due to aircraft charge, E_q, from that of the ambient field. To achieve this, one must consider the individual vector electric field components in the signal of each field mill. For example the total voltage output signal, *V*, in each field mill may consist of an equation of the form

$$V = aE_x + bE_y + cE_z + dE_q \quad (12),$$

where the E_x, E_y, and E_z are the vector components of the electric field, and the coefficients *a, b, c* and *d* must be found by either calibration of the aircraft, applying charge to a small model of the aircraft (only for conducting bodies e.g. Imyanitov and Chubarina 1967), or numerical modelling. By determining the coefficients and solving the matrix equation that results from each equation from each individual field mill, it is possible to calculate the individual E_x, E_y, E_z and E_q. Care must be taken when choosing the location of the electric field mills on the aircraft, to avoid proximity to sharp points such as propellers or wing tips which are prone to emission of corona ions. A common technique is to choose geometrically similar locations for placement of pairs of field mills, as this reduces the number of unwanted components of the electric field. For more detail on aircraft charging and distortion effects see Imyanitov and Chubarina 1967; Mazur et al. 1987; Jones 1990; MacGorman and Rust 1998 (Ch6); Koshak 2006 or Koshak et al. 2006.

7.3 Summary

Airborne measurements of atmospheric electricity have been made for more than 200 years, providing much data with which to understand the electrical characteristics of the atmosphere. The early measurement platforms of manned balloons have since been replaced with more manoeuvrable, safer platforms such as aircraft and free balloons, which are capable of reaching higher altitudes, and present less of a challenge to launch. During the last few hundred years, developments in technology and electronics have also reduced the physical size, weight and cost of sensors, to the point where some sensors are now suitable for flights on standard radiosondes, launched routinely by the world's meteorological services.

Airborne measurements have investigated areas that are central to the Global Electric Circuit hypothesis, for example, it has been demonstrated that the diurnal variation in ionospheric potential follows closely that of the Carnegie measurements of fair weather PG (Markson 1976), suggesting that local atmospheric electrical parameters at the surface are controlled globally. Airborne measurements have also shown that the ionospheric potential measured from two locations varies together (Muhleisen 1971), supporting the concept that the ionosphere is an equipotential. Recent measurements of the conduction current above thunderstorms find that the majority of thunderstorms produce a positive upward flowing current, which supports Wilson's hypothesis that thunderstorms provide the main contribution to charge in the ionosphere (Mach et al. 2010). The same measurements estimate that electrified shower clouds also contribute substantially (~10%) to the GEC (Mach et al. 2011).

Although the major characteristics of the Earth's electrical atmosphere are now understood, there remain some areas which warrant further research. These include:

- Measurement of charge on individual cloud droplets and conductivity in thunderstorms, in order to more fully understand thunderstorm electrification mechanisms.
- Further investigation of inverted polarity thunderstorms

- Lightning generation mechanisms (and importance of cosmic rays)
- Charge transfer in lightning strokes
- Differences between intra-cloud and cloud to ground lightning
- Investigation of Transient Luminous Events (TLEs) such as sprites and jets, as well as electric field and conductivity measurements above thunderstorms which produce these phenomena.
- Contribution of TLE's to the GEC
- Measurement of electric fields and conductivity in the mesosphere
- Effect of aerosols on thunderstorm development and flash rate
- Investigation of the response of atmospheric electric variables to solar activity, both locally and globally, and long and short term fluctuations (e.g. 11 year solar cycle and solar flares).
- Better understanding of the effect of charge on cloud microphysics; cloud responses to changes in cosmic ray ionisation, and the mechanism by which this can occur.
- Effect of charge on aerosol particle layers and their transport properties (e.g. volcanic ash, Saharan dust and aerosol layers).
- Atmospheric electricity on other planets

Measurements of atmospheric electricity aloft have enabled us to understand a wide variety of electrical phenomena, which is not fully possible from surface measurements alone. Airborne measurements remain essential to understanding the detailed nature of established and emerging atmospheric processes and their in situ nature means that there is no alternative but for them to continue in future.

Acknowledgements

This work was funded through a National Environment Research Council (NERC) studentship and contributed to by the NERC funded research project More Operational Radiosonde Sensors (MORSE) – NE/H002081/1. Thanks also to Prof. Giles Harrison for many insightful discussions and comments on the manuscript.

References

Anderson, R.V., J.C. Bailey, H. Tammet (1991) Errors in the gerdien measurement of atmospheric electric conductivity. Meteor. and Atmos. Phys. 46, 101-112.

Aplin, K.L., R.G. Harrison, M.J. Rycroft (2008) Investigating Earth's Atmospheric Electricity : a Role for Model Planetary Studies, Space. Sci. Rev., 137, 11-27.

Bailey, J.C., R.J. Blakeslee, K.T. Driscoll (1999) Evidence for the absence of conductivity variations above thunderstorms. 11th Int. Conf. Atm. Elec. NASA Conf. Publ., pp. 646-649.

Barcus, J.R., I. Iversen, P. Stauning (1986) Observations of the Electric Field in the Stratosphere Over an Arctic Storm System. J. Geophys. Res. 91, 9881-9892.

Barklie, R.H.D., W. Whitlock, G. Haberfield (1958) Observations on the reactions between small ions and (a) cloud droplets, (b) aitken nuclei. In: Recent Advances in Atmospheric Electricity. L.G. Smith (Ed.), Pergamon, New York, pp. 223-229.

Bateman, M.G., W.D. Rust, T.C. Marshall (1994) A Balloon-Borne Instrument for Measuring the Charge and Size of Precipitation Particles inside Thunderstorms. J. Atmos. and Ocean. Tech. 11, 161-169.

Bateman, M.G., W.D. Rust, B.F. Smull, et al. (1995) Precipitation charge and size measurements in the stratiform region of two mesoscale convective systems. J. Geophys. Res. 100, 16341-16356.

Bateman, M.G., T.C. Marshall, M. Stolzenburg, et al. (1999a) Precipitation charge and size measurements inside a New Mexico mountain thunderstorm. J. Geophys. Res. 104, 9643-9653.

Bateman, M.G., K.B. Eack, W.D. Rust, et al. (1999b) Electrical current along balloon rigging line inside thunderstorms. Atmospheric Research 51, 323-335.

Bateman, M.G., M.F. Stewart, S.J. Podgorny, et al. (2007) A Low-Noise, Microprocessor-Controlled, Internally Digitizing Rotating-Vane Electric Field Mill for Airborne Platforms. J. Atmos. and Ocean. Tech. 24, 1245-1255.

Bazilevskaya, G.A., I.G. Usoskin, E.O. Fluckiger, R.G. Harrison et al (2008) Cosmic ray induced ion production in the atmosphere. Space Science Reviews. 137, 149-173.

Beard, K.V., H.T. Ochs, III, C.H. Twohy (2004) Aircraft measurements of high average charges on cloud drops in layer clouds. Geophys. Res. Lett. 31, L14111.

Bering III, E.A., T.J. Rosenberg, J.R. Benbrook, et al. (1980) Electric Fields, Electron Precipitation, and VLF Radiation During a Simultaneous Magnetospheric Substorm and Atmospheric Thunderstorm. J. Geophys. Res. 85, 55-72.

Bering III, E.A., J.R. Benbrook, G.A. Garrett, A.M. Pareded et al. (2002) Sprite and Elve Electrodynamics, Advances in Space Research, 30, 11, 2585–2595.

Bering III, E.A., J.R. Benbrook, L. Bhusal, G.A. Garrett et al. (2004a) Observations of transient luminous events (TLEs) associated with negative cloud to ground (−CG) lightning strokes, Geophysical Research Letters. 31, L05104.

Bering III, E.A., L. Bhusal, J.R. Benbrook, G.A. Garrett et al. (2004b) The results from the 1999 sprites balloon campaign. Advances in Space Research 34, 1782-1791.

Bering III, E.A., R.H. Holzworth, B.D. Reddell, et al. (2005) Balloon observations of temporal and spatial fluctuations in stratospheric conductivity. Advances in Space Research 35, 1434-1449.

Berthelier, J.J, R. Graard, H. Laakso, M. Parrot (2000) ARES, atmospheric relaxation and electric field sensor, the electric field experiment on NETLANDER, Planetary and Space Science, 48, 1193-1200.

Berthelier, J.J., F. Simoes, J.P. Pommereau (2008) Observation of charged aerosol layers and distant lightning from electric field measurements onboard balloons, Geophysical Research Abstracts, 10, EGU2008-A-07063.

Blakeslee, R.J., H.J. Christian, B. Vonnegut (1989) Electrical Measurements Over Thunderstorms. J. Geophys. Res. 94, 13135-13140.

Boussaton, M.P., S. Coquillat, S. Chauzy, et al. (2004) A New Videosonde with a Particle Charge Measurement Device for In Situ Observation of Precipitation Particles. J. Atmos. and Ocean. Tech. 21, 1519-1531.

Brown J.G. (1930) The relation of space charge and potential gradient to the diurnal system of convection in the lower atmosphere. Terr. Magn. Atmos. Elec., 35, 1-15.

Brown K.A., P.R. Krehbiel, C.B. Moore, G.N. Sargent (1971) Electrical screening layers around charged clouds, J. Geophys. Res. 76, 12, 2825-2835.

Budyko, M.I. (1971) Results of observations of atmospheric electricity (The World Network, Additional Issue 1965-1969). USSR Chief Administration of the Hydro-Meteorological Service, Leningrad.

Burke, H.K., A.A. Few (1978) Direct measurements of the atmospheric conduction current. J. Geophys. Res. 83, 3093-3098.

Byrne, G.J., A.A. Few, M.E. Weber (1983) Altitude, thickness and charge concentration of charged regions of four thunderstorms during TRIP1981 based upon in situ balloon electric field measurements. Geophys. Res. Lett. 10, 39-42.

Byrne, G.J., A.A. Few, M.F. Stewart, et al. (1987) In situ meaurements and radar observations of a severe storm: electricity, kinematics and precipitation J. Geophys. Res. 92, 1017-1031.

Byrne, G.J., J.R. Benbrook, E.A. Bering, et al. (1988) Observations of the stratospheric conductivity and its variation at three latitudes. J. Geophys. Res. 93, 3879-3891.

Byrne, G.J., A.A. Few, M.F. Stewart (1989) Electric Field Measurements Within a Severe Thunderstorm Anvil. J. Geophys. Res. 94, 6297-6307.

Byrne, G.J., J.R. Benbrook, E.A. Bering III (1991) Balloon observations of stratospheric electricity above the South Pole: vertical electric field, conductivity, and conduction current, J. Atmos. Terr. Phys. 53,859-868.

Cairo, F., J. P. Pommereau, K. S. Law, H. Schlager et al, (2010) An introduction to the SCOUT-AMMA stratospheric aircraft, balloons and sondes campaign in West Africa, August 2006: rationale and roadmap, Atmospheric chemistry and physics, 10, 2237-2256.

Callahan, R.C., S.C. Coroniti, A.J. Parziale, et al. (1951) Electrical conductivity of air in the troposphere. J. Geophys. Res. 56, 545-551.

Cavallo T. (1776) Extraordinary electricity of the atmosphere observed at Islington on the month of October, 1775. Phil.Trans. Roy. Soc. Lond. 66, 407–411.

Chakravarty, S.C., S.P. Gupta, S. Chandrasekaran (1997) Middle atmospheric electrodynamics at low latitude, Adv. Space Res., 20, 2181–2189

Chalmers, J.A. (1957) Atmospheric Electricity. Pergamon Press, London.

Chapman, S. (1956) Electrostatic field measurmeents, corona discharge, and thunderclouds. Rep. C.A.L. 68. Cornell Aeronaut. Lab, Ithica, N.Y.

Chauzy, S., M. Chong, A. Delannoy, et al. (1985) The June 22 tropical squall line observed during COPT 81 experiment: electrical signature associated with dynamical structure and precipitation. J. Geophys. Res. 90, 6091-6098.

Christian, H.J. (1976) Vector electric field structure inside a New Mexico thundercloud. PhD Thesis, Rice University, Houston, TX.

Christian, H.J., A.A. Few (1977) The measurement of atmospheric electric fields using a newly developed balloon sensor. In: Electrical Processes in Atmospheres. H. Dolezalek, R. Reiter (Ed.), Dr. Dietrich Steinkopff Verlag, Darmstadt, pp. 231-237.

Christian, H.J., C.R. Holmes, J.W. Bullock, et al. (1980) Airborne and ground-based studies of thunderstorms in the vicinity of Langmuir Laboratory. Q. J. R. Met. Soc. 106, 159-174.

Christian, H.J., D.M. Mach, J. Bailey (1993) The Airborne Field Mill Project: A program summary. EOS, Trans. Amer. Geophys. Union 74, 152.

Chubb, J. (2010) An introduction to electrostatic measurements. Nova Science Publishers, New York.

Clark, J.F. (1957) Airborne measurement of atmospheric potential gradient. J. Geophys. Res. 62.

Clark, J.F. (1958) The fair-weather atmospheric electrical potential and its gradient. In: Recent advances in atmospheric electricicty. L.G. Smith (Ed.), Pergamon, New York, pp. 61-73.

Cobb, W.E. (1977) Atmospheric electric measurements at the south pole. In: Electrical Processes in Atmospheres. H. Dolezalek, R. Reiter (Ed.), Dr. Dietrich Steinkopff Verlag, Darmstadt, pp. 161-167.

Cupal, J.J., N.R. Kale, P.J. Wechsler, et al. (1989) An Instrument for the Simultaneous Measurement of the Image and Electric Charge of Hydrometeors. J. Atmos. and Ocean. Tech. 6, 697-705.

Curtis, H.O., M.C. Hyland (1958) Aircraft measurements of the ratio of negative to positive conductivity. In: Recent advances in Atmospheric Electricity. L.G. Smith (Ed.), Pergamon, New York, pp. 111-117.

Dalibart, T.F. (1752) Memoire lu a l'academie des Sciences Paris le 13 mai

Driscoll, K.T., R.J. Blakeslee, J.C. Bailey, et al. (1996) Atmospheric conductivity observations over a wide latitudinal range. 10th International conference on atmospheric electricity, Osaka, Japan, pp. 176-179.

Dye, J.E., J.J. Jones, W.P. Winn, et al. (1986) Early Electrification and Precipitation Development in a Small, Isolated Montana Cumulonimbus. J. Geophys. Res. 91, 1231-1247.

Dye, J.E., W.P. Winn, J.J. Jones, et al. (1989) The Electrification of New Mexico Thunderstorms 1. Relationship Between Precipitation Development and the Onset of Electrification. J. Geophys. Res. 94, 8643-8656.

Dye, J.E., J.C. Willett (2007) Observed Enhancement of Reflectivity and the Electric Field in Long-Lived Florida Anvils. Mon. Weath. Rev. 135, 3362-3380.

Dye, J.E., M.G. Bateman, H.J. Christian, et al. (2007) Electric fields, cloud microphysics, and reflectivity in anvils of Florida thunderstorms. J. Geophys. Res. 112, D11215.

Elster, J., H. Geitel, H. (1899) Uber die Existenz elektrischer Ionen in der Atmosphare, Terr. Magn. Atmos. Elect., 4, 213–234.

Evans, W.H. (1969) Electric Fields and Conductivity in Thunderclouds. J. Geophys. Res. 74, 939-948.

Everling, E., A. Wigand (1921) Spannungsgefälle und vertikaler Leitungsstrom in der freien Atmosphäre, nach Messungen bei Hochfarhten im Freiballon. Annalen der Physik 66, 261-282.

Farrell W.M., et al (2004) Electric and magnetic signatures of dust devils from the 2000–2001 MATADOR desert tests, J. Geophys. Res. 109, E03004.
Few, A.A., A.J. Weinheimer (1986) Factor of 2 error in balloon-borne atmospheric conduction current measurements. J. Geophys. Res. 91, 10,937-910,948.
Fitzgerald, D.R., H.C. Byers (1958) Aircraft observations of convective cloud electrification. In: Recent advances in atmospheric electricity. L.G. Smith (Ed.), Pergamon New York, p. 245.
Franklin, B. (1751) A letter from Mr Franklin to Mr Peter Collinson, F.R.S., concerning the effects of lightning, Philosophical Transactions of the Royal Society of London , Nov 14, 1751, p289.
Frier, G. D (1960) The electric field of a large dust devil, J. Geophys. Res. 65, 3504.
Freier, G. (1962) Conductivity of the air in thunderstorms. J. Geophys. Res. 67, 4683-4691.
Fulchignoni, M., F. Ferri, F. Angrilli, et al. (2005) In situ measurements of the physical characteristics of Titan's environment. Nature 438, 785-791.
Gaskell, W., A.J. Illingworth, J. Latham, et al. (1978) Airborne studies of electric fields and the charge and size of precipitation elements in thunderstorms. Q. J. R. Met. Soc. 104, 447-460.
Gerdien, H. (1904) Luftelektrische Messungen bei 2 Ballonfahrten. Nachrichten von der Gesellschaft der Wissenschaften zu Göttingen pp. 277–299.
Gerdien, H. (1905a) Messungen der dichte des vertikalen elektrischen Leitungsstromes in der freien atmosphäre bei der ballonfahrt am 11 V 1905. Nachrichten von der Gesellschaft der Wissenschaften zu Göttingen pp. 258–270.
Gerdien, H. (1905b) Messungen der Dichte des vertikalen elektrischen Leitungsstromes in der frein Atmosphare bei der Ballonfahrt am 30VIII 1905. Nachrichten von der Gessellschaft der Wissenschaften zu Gottingen.
Gerdien, H. (1905c) Ein neuer apparat zur messung der elektrishcen leitfahigkeit der luft. Nachrichten von der Gessellschaft der Wissenschaften zu Gottingen 1905, 240-251.
Gish, O.H., K.L. Sherman (1936) The National Geographic Society-U.S. Army AIr Corps Stratosphere Flight of 1935 in the Balloon Explorer II. Nat. Geo. Soc. Stratosphere Series, Washington, p. 94.
Gish, O.H. (1944) Evaluation and interpretation of the columnar resistance of the atmosphere. Terr. Magn. Atmos. Electr. 49, 159-168.
Gish, O.H., G.R. Wait (1950) Thunderstorms and the Earth's general electrification. J. Geophys. Res. 55, 473-484.
Gondot, P., A. Delannoy, P. Blanchet (1988) In-flight electrical conductivity measurements in convective cloud. 8th International Conference on Atmospheric Electricity, Upsala, Sweden, pp. 552-558.
Grenet, G. (1947) Essai d'explication de la charge electrique des nuages d'orages. Ann. de Geophys. 3, 306-307.
Griffiths, R.F., J. Latham, V. Myers (1974) The ionic conductivity of electrified clouds. Q. J. R. Met. Soc. 100, 181-190.
Gringel, W. (1978) Untersuchungen zur elektrischen Luftleitfahigkeit unter Berucksichtihung der Sonnenaktivitat und der Aerosolteilchenkonzentration bis 35km Hohe. PhD Thesis, Universitat Tubingen.
Gringel, W., R. Muhleisen (1978) Sahara dust concentration on the troposphere over the North Atlantic derived from measurements of air conductivity. Beitraege zur Physik der atmosphaere 51, 121-128.
Gringel, W., J.M. Rosen, D.J. Hoffman (1986) Electrical structure from 0-30 kilometers. In: The Earth's Electrical Environment. (Ed.), National Academy Press, Washinton D.C., pp. 166-182.
Gunn, R., W.C. Hall, G.D. Kinzer (1946) Army-Navy Precipitation-Static Project: Part I-The Precipitation-Static Interference Problem and Methods for Its Investigation. Proceedings of the IRE 34, 156p-161p.
Gunn, R. (1947) The Electrical Charge on Precipitation at Various Altitudes and Its Relation to Thunderstorms. Physical Review 71, 181.
Gunn, R. (1948) Electric field intensity inside of natural clouds. J. Appl. Phys. 19.
Gunn, R. (1950) The free electrical charge on precipitation inside an active thunderstorm. J. Geophys. Res. 55, 171-178.
Gunn, R. (1952) The electrification of cloud droplets in non precipitating cumuli. J. Met. 9, 397-402.

Gupta, S.P. (2000) Solar cycle variations of stratospheric conductivity over low latitude, Adv. Space Res., 26, 1225–1229.
Gupta, S.P. (2002) Semidiurnal variations of stratospheric conductivity at balloon float altitude, Adv. Space Res., 30, 2631-2635.
Gupta, S.P. (2004) Solar activity and atmospheric tide effect on the polar conductivity and the vertical electric field in the stratosphere at low latitude, Adv. Space Res., 34, 1798–1800.
Gurevich A.V., K.P. Zybin (2005) Runaway breakdown and the mysteries of lightning , Physics Today, 58, 5, 37.
Hale, L.C., D.P. Hoult, D.C. Baker (1968) A summary of blunt probe theory and experimental results. Space Res. 8, 320.
Harrison, R.G. (2001) A balloon-carried electrometer for high-resolution atmospheric electric field measurements in clouds Rev. Sci. Instrum. 72, 2738-2742.
Harrison, R.G. (2004) The Global Atmospheric Electrical Circuit and Climate. Surveys in Geophysics 25, 441-484.
Harrison, R.G., A.J. Bennett (2007) Cosmic ray and air conductivity profiles retrieved from early twentieth century balloon soundings of the lower troposphere. J. Atmos. Sol.-Terr. Phys. 69, 515-527.
Harrison, R.G., M.H.P. Ambaum (2008) Enhancement of cloud formation by droplet charging. Proc. R. Soc. A 464 2561-2573
Harrison, R.G., et al. (2010) Self-charging of the Eyjafjallajökull volcanic ash plume. Environ. Res. Lett. 5, 024004.
Hatakeyama, H., J. Kobayashi, T. Kitaoka, et al. (1958) A radiosonde instrument for the measurement of atmospheric electricity and its flight results. In: Recent advances in atmospheric electricity. L.G. Smith (Ed.), Pergamon New York.
Hess, V.F. (1911) Messungen der durchdringenden Strahlen bei zwei Freiballonfahrten. S.B. Akad. Wiss., Wein, 120, 1575-1584.
Higazi, K.A., J.A. Chalmers (1966) Measurements of atmospheric electrical conductivity near the ground. J. Atm. Terr. Phys. 25, 327-330.
Holzworth, R.H. (1977) Large scale DC electric fields in the Earth's environment, PhD Thesis, Univ. Of Calif., Berkley.
Holzworth, R.H., (1981) High latitude stratospheric electrical measurements in fair and foul weather under various solar conditions, J. Atmos. Terr. Phys., 43, 1115-1125.
Holzworth, R.H. (1984) Hy-Wire Measurements of Atmospheric Potential. J. Geophys. Res. 89, 1395-1401.
Holzworth, R.H. (1991) Conductivity and electric field variations with altitude in the stratosphere, J. Geophys. Res., 96, 12 857-12 864.
Holzworth, R.H., F.S. Mozer (1979) Direct evidence of solar flare modification of stratospheric electric fields, J. Geophys. Res., 84, 363-367.
Holzworth, R.H., K.W. Norville (1987) Solar flare perturbations in stratospheric current systems, Geophys. Res. Lett., 14, 852-855.
Holzworth, R.H., M.H. Dazey, E.R. Schnauss, et al. (1981) Direct measurement of lower atmospheric vertical potential differences. Geophys. Res. Lett. 8, 783-786.
Holzworth, R.H., T. Onsager, P. Kintner, S. Powell (1984) Planetary-Scale Variability of the Fair-Weather Vertical Electric Field in the Stratosphere, Phys. Rev. Lett. 53, 1398–1401.
Holzworth, R.H., K.W. Norville, P.M. Kintner, et al. (1986) Stratospheric Conductivity Variations Over Thunderstorms. J. Geophys. Res. 91, 13257-13263.
Holzworth, R.H., E.A. Bering (1998) Ionospheric electric fields from stratospheric balloon-borne probes. In: Measurement Techniques in Space Plasmas: Fields, JGR Monograph. R. Pfaff, J. Borovsky (Ed.), pp. 76-86.
Holzworth, R.H., E.A. Bering, M.F. Kokorowski, et al. (2005a) Balloon observations of temporal variation in the global circuit compared to global lightning activity. Adv. Space Res. 36, 2223-2228.
Holzworth, R.H., M. P. McCarthy, J. N. Thomas, J. Chin et al. (2005b) Strong electric fields from positive lightning strokes in the stratosphere. Geophys. Res. Lett. 32, L04809.

Hoppel, W.A., B.B. Philips (1971) The Electrical Shielding Layer Around Charged Clouds and its Role in Thunderstorm Electricity. Journal of Atmospheric Sciences, 28, 1258-1271.
Hoppel, W.A., R.V. Anderson, J.C. Willett (1986) Atmospheric electricity in the planetary boundary layer. The Earth's Electrical Environment, Studies in Geophysics. National Academy Press, Washington, pp. 149–165
Horowitz, P., W. Hill (1989) The art of electronics. Cambridge University Press.
Houze, R.A., B.F. Smull, P. Dodge (1990) Mesoscale Organization of Springtime Rainstorms in Oklahoma. Monthly Weather Review 118, 613-654.
Houze, R.A., Jr. (2004) Mesoscale convective systems. Rev. Geophys. 42, RG4003.
Hu, H., R.H. Holzworth, Y.Q. Li (1989) Thunderstorm Related Variations in Stratospheric Conductivity Measurements. J. Geophys. Res. 94, 16429-16435.
Hu, H., R.H. Holzworth (1996) Observations and parametrization of the stratospheric electrical conductivity. J. Geophys. Res. 101, 29539-29552.
Hu, W., S. Cummer, W. A. Lyons, T. E. Nelson (2002) Lightning charge moment changes for the initiation of sprites. Geophys. Res. Lett., 29, 1279.
Hunter, S.M., T.J. Schuur, T.C. Mapshall, et al. (1992) Electric and Kinematic Structure of the Oklahoma Mesoscale Convective System of 7 June 1989. Mon. Weath. Rev. 120, 2226-2239.
Idrac, P. (1928) Recherches sure le champ electrique de l'atmosphere auxgrandes altitudes a l'observatoire Trappes. Meml. Off. Natn. Met. Fr.
Imyanitov, I.M., E.V. Chubarina (1967) Electricity of the free atmosphere. Israel Program for Scientific Translations, Jerusalem.
Israel, H. (1971) Atmospheric Electricity Vol.1. Israel Program for Scientific Translations, Jerusalem.
Israel, H. (1973) Atmospheric Electricity Vol.2. Israel Program for Scientific Translations, Jerusalem.
John, T., P. Chopra, S.C. Garg (2009) Effect of photoelectric emission on blunt probe conductivity measurements in the stratosphere. J. Atmos. Sol.-Terr. Phys. 71, 905-910.
Jones, J.J. (1990) Electric Charge Acquired by Airplanes Penetrating Thunderstorms. J. Geophys. Res. 95, 16589-16600.
Jones, O.C., R.S. Maddever, J.H. Sanders (1959) Radiosonde measurment of vertical electrical field and polar conductivity. J. Sci. Instrum. 36, 24-28.
Jonsson, H.H. (1990) Possible sources of errors in electrical measurements made in thunderclouds with balloon-borne instrumentation. J. Geophys. Res. 95, 22539-22545.
Jonsson, H.H., B. Vonnegut (1995) Comment on "Negatively charged precipitation in a New Mexico thunderstorm" by Thomas C. Marshall and Stephen J. Marsh, and "Charged precipitation measurements before the first lightning flash in a thunderstorm" by Stephen J. Marsh and Thomas C. Marshall. J. Geophys. Res. 100, 16867-16868.
Junge, C.E., C.W. Chagnon, J.E. Manson (1961) Stratospheric aerosols. J. Meteor. 18, 81-108.
Kamra, A.K. (1979) Contributions of Cloud and Precipitation Particles to the Electrical Conductivity and the Relaxation Time of the Air in Thunderstorms. J. Geophys. Res. 84, 5034-5038.
Kasemir, H.W. (1955) Measurement of the air-Earth current density. Proceedings of the Conference on Atmospheric Electricity, Geophys. Res. Pap. 42, Air Force Cambridge Res. Cent., Bedford., Mass., pp. 91-95.
Kasemir, H.W. (1960) A radiosonde for measuring the air-earth current density. USA SRDL Tech. Rep. 2125. U.S. Army Signal Res. and Dev. Lab, Ft. Monmouth, N.J.
Kellogg, P.J., M. Weed (1968) Balloon measurements of ionospheric electric fields Proceedings of Fourth International Conference on the Universal Aspects of Atmospheric Electricity, Tokyo.
Khain, A., V. Arkhipov, M. Pinsky, et al. (2004) Rain Enhancement and Fog Elimination by Seeding with Charged Droplets. Part I: Theory and Numerical Simulations. J. App. Met. 43, 1513-1529.
Klein, S.A., D.L. Hartmann (1993) The seasonal cycle of low stratiform clouds. J. Climate 6, 1587-1606.
Koenigsfeld, H., P. Piraux (1950) Un novel electrometre portatif pour la mesure des charges electrostatiques par systeme electronique; son application a la radiosonde. Mem. Inst. Met. Belg. 45, 610.

Koenigsfeld, L. (1953) Investigations of the potential gradient at the Earth's ground surface and within the free troposphere. In: Thunderstorm electricity. (Ed.), University of Chicago Press, Chicago, pp. 24-45.
Koenigsfeld, L. (1955) Study of the variation of potential gradient with altitude and correlated meteorological conditions. Proc. Conf. Atmos. Electr. , Wentworth-by-the-sea, New Hampsire, pp. 21-25.
Kokorowski, M., J.G. Sample, R.H. Holzworth, E.A. Bering (2006), Rapid fluctuations of stratospheric electric field following a solar energetic particle event, Geophys. Res. Lett., 33, L20105.
Kondo, Y., R. Reiter, H. Jäger, et al. (1982a) Stratospheric aerosol inferred from electrical conductivity during a volcanically quiescent period. Pure and App. Geophys. 120, 1-10.
Kondo, Y., R. Reiter, H. Jäger, et al. (1982b) The effect of the Mt St Helens eruption on tropospheric and stratospheric ions. Pure and App. Geophys. 120, 11-17.
Koshak, W.J. (2006) Retrieving Storm Electric Fields from Aircraft Field Mill Data. Part I: Theory. J. Atmos. and Ocean. Tech. 23, 1289-1302.
Koshak, W.J., D.M. Mach, H.J. Christian, et al. (2006) Retrieving Storm Electric Fields from Aircraft Field Mill Data. Part II: Applications. J. Atmos. and Ocean. Tech. 23, 1303-1322.
Kok, J.F., N.O. Renno (2008), Enhancement of the emission of mineral dust aerosols by electric forces, Geophys. Res. Lett. 33, L19S10.
Kraakevik, J.H., J.F. Clark (1958) Airborne measurements of atmospheric electricity. Trans. Am. Geophys. Union 39, 827-834.
Kraakevik, J.H. (1958) The airborne measurements of atmospheric conductivity. J. Geophys. Res. 63, 161-169.
Kraakevik, J.H. (1961) Measurements of Current Density in the Fair Weather Atmosphere. J. Geophys. Res. 66, 3735-3748.
Krehbiel, P. (1986) The electrical structure of thunderstorms. National Academy Press, Washington D.C. .
Latham, J., C.D. Stow (1969) Airborne studies of the electrical properties of large convective clouds. Q. J. R. Met. Soc. 95, 486-500.
Lecolazet, R. (1948) Les phenomenes electriques a las frontiere de deux atmospheres differentes. Annls. Geophys. 4, 181-192.
Lemonnier, L.G. (1752) Observations sur l'electricite de l'air. Mem. Acad. Sci. 2, 233.
Linke, F. (1905) Luftelektrische Messungen bei Zwolf Ballonfahrten. Meteor. Z., p. 340.
Lutz C.W. (1939) Die wichtigstenluftelektrischen Grossen fur Munchen. Beitr .Geophys. 54, 337-347.
Lyons, W. A., T.E. Nelson, E. R. Williams, S. A. Cummer, M. A. Stanley, (2003) Characteristics of Sprite-Producing Positive Cloud-to-Ground Lightning during the 19 July 2000 STEPS Mesoscale Convective Systems. *Mon. Wea. Rev.*, 131, 2417–2427.
MacGorman, D.R., W.D. Rust (1998) The electrical nature of storms. Oxford University Press, New York.
MacGorman, D. R., W. D. Rust, P. Krehbiel, W. Rison, et al. (2005) The electrical structure of two supercell storms during STEPS. *Mon. Wea. Rev.*, 133, 2583–2607.
Mach, D.M., R.J. Blakeslee, M.G. Bateman, et al. (2009) Electric fields, conductivity, and estimated currents from aircraft overflights of electrified clouds. J. Geophys. Res. 114, D10204.
Mach, D.M., R.J. Blakeslee, M.G. Bateman., J.C. Bailey (2010) Comparisons of total currents based on storm location, polarity, and flash rates derived from high-altitude aircraft overflights, J. Geophys. Res. **115**, D03201.
Mach, D.M., R.J. Blakeslee, M.G. Bateman (2011) Global electric circuit implications of combined storm electric current measurements and satellite-based diurnal lightning statistics, J. Geophys. Res. 116,D05201.
Markson, R. (1976) Ionospheric Potential Variations Obtained From Aircraft Measurements of Potential Gradient. J. Geophys. Res. 81, 1980-1990.
Markson, R. (1977) Airborne atmospheric electrical measurements of the variation of ionospheric potential and electrical structure in the exchange layer over the ocean. In: Electrical Processes in Atmospheres. H. Dolezalek, R. Reiter (Ed.), Dr. Dietrich Steinkopff Verlag, Darmstadt, pp. 450-459.
Markson, R. (1984) Comment on "Hy-Wire Measurements of Atmospheric Potential" by R. H. Holzworth. J. Geophys. Res. 89, 2629-2635.

Markson, R. (1985) Aircraft measurements of the atmospheric electrical gobal circuit during the period 1971-1984. J. Geophys. Res. 90, 5967-5977.
Markson, R., L.H. Ruhnke, E.R. Williams (1999) Global scale comparison of simultaneous ionospheric potential measurements. Atmos. Res. 51, 315-321.
Markson, R. (2007) The Global Circuit Intensity: Its Measurement and Variation over the Last 50 Years. Bulletin of the American Meteorological Society 88, 223-241.
Marsh, S.J., T.C. Marshall (1993) Charged Precipitation Measurements Before the First Lightning Flash in a Thunderstorm. J. Geophys. Res. 98, 16605-16611.
Marshall, T.C., W.P. Winn (1982) Measurements of Charged Precipitation in a New Mexico Thunderstorm: Lower Positive Charge Centers. J. Geophys. Res. 87, 7141-7157.
Marshall, T.C., W.D. Rust, W.P. Winn, et al. (1989) Electrical Structure in Two Thunderstorm Anvil Clouds. J. Geophys. Res. 94, 2171-2181.
Marshall, T.C., W.D. Rust (1991) Electric Field Soundings Through Thunderstorms. J. Geophys. Res. 96, 22297-22306.
Marshall, T.C., B. Lin (1992) Electricity in Dying Thunderstorms. J. Geophys. Res. 97, 9913-9918.
Marshall, T.C., S.J. Marsh (1993) Negatively Charged Precipitation in a New Mexico Thunderstorm. J. Geophys. Res. 98, 14909-14916.
Marshall, T.C., W.D. Rust (1993) Two Types of Vertical Electrical Structures in Stratiform Precipitation Regions of Mesoscale Convective Systems. Bull. Amer. Meteor. Soc. 74, 2159-2170.
Marshall, T.C., S.J. Marsh (1995) Reply. J. Geophys. Res. 100, 16869-16871.
Marshall, T.C., W. Rison, W.D. Rust, et al. (1995a) Rocket and balloon observations of electric field in two thunderstorms. J. Geophys. Res. 100, 20815-20828.
Marshall, T.C., M.P. McCarthy, W.D. Rust (1995b) Electric field magnitudes and lightning initiation in thunderstorms. J. Geophys. Res. 100, 7097-7103.
Marshall, T.C., M. Stolzenburg, P.R. Krehbiel, et al. (2009) Electrical evolution during the decay stage of New Mexico thunderstorms. J. Geophys. Res. 114, D02209.
Mazur, V., L.H. Ruhnke, T. Rudolph (1987) Effect of E-Field Mill Location on Accuracy of Electric Field Measurements With Instrumented Airplane. J. Geophys. Res. 92, 12013-12019.
Mecklenburg, W., P. Lautner (1940) Zur Messung des potential gradienten und der raumladung in der freien atmosphare. Z. Phys. 115, 9-10.
Merceret, F.J., H. Christian (2000) KSC ABFM 2000 - A field program to facilitate safe relaxation of the lightning launch commit criteria for America's space program. Ninth Conf. on Aviation, Range and Aerospace Meteorology. Amer. Meteor. Soc., Orlando, FL, pp. 447-449.
Merceret, F.J., J.G. Ward, D.M. Mach, et al. (2008) On the Magnitude of the Electric Field near Thunderstorm-Associated Clouds. J. App. Met. and Clim. 47, 240-248.
Mitchell, J.D., L.C. Hale (1973) Observations of the lowest ionosphere. Space Res. 13, 471.
Mo, Q., A.G. Detwiler, J. Hallett, et al. (2003) Horizontal structure of the electric field in the stratiform region of an Oklahoma mesoscale convective system. J. Geophys. Res. 108, 4225.
Mo, Q., A.G. Detwiler, J. Helsdon, et al. (2007) Hydrometeor charges observed below an electrified cloud using a new instrument. J. Geophys. Res. 112, D13207.
Moore, C.B., C.B. Vonnegut, A.T. Botka (1958) Results of an experiment to determine initial precedence of organised electrification and precipitation in thunderstorms. In: Recent advances in atmospheric electricicty. L.G. Smith (Ed.), Pergamon, New York, pp. 333-360.
Moore, C.B., B. Vonnegut, F.J. Mallahan (1961) Airborne Filters for the Measurement of Atmospheric Space Charge. J. Geophys. Res. 66, 3219-3226.
Morita, Y., H. Ishikawa, M. Kanada (1971) The Vertical Profiles of the Small Ion Density and the Electric Conductivity in the Atmosphere in 19 Kilometers. J. Geophys. Res. 76, 3431-3436.
Mozer, F.S., R. Serlin (1969) Magnetospheric electric field measurements with balloons. J. Geophys. Res. 74, 4739.
Mühleisen, R. (1951) Zur methodik der luftelekitishcen potentialmessung: Einfluss des windes bei radioaktiven kollektoren. Z. Naturf. 6, 667-671.

Mühleisen, R.P. (1971) New determination of the air-earth current over the ocean and measurements of ionosphere potentials. Pure and Applied Geophysics 84, 112-115.
Mühleisen, R.P. (1977) The global circuit and its parameters. In: Electrical Processes in Atmospheres. H. Dolezalek, R. Reiter (Ed.), Dr. Dietrich Steinkopff Verlag, Darmstadt, pp. 467–476.
Nicoll, K.A., R.G. Harrison (2008) A double Gerdien instrument for simultaneous bipolar air conductivity measurements on balloon platforms. Rev. Sci. Instrum. 79, 084502.
Nicoll, K.A., R.G. Harrison (2009) A lightweight balloon-carried cloud charge sensor. Rev. Sci. Instrum. 80, 014501.
Nicoll, K.A., R.G. Harrison (2010) Experimental determination of layer cloud edge charging from cosmic ray ionisation. Geophys. Res. Lett. 37, L13802.
Nicoll, K.A., et al. (2011) Observations of Saharan dust layer electrification. Environ. Res. Lett. 6, 014001.
Norville, K., R.H. Holzworth, (1987) Global circuit variability from multiple stratospheric electrical measurements, . Geophys. Res.,92, 5685-5695.
Obolensky, W.N. (1925) Uber Elektrishce Ladungen in der Atmosphare. Ann. Phys. Lps. 77, 644-666.
Olson, D.E. (1971) Evidence for auroral effects on atmospheric electricity. Pure and App. Geophys. 84, 118-138.
Paltridge, G. W. (1964), Measurement of the Electrostatic Field in the Stratosphere, J. Geophys. Res., 69, 1947–1954.
Paltridge, G.W. (1965) Experimental measurements of the small-ion density and electrical conductivity of the stratosphere. J. Geophys. Res. 70, 2751-2761.
Peltier A. (1842) Recherches sur las cause des phenomenes electriques de l'atmosphere et sur les moynes d'en recueiller la manifestation. Ann. Chim. Phys. 4, 385.
Petrov, G.D. (1961) On the Distribution of Droplet Charges in Cumulus Clouds. Izv. Akad. Nauk S S S R, Ser. Geofiz 7, 1085.
Phillips, B.B. (1967) Ionic equilibrium and the electrical conductivity in thunderclouds. Mon. Weath. Rev. 95.
Pinto, I.R.C.A., O. Pinto, Jr., W.D. Gonzalez, et al. (1988) Stratospheric electric field and conductivity measurements over electrified convective clouds in the South American region. J. Geophys. Res. 93, 709-715.
Raj, P.E., P.C.S. Devara, A.M. Selvam, et al. (1993) Aircraft observations of electrical conductivity in warm clouds. Adv. Atmos. Sci. 10, 95-102.
Renno, N.O., V.J. Abreu, J. Koch, P.H. Smith et al (2004) MATADOR 2002 - A pilot field experiment on convective plumes and dust devils. J. Geophys. Res. 109, E7, 5.
Roble, R.G., I. Tzur (1986) The global atmospheric-electrical circuit. The Earth's Electrical Environment. National Academy Press, Washington D.C., pp. 206-231.
Romas, J. de. (1753) Mémoire où après avoir donné un moyen aisé pour elever fort haut, et a peu de frais un corps électrisable isolé, on rapporte des observations frappantes qui prouvent que plus le corps isolé est élevé au-dessus de la terre, plus le feu d'électricité est abondant. Mem. Acad Bordeux.
Rosen, J.M., D.J. Hofmann (1981) Balloon-Borne Measurements of the Small Ion Concentration. J. Geophys. Res. 86, 7399-7405.
Rosen, J.M., D.J. Hofmann, W. Gringel, et al. (1982) Results of an international workshop on atmospheric electrical measurements. J. Geophys. Res. 87, 1219-1227.
Rosen, J.M., D.J. Hofmann, W. Gringel (1985) Measurements of Ion Mobility to 30 km. J. Geophys. Res. 90, 5876-5884.
Rossman, F. (1950) Luftelektrische Messungen mittels Segelflugzeugen. Berichte d.Deutsch. Wetterdienstes der U.S. Zone.
Roussel-Dupré, R., J. J. Colman, E. Symbalisty, D. Sentman, V. P. Pasko (2008) Physical Processes Related to Discharges in Planetary Atmospheres , Space Science Reviews, 137, 51-82.
Ruhnke, L.H. (1969) Area averaging of atmospheric electric currents. J. Geomagn. Geoelectr. 21, 453-462.
Rust, W.D., C.B. Moore (1974) Electrical conditions near the bases of thunderclouds over New Mexico. Q. J. R. Met. Soc. 100, 450-468.

Rust, W.D., T.C. Marshall (1996) On abandoning the thunderstorm tripole-charge paradigm. J. Geophys. Res. 101, 23499-23504.
Rust, W.D., D.R. MacGorman (2002) Possibly inverted-polarity electrical structures in thunderstorms during STEPS. Geophys. Res. Lett. 29, 1571.
Rust, W.D., D.R. MacGorman, E.C. Bruning, et al. (2005) Inverted-polarity electrical structures in thunderstorms in the Severe Thunderstorm Electrification and Precipitation Study (STEPS). Atmos. Res. 76, 247-271.
Rycroft, M., R. Harrison, K. Nicoll, et al. (2008) An Overview of Earth's Global Electric Circuit and Atmospheric Conductivity. Space Sci. Rev. 137, 83-105.
Saba, M.M.F., O. Pinto, Jr., I.R.C.A. Pinto (1999) Stratospheric conductivity measurements in Brazil. J. Geophys. Res. 104, 27203-27208.
Sagalyn, R.C., G.A. Faucher (1954) Aircraft investigation of the large ion content and conductivity of the atmosphere and their relation to meteorological factors. J. Atmos. and Terr. Phys. 5, 253-272.
Sagalyn, R.C., G.A. Faucher (1956) Space and time variations of charged nuclei and electrical conductivity of the atmosphere. Q. J. R. Met. Soc. 82, 428-445.
Sagalyn, R.C. (1958) Significance of the ratio of the polar conductivities in regions of variable pollution content. In: Recent advances in atmospheric electricity. L.G. Smith (Ed.), Pergamon, New York, pp. 235-237.
São Sabbas, F.T., M. J. Taylor, P.-D. Pautet, M. Bailey (2010) Observations of prolific transient luminous event production above a mesoscale convective system in Argentina during the Sprite2006 Campaign in Brazil , J. Geophys. Res., 115, A00E58.
Saunders, C.P.R. (1993) A review of thunderstorm electrification processes. J. App. Met. 32, 642-655.
Schuur, T.J., W.D. Rust, B.F. Smull, et al. (1991) Electrical and Kinematic Structure of the Stratiform Precipitation Region Trailing an Oklahoma Squall Line. J. Atmos. Sci. 48, 825-842.
Scott, J.P., W.H. Evans (1969) The electrical conductivity of clouds. Pure and App. Geophys. 75, 219-232.
Scrase, F.J. (1933) The air-Earth current at Kew Observatory. Geophys. Mem. Lond., 58.
Scrase, F.J. (1935) Some measurements of the variation of potnetial gradient with height near the ground at Kew Observatory. Geophys. Mem. Lond., 75, 1-20.
Selvam, A.M., A.S.R. Murty, S.K. Paul, et al. (1978) Airborne electrical and microphysical measurements in clouds in maritime and urban environments. Atmos. Env. 12, 1097-1101.
Sentman, D.D. , E.M. Wescott (1993) Observations of upper atmospheric optical flashes recorded from an aircraft. Geophys. Res. Lett. 20, 2857-2860.
Shepherd, T.R., W.D. Rust, T.C. Marshall (1996) Electric Fields and Charges near 0°C in Stratiform Clouds. Mon. Weath. Rev. 124, 919-938.
Shishkin, N.S. (1965) The role of the coagulation of charged cloud particles in the development of thunderstorm phenomena. In: Problems of atmospheric and space electricity S.C. Coroniti (Ed.), Elsevier, Amsterdam, pp. 268-279.
Simpson, G., F.J. Scrase (1937) The Distribution of Electricity in Thunderclouds. Proc. R. Soc. Lond. Series A. Mathematical and Physical Sciences 161, 309-352.
Simpson, G., G.D. Robinson (1941) The Distribution of Electricity in Thunderclouds, II. Proc. R. Soc. Lond. Series A. Mathematical and Physical Sciences 177, 281-329.
Smiddy, M., J.A. Chalmers (1960) Measurements of space charge in the lower atmosphere using double field mills. Q. J. R. Met. Soc. 86, 79-84.
Srivastava, G.P., B.B. Huddar, A. Mani (1972) Electrical conductivity and potential gradient measurements in the free atmosphere over India. Pure and App. Geophys. 100, 81-93.
Stergis, C.G., S.C. Coronti, A. Nazarek, et al. (1955) Conductivity measurements in the stratosphere. J. Atmos. Terr. Phys. 6, 233-242.
Stergis, C.G., G.C. Rein, T. Kangas (1957a) Electric field measurements in the stratosphere, J. Atmos. Terr. Phys., 11, 77-82.
Stergis, C.G., G.C. Rein, T. Kangas (1957b) Electric field measurements above thunderstorms. J. Atmos. Terr. Phys 11, 83-90.

Stolzenberg, M., T.C. Marshall (1994) Testing models of thunderstorm charge distributions with Coulomb's law. J. Geophys. Res. 99, 25921-32.
Stolzenburg, M., T.C. Marshall, W.D. Rust, et al. (1994) Horizontal Distribution of Electrical and Meteorological Conditions across the Stratiform Region of a Mesoscale Convective System. Mon. Weath. Rev. 122, 1777-1797.
Stolzenburg, M., T.C. Marshall (1998) Charged precipitation and electric field in two thunderstorms. J. Geophys. Res. 103, 19777-19790.
Stolzenburg, M., W.D. Rust, B.F. Smull, et al. (1998a) Electrical structure in thunderstorm convective regions 1. Mesoscale convective systems. J. Geophys. Res. 103, 14059-14078.
Stolzenburg, M., W.D. Rust, T.C. Marshall (1998b) Electrical structure in thunderstorm convective regions 2. Isolated storms. J. Geophys. Res. 103, 14079-14096.
Stolzenburg, M., W.D. Rust, T.C. Marshall (1998c) Electrical structure in thunderstorm convective regions 3. Synthesis. J. Geophys. Res. 103, 14097-14108.
Stolzenberg, M., T.C. Marshall, W.D. Rust, et al. (2002) Two simultaneous charge structures in thunderstorm convection. J. Geophys. Res. 107, 4352-4364.
Stolzenberg, M., T.C. Marshall, P. Krehbiel (2004) Duration and Extent of Large Electric Fields in a Thunderstorm Anvil After the Last Lightning Flash. AGU Fall Meet. Suppl., pp. AE33A-0191.
Stolzenburg, M., T.C. Marshall (2008) Charge Structure and Dynamics in Thunderstorms. In: Planetary Atmospheric Electricity. F. Leblanc, K.L. Aplin, et al. (Ed.), Springer New York, pp. 355-372.
Takahashi, T. (1965) Measurement of electric charge in thundercloud by radiosonde. J. Met. Soc. Jap. 43, 206-217.
Takahashi, T. (1978) Electrical properties of oceanic tropical clouds at Ponape, Micronesia. Mon. Weath. Rev. 106.
Takahashi, T. (1983) Electric structure of oceanic tropical clouds and charge separation processes. J. Meteor. Soc. Japan. 61, 656-668.
Takahashi, T. (1990) Near absence of lightning in torrential rainfall producing micronesian thunderstorms. Geophys. Res. Lett. 17, 2381-2384.
Takahashi, T., K. Suzuki, C. Wang, et al. (1995) Precipitation mechanisms of cloud systems developed in a semi arid area of Pingliang, China:videosonde observations. J. Meteor. Soc. Japan 73, 1191-1211.
Takahashi, T., T. Tajiri, Y. Sonoi (1999) Charges on Graupel and Snow Crystals and the Electrical Structure of Winter Thunderstorms. J. Atmos. Sci. 56, 1561-1578.
Tammet, H., S. Israelsson, Knudsen, E., T.J. Tuomi (1996) Effective area of a horizontal long-wire antenna collecting the atmospheric electric vertical current. J. Geophys. Res. 101, 29671-29677.
Tessendorf, S. A., K. C. Wiens, and S. A. Rutledge (2007), Radar and lightning observations of the 3 June 2000 electrically inverted storm from STEPS, Mon. Weather Rev., 135, 3665 – 3681.
Thomas, J.N., R.H. Holzworth, J. Chin (2004) A new high voltage electric field instrument for studying sprites. IEEEE Trans. Geo. Remote Sensing 42 (7), 1399-1404.
Thomas, J. N., R. H. Holzworth, and M. P. McCarthy (2009), In situ measurements of contributions to the global electrical circuit by a thunderstorm in southeastern Brazil, Atmos. Res., 91, 153–160.
Tinsley, B.A. (2000) Influence of solar wind on the global electric circuit , and inferred effects on cloud microphysics, temperature and dynamics in the troposphere. Space Sci. Rev. 94, 231-258.
Tinsley, B.A., R.P. Rohrbaugh, M. Hei, et al. (2000) Effects of Image Charges on the Scavenging of Aerosol Particles by Cloud Droplets and on Droplet Charging and Possible Ice Nucleation Processes. J. Atmos. Sci. 57, 2118-2134.
Torreson, O.W., W.C. Parkinson, O.H. Gish, et al. (1946) Ocean atmospheric–electric results. Oceanography III: Scientific Results of Cruise VII During 1928–1929 under Command of Captain J.P. Ault Carnegie Institution of Washington, Washington D.C., p. 103.
Tuma, J. (1899) Beiträge zur Kenntniss der atmosphärischen Elektricität III. Sitz. Ak. Wiss. Wien
Uchikawa, K. (1977) Annual variations of the ionospheric potential, the air-Earth current density and the columnar resistance measured by radiosondes, In: Electrical Processes in Atmospheres. H. Dolezalek, R. Reiter (Ed.), Dr. Dietrich Steinkopff Verlag, Darmstadt, pp. 460-463.

Vali, G., J.J. Cupal, C.P.R. Saunders, et al. (1984) Airborne measurements of the electrical charges of hydrometeors. 9th International Cloud Physics Conference, Tallinn, Estonia, pp. 751-754.
Venkiteshwaran, S.P., N.C. Dhar, B.B. Huddar (1953) On the measurement of the electrical potential gradient in the upper air over Poona by Radiosondes. Proc. Indian Acad. Sci. 37, 260.
Venkiteshwaran, S.P. (1958) Measurement of the electrical potential gradient and conductivity by radiosonde at Poona, India. In: Recent advances in atmospheric electricity. L.G. Smith (Ed.), Pergamon New York, pp. 89-100.
Venkiteshwaran, S.P., A. Mani, B.B. Huddar, et al. (1962) Some observations of electric potential gradient and conductivity in cirrus cloud levels over Poona. Indian J. Met. Geophys. 13, 175-178.
Vonnegut, B. (1953) Possible Mechanism for the formation of thunderstorm electricity. Bull. Amer. Meteor. Soc. 34, 378.
Vonnegut, B., M. Blume (1957) Preliminary investigation of the distribution of space charge in the lower atmosphere. In: Artificial Stimulation of Rain: Proc. of the First Conf. on the Phys. of Cloud and Precipitation. H. Weikmann, W. Smith (Ed.), Pergamon pp. 131-141.
Vonnegut, B., C.B. Moore, A.T. Botka (1959) Preliminary Results of an Experiment to Determine Initial Precedence of Organized Electrification and Precipitation in Thunderstorms. J. Geophys. Res. 64, 347-357.
Vonnegut, B. (1963) Some facts and speculations concerning the origin and role of thunderstorm electricity. Meteorolog. Monogr. 5, 224-241.
Vonnegut, B., C.B. Moore, R.P. Espinola, et al. (1966) Electric potential gradients above thunderstorms. J. Atmos. Sci. 23, 764-770.
Vonnegut, B. (1969) Discussion of Paper by W. H. Evans, "Electric Fields and Conductivity in Thunderclouds". J. Geophys. Res. 74, 7053-7055.
Vonnegut, B., R. Markson, C.B. Moore (1973) Direct Measurement of Vertical Potential Differences in the Lower Atmosphere. J. Geophys. Res. 78, 4526-4528.
Wall, W. (1708) Phil. Trans. 26, p79.
Weber, M.E., A.A. Few (1978) A balloon borne instrument to induce corona currents as a measure of electric fields in thunderclouds. Geophys. Res. Lett. 5, 253-256.
Weber, M.E., H.J. Christian, A.A. Few, et al. (1982) A Thundercloud Electric Field Sounding: Charge Distribution and Lightning. J. Geophys. Res. 87, 7158-7169.
Weber, M.E., M.F. Stewart, A.A. Few (1983) Corona Point Measurements in a Thundercloud at Langmuir Laboratory. J. Geophys. Res. 88, 3907-3910.
Weinheimer, A.J., J.E. Dye, D.W. Breed, et al. (1991) Simultaneous Measurements of the Charge, Size, and Shape of Hydrometeors in an Electrified Cloud. J. Geophys. Res. 96, 20809-20829.
Wiens, K. C., S. A. Rutledge, and S. A. Tessendorf (2005), The 29 June 2000 supercell observed during STEPS. Part II: Lightning and charge structure, J. Atmos. Sci., 62, 4151– 4177.
Whipple, F.J.W., F.J. Scrase (1936) Point discharge in the electric field of the Earth. Geophys. Mem. Lond. 68, 1-20.
Willett, J.C., W.D. Rust (1981) Direct Measurements of the Atmospheric Electrical Potential, Using Tethered Balloons. J. Geophys. Res. 86, 12139-12142.
Williams, E.R. (1985) Large-Scale Charge Separation in Thunderclouds. J. Geophys. Res. 90, 6013-6025.
Williams, E. R. (2001) The electrification of severe storms. *Severe Convective Storms, Meteor. Monogr*., No. 50, Amer. Meteor. Soc., 527–561.
Wilson, C.T.R. (1906) On the measurement of the Earth-air current and on the origin of atmospheric electricity. Proc. Camb. Philos. Soc. 13, 363-382.
Wilson, C.T.R. (1920) Investigation on lightning discharges and on the electric field of thunderstorms. Phil. Trans. Roy. Soc. Lond. A221, 73-115.
Winn, W.P., G.W. Schwede, C.B. Moore (1974) Measurements of Electric Fields in Thunderclouds. J. Geophys. Res. 79, 1761-1767.
Winn, W.P., L.G. Byerley (1975) Electric field growth in thunderclouds. Q. J. R. Met. Soc. 101, 979-994.

Winn, W.P., C.B. Moore, C.R. Holmes, et al. (1978) Thunderstorm on July 16, 1975, Over Langmuir Laboratory: A Case Study. J. Geophys. Res. 83, 3079-3092.
Winn, W.P., C.B. Moore, C.R. Holmes (1981) Electric Field Structure in an Active Part of a Small, Isolated Thundercloud. J. Geophys. Res. 86, 1187-1193.
Woessner, R.H., W.E. Cobb, R. Gunn (1958) Simultaneous measurement of the positive and negative light ion conductivities to 26km. J. Geophys. Res. 63, 171-180.
Yair, Y. (2008) Charge Generation and Separation Processes. In: Planetary Atmospheric Electricity. F. Leblanc, K.L. Aplin, et al. (Ed.), Springer New York, pp. 119-131.
Zhou, L., B.A. Tinsley (2007) Production of space charge at the boundaries of layer clouds, J. Geophys. Res. 112, D11203.

List of Figures

Figure 1 Standard diurnal variation in potential gradient (PG) as measured by the Carnegie research ship (grey, left hand axis) and global thunderstorm area (black, right hand axis) (data from Israel (1973)).

Figure 2 (a) Principle of the potential probe technique for measurement of electric field (taken from Harrison (2004), with permission), showing the position of the collector (radioactive probe, burning fuse or water dropper) at height z above the surface. The potential of the collector, V(z), is measured, relative to the surface (taken to be ground). (b) Mounting of water dropper sensors on a balloon basket, showing the water supplies to the sensors beneath the basket (Tuma 1899). (c) Electric field mill developed by J.C.I Chubb (http://www.jci.co.uk/products.html), deployed on the atmospheric field site at the University of Reading, UK.

Figure 3 Fair weather vertical profiles of the magnitude of the vertical electric field measured from an aircraft over Leningrad by Imyanitov and Cubarina (1967). Each line represents a "category" of electric field profile. Category 1 (dotted line) – positive E_z monotonously decreasing with height (72 flights); category 3 (solid black line) – E_z not varying monotonously with height, but has a maximum usually between 300-700m (79 flights). Data from Imyanitov and Chubarina (1967).

Figure 4 Comparison of balloon borne ionospheric potential measurements made from Weissenau, Germany, and the research ship Meteor over the north Atlantic between 17 March and 2 April 1969. The blue line denotes a least squares fit, with the equation y = 0.651x + 77.2. Data from Budyko (1971).

Figure 5 (a) conceptual representation of the Gerdien condenser conductivity apparatus. (b) Rendering of Gerdien's original conductivity apparatus, showing the horizontal sampling tube inlet (left), electrometers attached to the electrodes, and aspirating fan (right) (Gerdien 1904). (c) Subsequent conductivity apparatus developed by Gerdien for use on manned balloons (Gerdien 1905c). (d) Photograph of more modern balloon based bipolar conductivity apparatus for radiosonde use, described in Nicoll and Harrison (2008).

Figure 6 (a) Parameterisations of fair weather vertical profiles of conductivity from measurements by various investigators. Thick black solid line – Woessner et al (1958); black dashed line - Gringel (1978) (solar maximum); blue dot dashed line – Gringel (1978) (solar minimum); thin red line – Rosen et al (1985); dashed red line – Callahan et al (1951); thin blue line – Gish and Sherman (1936). (b) Solid black line - Parameterization of positive conductivity at 20km for a range of geomagnetic latitudes during 1993, as measured by Driscoll et al (1996) from a high altitude aircraft. Dashed black line - conductivity parameterization from Hu and Holzworth (1996), measured by high altitude constant level balloons at 26km.

Figure 7 Measurements of atmospheric electrical parameters from a high altitude balloon at 26km during a solar energetic particle event on 16th February 1984 (geographical coordinates 44.6°S, 142.7° E). Positive and negative relaxation time constants (τ+ and τ-) are shown on the upper LHS axis, with corresponding polar conductivities on the upper RHS axis. Vertical electric field, Ez is shown on the lower LHS axis. The vertical line at 0910 denotes the start of the solar energetic particle event. Reproduced from Holzworth and Norville (1987), with permission from AGU.

Figure 8 Vertical profiles through the boundary layer measured from an instrumented aircraft by Sagalyn and Faucher (1954) during August 1953. (a) shows the profile of conductivity and electric field, and (b) the corresponding layer of space charge that accumulates at the top of the layer, associated with the temperature inversion. Taken from Tinsley (2000), with permission.

Figure 9 Vertical profile through layer of volcanic ash on 19th April 2010 over Scotland. (a) aerosol particle concentration inside the plume for bins of different diameter d: 0.6 to 1.4 μm grey circles, 1.4 to 2.6 μm black circles, with fitted smoothing spline (solid line) for the total particle concentration. (b) Measured charge density inside the plume. Adapted from Harrison et al (2010), with permission.

Figure 10 Balloon-borne measurements of electric field (E, left hand trace), positive conductivity (σ+, middle trace) and temperature (T) through a layer of stratocumulus cloud over Oxford, UK (taken from Jones et al (1959), with permission).

Figure 11 Vertical profiles of various parameters measured inside an extensive layer of stratiform cloud over the UK. (a) cloud droplet number concentration, (b) electrode voltage on balloon-borne charge sensor (CECD), (c) space charge derived from CECD electrode voltage, where measured values are shown by black points with red error bars. The black solid line and grey dotted lines denote space charge calculated according to theory (for a range of J_c values from 1-3pAm^{-2}). N.B. the balloon was descending through the cloud layer during these measurements. Taken from Nicoll and Harrison (2010).

Figure 12 (a) Schematic of the balloon borne Electric Field Meter (EFM) designed by Winn et al (1978), showing the two aluminium spheres which act as the sensing electrodes and contain the measurement electronics. Reproduced from Marshall et al (1995a), with permission from AGU. (b) Schematic of the Balloon Electric Field Sensor (BEFS). The conducting surface of the balloon, made from aluminium coated mylar, serves as the sensing element of the instrument. The external electric field induces a current in the conductor, which is related to the orientation of the balloon. Reproduced from Weber et al (1982), with permission from AGU.

Figure 13 Electric field soundings representative of the typical charge structure found inside (a) updraft regions, and (b) outside updraft regions in thunderstorms. Inside the updraft there are typically four distinct charge regions, whilst outside there are six main charge regions. Taken from Stolzenberg et al (2002), with permission from AGU.

Figure 14 Small section of a balloon borne Electric Field Meter sounding made on July 17th 1992 through the upper part of a thunderstorm and above cloud top. The transient change in electric field at 13.6km is due to a lightning discharge in the storm below. Taken from Marshall et al (1995a) with permission from AGU.

Figure 15 Schematic of bipolar conductivity sensor used on the tethered balloon thunderstorm flights of Rust and Moore (1974). The ion-collecting electrode was recessed inside a 30cm diameter spherical aluminium housing to minimize the risk of point discharge and impacts with charged precipitation particles. Taken from Rust and Moore (1974), with permission.

Figure 16 (a) Particle charge instrument designed by Marshall and Winn (1982). The upper sphere contains three aluminium induction cylinders to detect charged precipitation particles, whilst the lower sphere contains the measurement electronics, transmitter, and batteries. Each sphere is 15cm in diameter. The spheres are mounted on a boom of 2.5cm diameter PVC tubing. (b) Vertical cross section of the particle charge instrument by Marshall and Winn (1982), showing the three induction cylinders in one sphere, and the electronics in the other. Both figures from Marshall and Winn (1982), with permission from AGU.

Figure 17 Atmospheric electrical measurements obtained inside a thunderstorm on 1st August 1984. (a) Electric field, measured by the balloon electric field meter of Winn et al (1978) (b) number of charged particles per minute , measured by the apparatus described in Marshall and Winn (1982) (positively charge particles are plotted above the time axis, negatively charged below).Taken from Marshall and Marsh (1993), with permission from AGU.

List of Tables

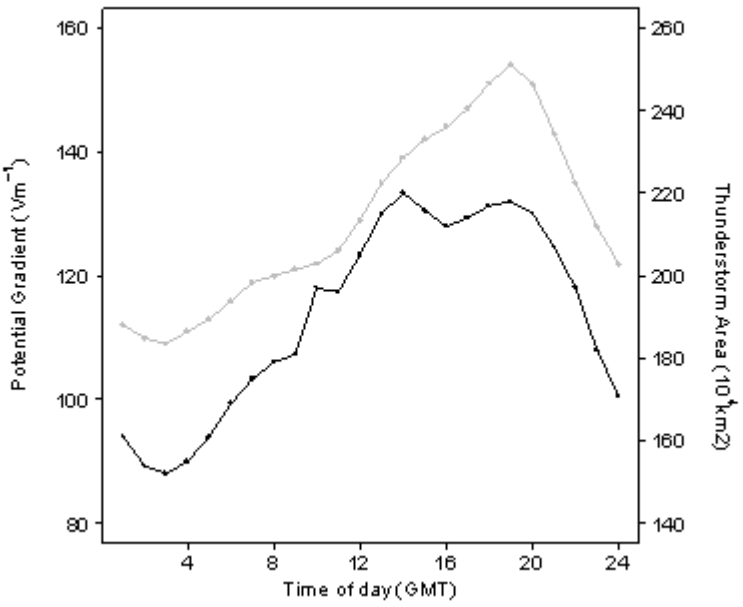

Figure 1

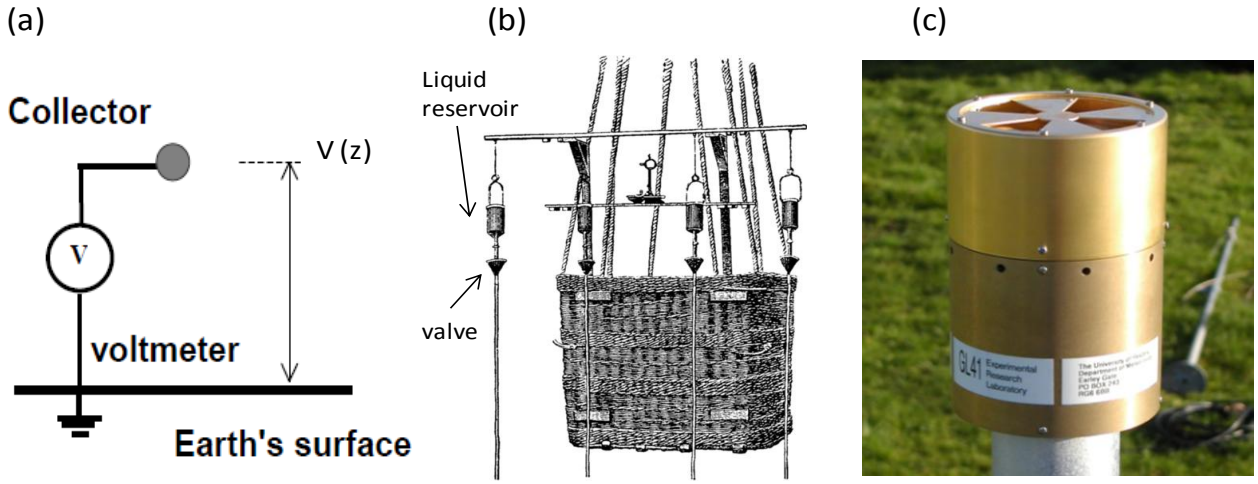

Figure 2

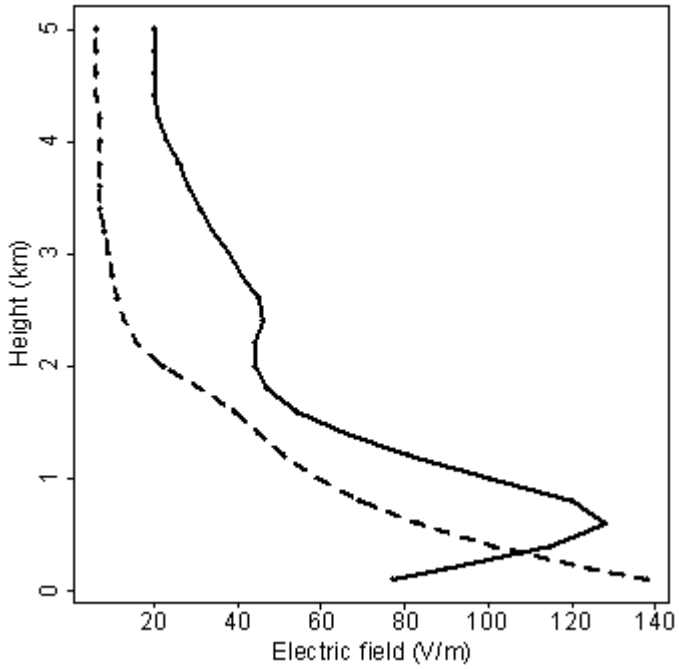

Figure 3

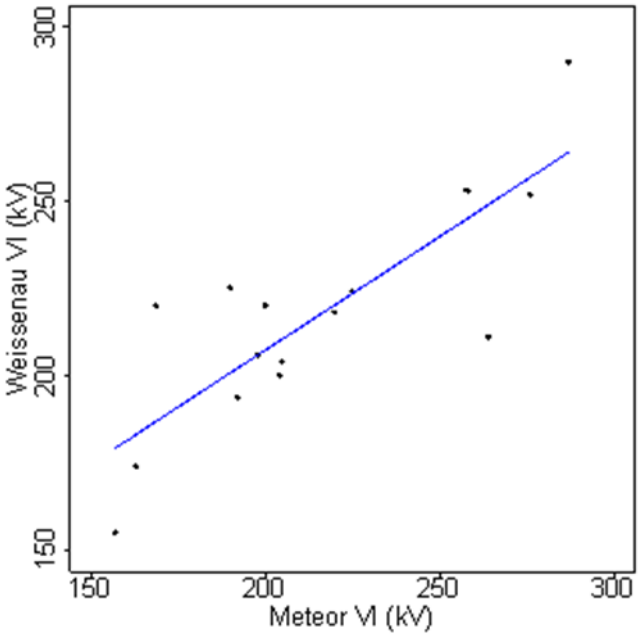

Figure 4

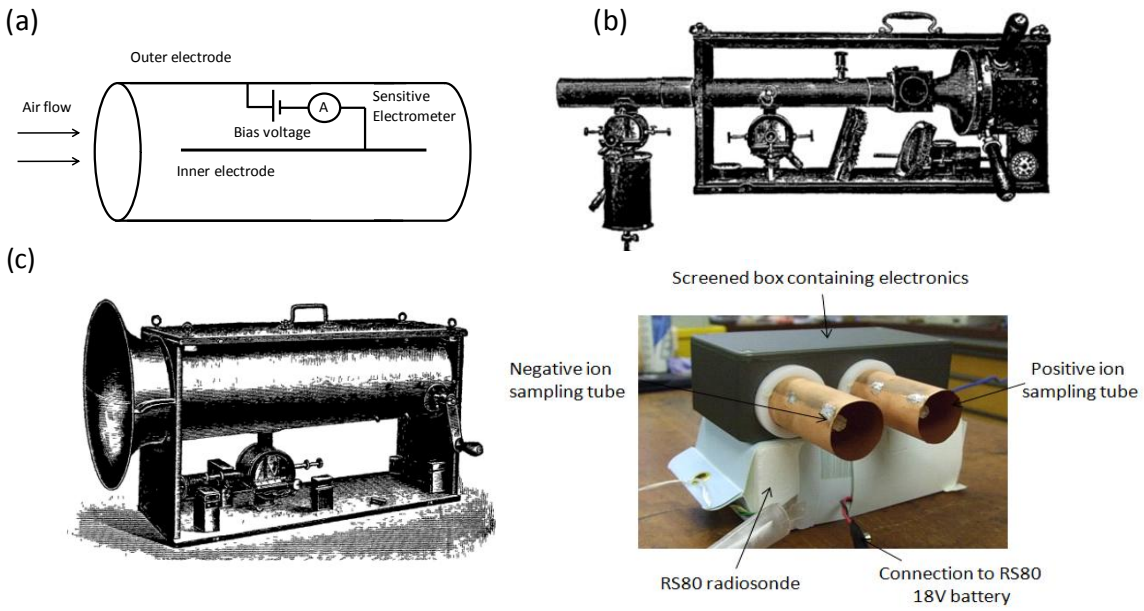

Figure 5

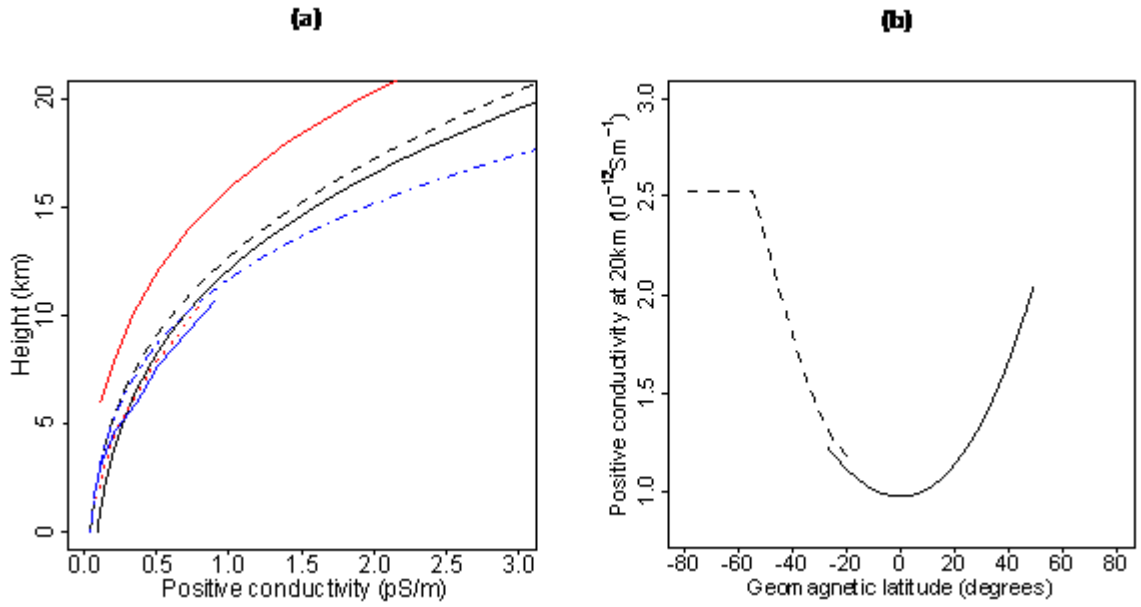

Figure 6

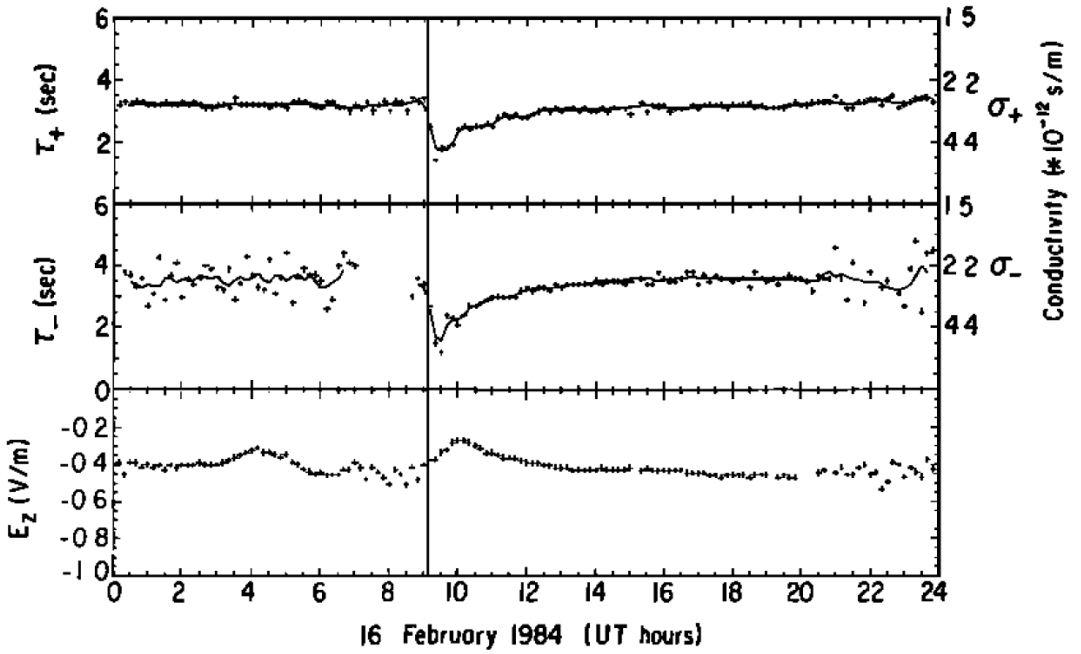

Figure 7

(a) (b)

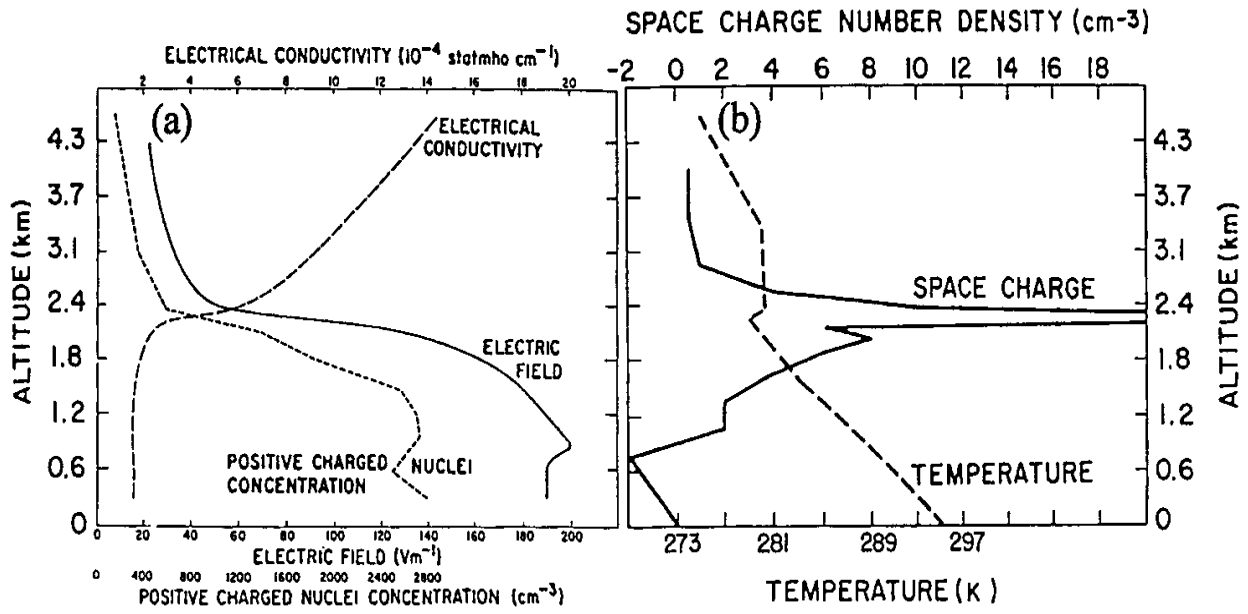

Figure 8

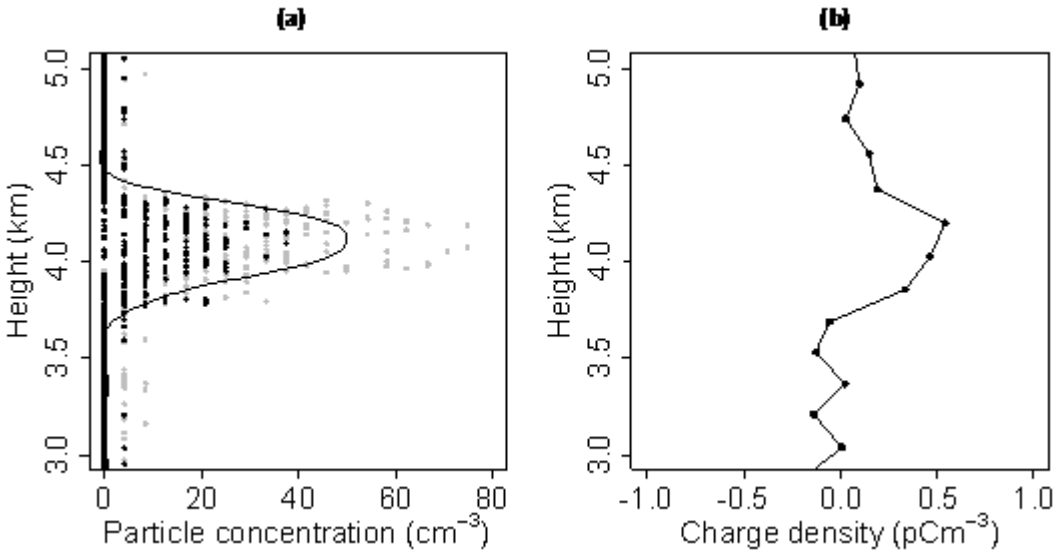

Figure 9

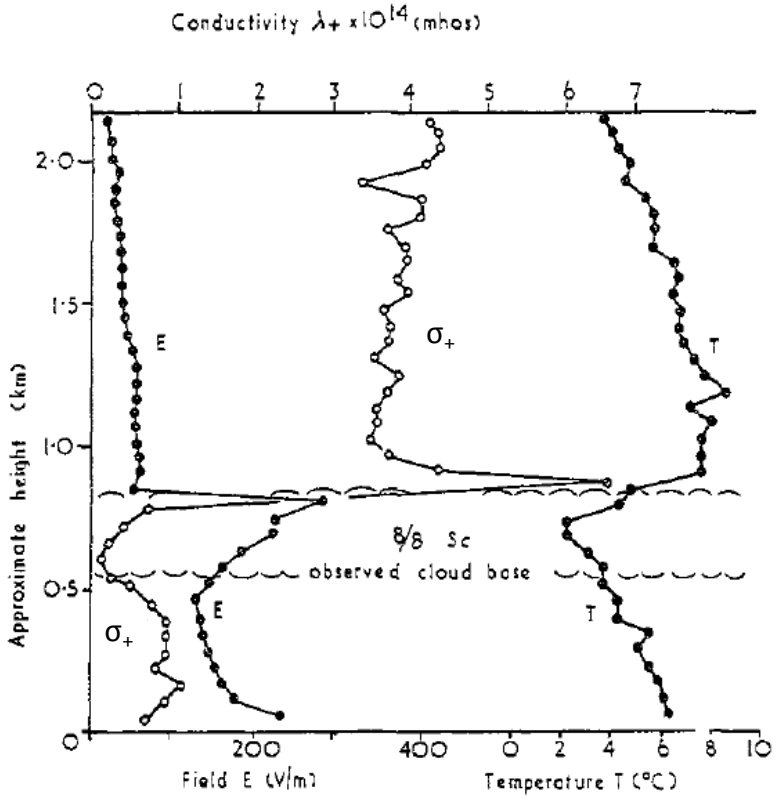

Figure 10

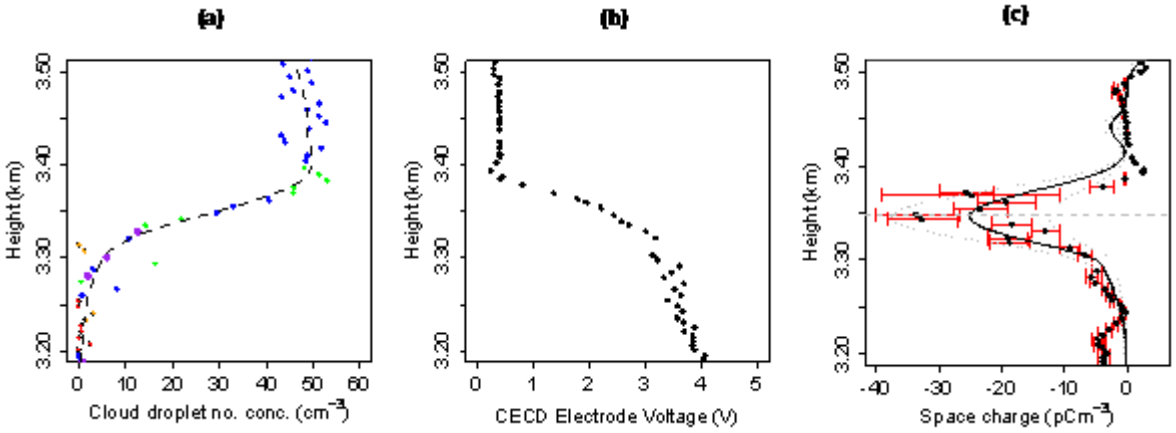

Figure 11

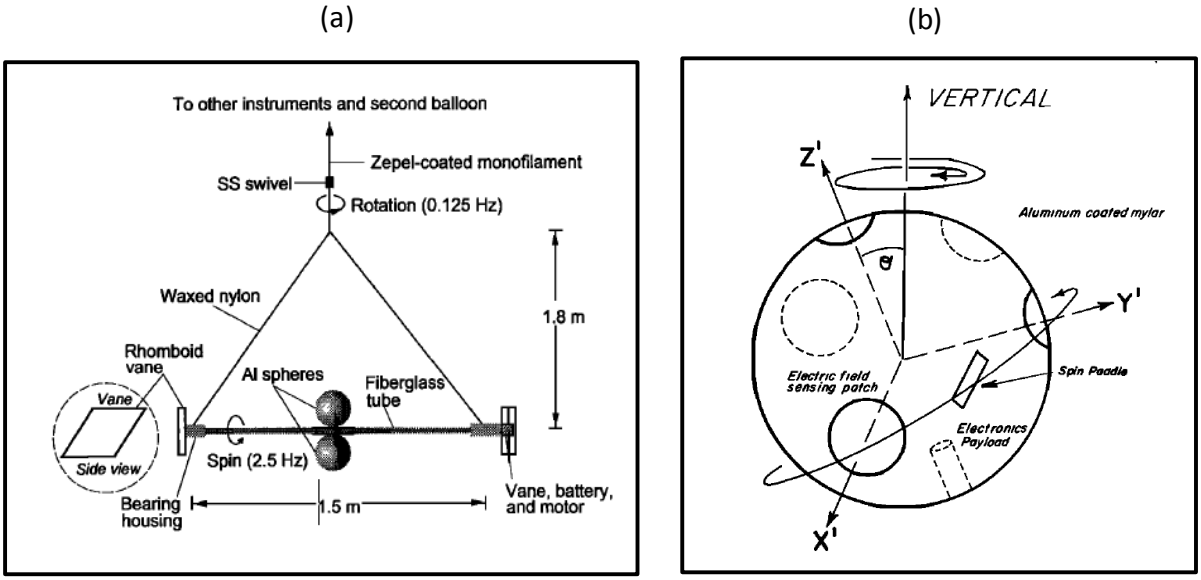

Figure 12

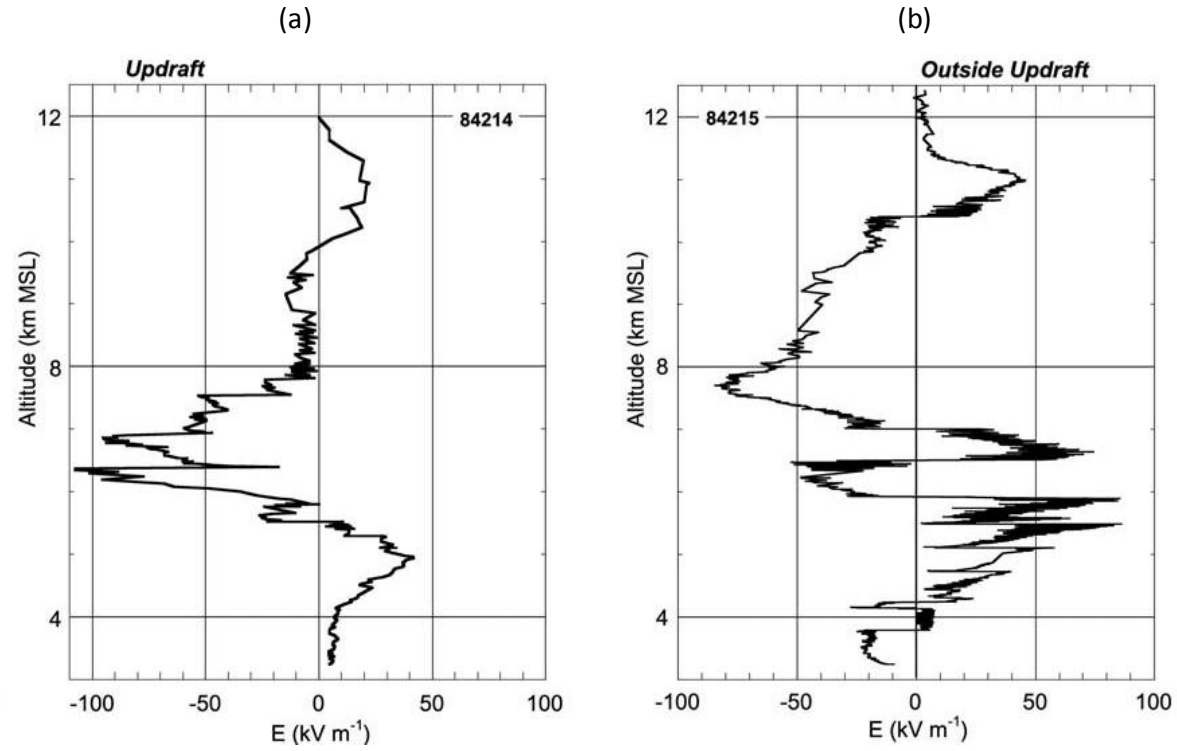

Figure 13

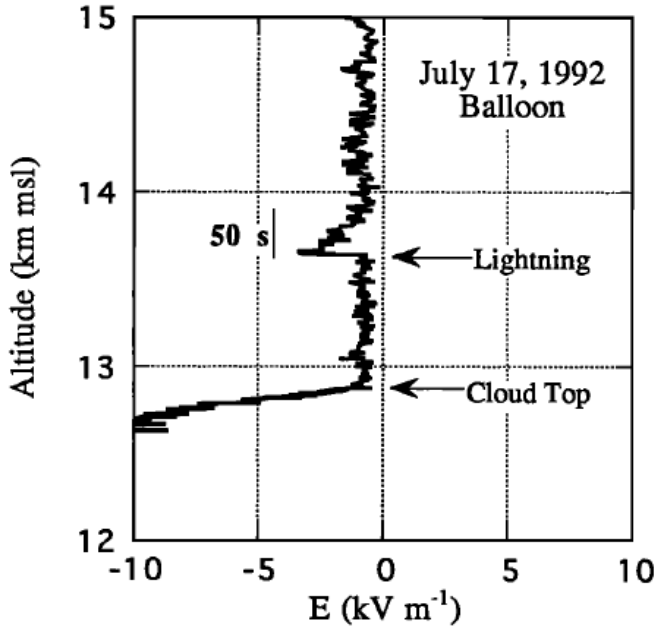

Figure 14

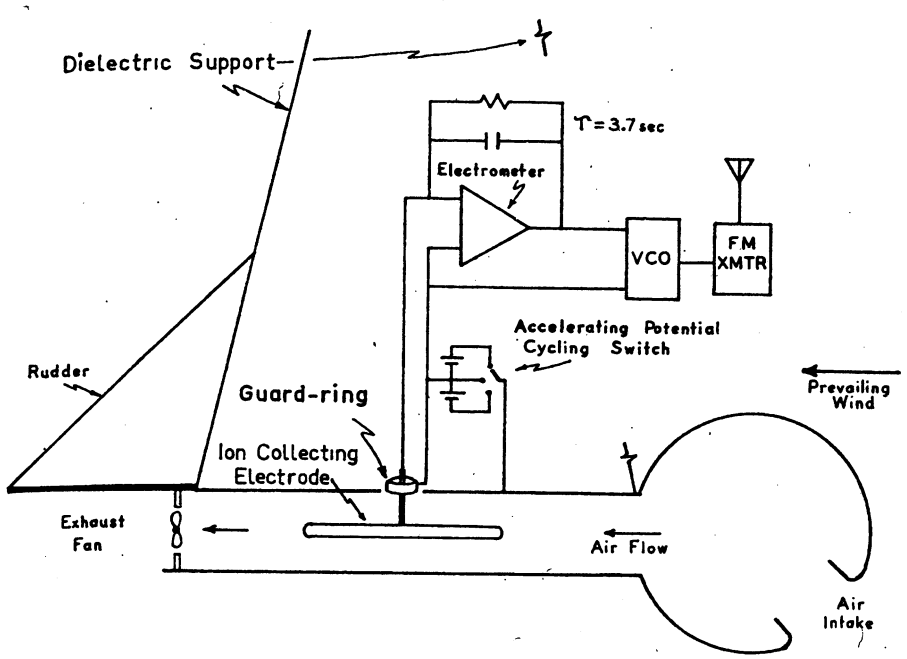

Figure 15

(a) (b)

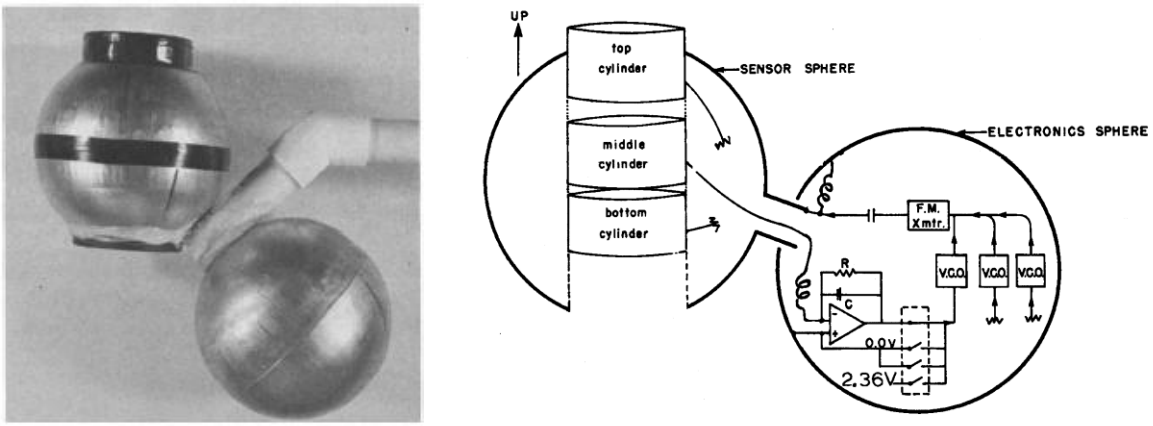

Figure 16

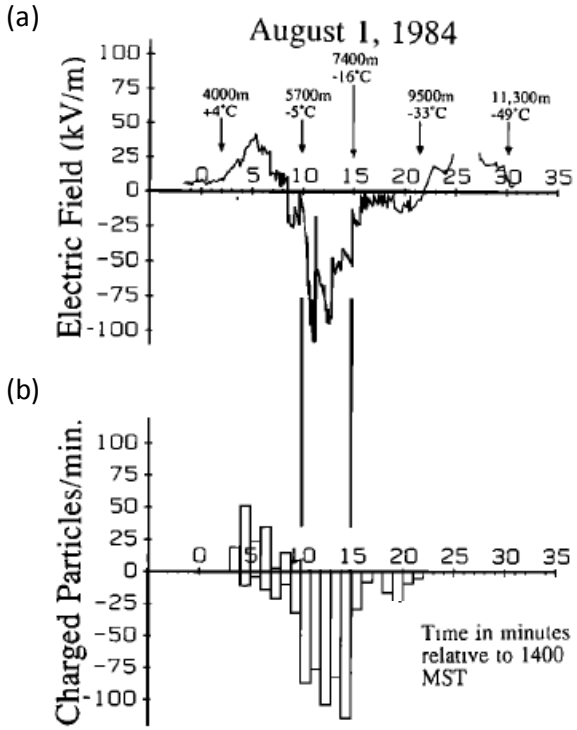
(a)
August 1, 1984
Electric Field (kV/m)
100
75
50
25
0
-25
-50
-75
-100
4000m
+4°C
5700m
-5°C
7400m
-16°C
9500m
-33°C
11,300m
-49°C
0 5 10 15 20 25 30 35
(b)
Charged Particles/min.
100
75
50
25
0
-25
-50
-75
-100
0 5 10 15 20 25 30 35
Time in minutes
relative to 1400
MST

Figure 17

Investigator	Height (km)	Location	Conductivity ratio (σ_-/σ_+)
Gish and Sherman (1936)	5 11 18	South Dakota	1.06 1.05 0.99
Callahan et al (1951)	1.5 to 9km	Various locations around the USA	1
Kraakevik (1958)	Within Boundary layer Above Boundary layer 6	Not noted Not noted Greenland	1.04 ± 0.13 1.08 ± 0.1 1.2
Curtis and Hyland (1958)	Above Boundary layer	Not noted	>1
Sagalyn (1958)	0.15-5 0.15-5	Atlantic ocean Texas	1.05 ± 0.1 1.03 ± 0.08
Woessner et al (1958)	<7 7 to 18 >18	Washington D.C.	0.7 to 1.6 0.9 to 1.33 1
Gringel et al (1986)	<15 15-20 20-25	Not noted	1.12 1 0.9

Table 1

Fair weather measurements aloft				
Investigator	**Measurement platform**	**Parameters measured**	**Instrumentation**	**Location**
Tuma (1899)	Manned balloon	E_z	Water dropper	Salzburg, Austria
Gerdien (1903,1904,1905a,1905b)	Manned balloon	E_z and σ	Water dropper and Gerdien condenser	Göttingen and Berlin, Germany
Everling and Wigand (1921)	Manned balloon	E_z and σ	Water dropper	Bitterfeld, Germany
Gish and Sherman (1936)	Manned balloon	σ	Gerdien condenser	South Dakota, USA
Idrac (1928)	Free balloon	E_z	Glow collectors (“wicks”)	France
Koenigsfeld and Piraux (1950)	Free balloon	E_z	Potential probe (radioactive)	Belgium
Callahan et al (1951)	Aircraft	σ_+ and σ_-	Gerdien condenser	USA
Venkiteshwaran et al (1953)	Free balloon	E_z	Potential probe (radioactive)	Pune, India
Koenigsfeld (1953, 1955)	Free balloon	E_z	Potential probe (radioactive)	Belgium
Stergis et al (1955)	Free balloon	σ	Gerdien condenser	New Mexico, USA
Stergis et al (1957a)	Free balloon	E_z	Potential probe (radioactive)	USA
Clark (1957,1958)	Aircraft	E_z	Electric field mill	Greenland, California and Gulf of Mexico
Kraakevik (1958, 1961)	Aircraft	σ_+ and σ_-	Gerdien condensers	Greenland
Curtis and Hyland (1958)	Aircraft	σ_+, σ_- and n	Gerdien condensers	Massachusetts, USA
Woessner et al (1958)	Free balloon	σ_+ and σ_-	Gerdien condensers	Washington D.C., USA
Venkiteshwaran (1958)	Free balloon	E_z and σ	Potential probe (radioactive)and Gerdien condenser	Poona, India
Hatakeyama et al (1958)	Free balloon	E_z and σ	Potential probe (radioactive), electric field mill and Gerdien condenser	Japan
Moore et al (1961)	Aircraft	E_z and ρ	Potential probe (radioactive), Obolensky filter	Illinois, USA
Paltridge (1964)	Free balloon	E_z	Potential probe	Melbourne, Australia
Paltridge (1965)	Free balloon	σ and n	Gerdien condensers	Victoria, Australia
Imyanitov and Chubarina (1967)	Aircraft	E_z	Electric field mill	Russia
Morita et al (1971)	Free balloon	σ and n	Gerdien condensers	Fukushima, Japan
Muhleisen (1971)	Free balloon	E_z and V_I	Electric field mill	Atlantic ocean, near equator; and Weissenau, southern Germany
Olson (1971)	Free balloon	J_c	Vertical antenna	Minnesota, USA and Manitoba, Canada
Srivastava et al (1972)	Free balloon	E_z and σ	Potential probe (radioactive) and Gerdien condenser	India
Vonnegut et al (1973)	Tethered balloon	E_z and V_I	Potential probe (radioactive) with high voltage supply on tether	New Mexico, USA
Gathman and Anderson (1976)	Aircraft	E_z and σ	Electric field mill and Gerdien condenser	Various worldwide locations
Uchikawa (1977)	Free balloon	J_c	Vertical antenna	Tateno, Japan

Muhelisen (1977)	Free balloon	E_z and V_I	Electric field mill	Weissenau, southern Germany
Markson (1977)	Aircraft	E_z and V_I	Potential probe (radioactive)	Various locations around the USA and Carribean
Cobb (1977)	Free balloon	J_c	Vertical antenna	Antarctica
Gringel (1978)	Free balloon	σ	Gerdien condenser	Germany
Holzworth (1981)	High altitude balloon	E_x,E_y,E_z and σ	Double Langmuir probe and relaxation probe	Northern auroral zone
Holzworth et al (1981)	Tethered balloon	E_z and V_I	Conducting collector	Virginia, USA
Willet and Rust (1981)	Tethered balloon	E_z and V_I	Potential probe (radioactive) with high voltage supply on tether	New Mexico, USA
Rosen and Hofmann (1981)	Free balloon	n	Modified Gerdien condenser	Wyoming, USA
Rosen et al (1982)	Free balloon	E_z, σ, J_c, n	E - Potential probe (radioactive), vertical wire antenna σ - Gerdien condenser, relaxation probe J_c – Vertical wire antenna n – Gerdien condenser	Wyoming, USA
Holzworth et al (1984)	High altitude balloon	E_x,E_y,E_z and σ	Double Langmuir probe and relaxation probe	Southern hemisphere - launched from New Zealand
Holzworth (1984)	Tethered balloon	E_z and V_I	Conducting collector	Virginia, USA
Markson (1985)	Aircraft	E_z and V_I	Electric field mill	Boston, USA; and Quebec, Canada
Rosen et al (1985)	Free balloon	σ and n	Modified Gerdien condenser	Wyoming, USA
Norville and Holzworth (1987)	High altitude balloon	E_x,E_y,E_z and σ	Double Langmuir probe and relaxation probe	Southern hemisphere - launched from New Zealand
Byrne et al (1988)	High altitude balloon	E_x,E_y,E_z and σ	Double Langmuir probe and relaxation probe	Texas, USA; Quebec, Canada and Antarctica
Holzworth (1991)	High altitude balloon	E_x,E_y,E_z and σ	Double Langmuir probe and relaxation probe	Southern hemisphere - launched from New Zealand
Byrne et al (1991)	High altitude balloon	E_x,E_y,E_z and σ	Double Langmuir probe and relaxation probe	Antarctica
Driscoll et al (1996)	Aircraft	σ	Gerdien condenser	Various worldwide locations
Hu and Holzworth (1996)	High altitude balloon	E_x,E_y,E_z and σ	Double Langmuir probe and relaxation probe	New Zealand and Antarctica
Chakravarty et al (1997)	High altitude balloon	σ	Gerdien condenser and Relaxation probe	Hyderabad, India
Gupta (2000)	High altitude balloon	σ	Relaxation probe	Hyderabad, India
Gupta (2002)	High altitude balloon	σ	Relaxation probe	Hyderabad, India
Gupta (2004)	High altitude balloon	E_z and σ	Double Langmuir probe and relaxation probe	Hyderabad, India
Markson et al (1999)	Free balloon	E_z and V_I	Radioactive probe	Massachusetts, USA and Darwin, Australia
Harrison (2001)	Free balloon	ρ	Displacement current sensor	Reading, UK
Bering et al (2005)	High altitude balloon	E_x,E_y,E_z and σ	Double Langmuir probe and relaxation probe	Antarctica
Holzworth et al (2005a)	High altitude balloon	E_x,E_y,E_z and σ	Double Langmuir probe and relaxation probe	Antarctica
John and Garg (2009)	High altitude balloon	σ	Relaxation probe	Hyderabad, India

Table 2

Cloud Type	No. of flights	Mean cloud thickness (m)	Mean $\|E_z\|$ (Vm^{-1})	Max E_z (Vm^{-1})	Min E_z (Vm^{-1})	Mean $\|\rho\|$ (pCm^{-3})	Max ρ (pCm^{-3})	Min ρ (pCm^{-3})
St	116	500	160	550	-150	9	53	58
Sc	357	500	180	1400	-160	10	137	82
As	218	950	320	6450	-145	27	1236	969
Cs	48	1100	280	2000	-90	13	58	102

Table 3

Measurements in convective clouds and thunderstorms				
Investigator	**Measurement platform**	**Parameters measured**	**Instrumentation**	**Location**
Simpson and Scrase (1937)	Free balloon	E	Alti-electrograph	London, UK
Simpson and Robinson (1941)	Free balloon	E	Alti-electrograph	London, UK
Gunn (1947)	Aircraft	E	Electric field mill	USA
Chapman (1956)	Free balloon	E	Vertically separated point discharge probes	USA
Fitzgerald and Byers (1958)	Aircraft	E	Electric field mills	USA and Caribbean
Vonnegut et al (1959)	Tethered balloon	E	Electric field mill	New Mexico, USA
Latham and Stow (1969)	Aircraft	E and q	Electric field mill and induction cylinder	Arizona, USA
Evans (1969)	Dropsonde	E and σ	Electric field mill (σ derived from same instrument)	Arizona, USA
Scott and Evans (1969)	Dropsonde	σ	Modified Gerdien condenser	Arizona, USA
Winn and Moore (1971)	Rocket	E	Electric field mill	New Mexico, USA
Rust and Moore (1974)	Tethered balloon	E, σ and q	Electric field mill, modified Gerdien condenser, Faraday funnel and induction cylinder	New Mexico, USA
Winn et al (1974)	Rocket	E	Electric field mill	New Mexico, USA
Winn and Byerley (1975)	Free balloon	E	Electric Field Meter (EFM)	New Mexico, USA
Christian (1976)	Free balloon	E	Balloon Electric Field Sensor (BEFS)	New Mexico, USA
Christian and Few (1977)	Free balloon	E	Balloon Electric Field Sensor (BEFS)	New Mexico, USA
Winn et al (1978, 1981)	Free balloon	E	Electric Field Meter (EFM)	New Mexico, USA
Weber and Few (1978)	Free balloon	E	Corona probe	New Mexico, USA
Takahashi (1978)	Free balloon	q	Induction cylinder	Ponape, Micronesia
Gaskell et al (1978)	Aircraft	E and q	Electric field mills and induction cylinder	New Mexico, USA
Weber (1980)	Free balloon	E	Balloon Electric Field Sensor (BEFS)	New Mexico, USA
Christian et al (1980)	Aircraft	E and q	Electric field mills and induction cylinder	New Mexico, USA
Marshall and Winn (1982)	Free balloon	E and q	Electric Field Meter (EFM) and induction cylinder	New Mexico, USA
Weber et al (1982)	Free balloon	E	Balloon Electric Field Sensor (BEFS)	New Mexico, USA
Weber et al (1983)	Free balloon	E	Corona probe	New Mexico, USA
Byrne et al (1983, 1987, 1989)	Free balloon	E	Corona probe	Oklahoma, USA
Takahashi (1983)	Free balloon	E and q	Radioactive collector and induction cylinder	Ponape, Micronesia
Dye et al (1986, 1989)	Aircraft	E and q	Electric field mills and induction cylinder	Montana and New Mexico, USA
Marshall et al (1989, 1995a)	Free balloon	E	Electric Field Meter (EFM)	New Mexico and Oklahoma, USA
Takahashi (1990)	Free balloon	q	Induction cylinder with video sonde	Ponape, Micronesia

Schurr et al (1991)	Free balloon	E	Electric Field Meter (EFM)	Oklahoma, USA
Hunter et al (1992)	Free balloon	E	Electric Field Meter (EFM)	Oklahoma, USA
Marshall and Rust (1991, 1993)	Free balloon	E	Electric Field Meter (EFM)	Alabama, New Mexico and Oklahoma, USA
Weinheimer et al (1991)	Aircraft	q	Induction cylinder	New Mexico, USA
Marshall and Lin (1992)	Free balloon	E	Electric Field Meter (EFM)	New Mexico, USA
Bateman et al (1994)	Free balloon	E and q	Electric Field Meter (EFM) and induction cylinder	Oklahoma, USA
Marsh and Marshall (1993)	Free balloon	E and q	Electric Field Meter (EFM) and induction cylinder	New Mexico, USA
Marshall and Marsh (1993)	Free balloon	E and q	Electric Field Meter (EFM) and induction cylinder	New Mexico, USA
Marshall et al (1995b)	Free balloon and rocket	E	Electric Field Meter (EFM) on balloon, electric field mills on rocket	New Mexico, USA
Stolzenberg et al (1994, 1998a, 1998b, 1998c, 2007)	Free balloon	E	Electric Field Meter (EFM)	Oklahoma and New Mexico, USA
Takahashi et al (1995,1998,1999)	Free balloon	q	Induction cylinder with video sonde	Ponape, Micronesia and Japan
Bateman et al (1995, 1999a)	Free balloon	E and q	Electric Field Meter (EFM) and induction cylinder	Oklahoma and New Mexico, USA
Shepherd et al (1995)	Free balloon	E	Electric Field Meter (EFM)	Oklahoma and New Mexico, USA
Stolzenberg and Marshall (1998)	Free balloon	E and q	Electric Field Meter (EFM) and induction cylinder	New Mexico, USA
Stolzenberg et al (2001)	Free balloon	E	Electric Field Meter (EFM)	Southern Great Plains, USA
Stolzenberg and Marshall (2002)	Free balloon	E	Electric Field Meter (EFM)	Oklahoma, USA
Rust and MacGorman (2002)	Free balloon	E	Electric Field Meter (EFM)	Colorado/Kansas, USA
Mo et al (2003)	Aircraft and free balloon	E	Electric field mills on aircraft and Electric Field Meter (EFM) on balloon	Colorado/Kansas, USA
Stolzenberg et al (2004)	Free balloon	E	Electric Field Meter (EFM)	USA
Rust et al (2005)	Free balloon	E	Electric Field Meter (EFM)	Colorado/Kansas, USA
MacGorman et al (2005)	Free balloon	E	Electric Field Meter (EFM)	Colorado/Kansas, USA
Dye an Willet (2007)	Aircraft	E	Electric field mills	Florida, USA
Dye et al (2007)	Aircraft	E	Electric field mills	Florida, USA
Mo et al (2007)	Aircraft	E and q	Electric field mills and induction cylinder	Colorado/Kansas, USA
Merceret et al (2007)	Aircraft	E	Electric field mills	Florida, USA
Marshal et al (2009)	Free balloon	E	Electric Field Meter (EFM)	New Mexico, USA

Table 4

	Land storms		Oceanic storms		All storms	
	Lightning	***No lightning***	***Lightning***	***No lightning***	***Lightning***	***No lightning***
Upward current (A) (positive polarity)	0.43 *(368)*	0.09 *(81)*	1.0 *(133)*	0.19 *(177)*	0.6 *(501)*	0.15 *(258)*
Upward current (A) (negative polarity)	-0.30 *(29)*	-0.12 *(10)*	-0.19 *(6)*	-0.17 (11)	-0.29 *(35)*	-0.16 *(21)*
Upward current (A) (zero)	0 *(2)*	0 *(24)*	0 *(4)*	0 *(5)*	0 *(6)*	0 *(29)*

Table 5

Problem	Possible solutions
Platform issues	
Charging of measurement platform from impacts with charged precipitation, aerosol particles or cloud droplets; induction from changing electric fields; emission of corona ions in regions of high electric fields; and in the case of aircraft, emission of exhaust gases. Charging of surfaces perturbs the local electric field in the region of measurement, and should be minimized.	*Balloon:* suspend the instrument package far below the balloon (distances in literature range from 10m to >100m, depending on balloon size and meteorological conditions during launch). Horizontal booms have also been used, particularly when measuring precipitation charge, to avoid contamination from charged particles emitted from the balloon surface. *Aircraft*: Account for the contribution of aircraft charge to the measured electric field by measuring electric field from different points on the aircraft (common practice to mount 5 or 6 electric field mills at strategic locations around the aircraft), see section 7.2 for details.
Current flow in balloon rigging lines during high humidity conditions in large electric fields (e.g. Jonsson 1990; Jonsson and Vonnegut 1995; Bateman et al 1999b). In electric fields of several kVm^{-1}, conduction currents of 10-100nA can flow through rigging lines connecting instrument packages to balloons. This may perturb the ambient electric field around the location of sensors, or by emission of corona ions from ends of the line.	At temperatures colder than -5°, conduction currents decrease rapidly, and should not cause serious problem during most of a balloon flight (Marshall and Marsh 1995). However, to avoid the risk of electrical breakdown, rigging lines should be made of hydrophobic material, e.g. Zepel-treated nylon, Teflon coated nylon or wax coated, as these have an increased resistance above untreated nylon.
Instrument Issues	
Triboelectric charging of non-conductive instrument surfaces by impacts from charged particles can strongly perturb the surrounding ambient electric field, leading to erroneous measurements.	Minimise this effect by increasing the conductivity of the outer surfaces e.g. coating them with conductive paint, spray, or wrapping them in tinfoil (e.g. Takahashi et al 1999).
Triboelectric charging of central electrode in conductivity apparatus. This effect leads to spurious changes in the central electrode current/voltage from impacts with charged precipitation particles/cloud droplets, which can wrongly be interpreted as changes in conductivity.	Although this effect is difficult to avoid, it is possible to determine when it occurs, by measuring the offset current in the central electrode, caused solely by charged particles. This can be achieved by either zeroing the bias voltage at regular intervals e.g. Scott and Evans (1969), or reducing the air flow rate to the tube so that no ions are deliberately collected (e.g. Kraakevik 1958).
Interference from external electric fields in conductivity apparatus. Measurement of conductivity is based on deflection of ions to a central electrode in an applied electric field. Interference from large external fields, which penetrate the ends of the conductivity sampling tube can perturb the conductivity measurement.	Careful design of the conductivity apparatus to ensure that the central electrode is placed well within the outer shielding tube is required, and some investigators have also experimented with wire mesh attached to the external ends of the outer shielding tube (e.g. Rosen and Hoffmann 1981), but care must be taken not to substantially reduce the airflow in the sampling tube.

Inlets are a common occurrence in aircraft instrumentation, particularly for the measurement of conductivity, but issues with the conductivity measurement can arise due to diffusion of ions to the inlet walls (e.g. Anderson and Bailey 1991).	The diameter of the inlet pipe, as well as the angle of airflow (e.g. 90 degree bends) must be carefully considered when using inlets for the measurement of conductivity, see Higazi and Chalmers (1966) and Anderson and Bailey (1991) for more details on this. Repulsion of ions can also arise at the inlet, due to the distortion of the local electric filed by the tube. This can be minimized by "guarding" the inlet i.e. maintaining it at the local atmospheric potential. This technique also helps to reduce leakage currents in the electronic circuitry, and is described in more detail in Horowitz and Hill (1989).
Corona discharge from sharp points on apparatus is a common problem in environments where electric fields of >several kVm^{-1} are present. The additional corona ions that are emitted perturb the ambient electrical conditions, giving rise to spurious measurements.	The most common method to avoid this is to design the apparatus with the least number of sharp points possible, and spherical designs are particularly good for this. The conductivity apparatus of Rust and Moore (1974), shown in Figure 15 provides an example of this, as the purpose of the spherical inlet around the conductivity sampling tube is to minimise corona discharge from the central electrode.
Splashing of droplets in particle charge apparatus. Measurement of charge on precipitation particles or cloud droplets is commonly made using the induction technique, which requires a particle/droplet to pass cleanly through an induction cylinder without touching the sides. Impaction effects from interactions between particles/droplets and the induction cylinder is a common occurrence, leading to spurious effects.	A simple avoidance method is to install an extra induction ring above the main measuring one, solely to detect impaction events (e.g. Marshall and Winn 1982). Another method, used by Gunn (1950), was to install the induction cylinder within a truncated cone, so that impacts would occur between particles and the cone. A similar approach was also adopted on the balloon borne apparatus of Takahashi et al (1999), who used a sponge to absorb impacts with particles above the induction ring.

Table 6 Summary of commonly encountered problems when making airborne measurements of atmospheric electrical parameters, and their possible solutions